NASA Contractor Report 3511

Terminal Area Automatic Navigation, Guidance, and Control Research Using the Microwave Landing System (MLS)

Part 2 – RNAV/MLS Transition Problems for Aircraft

Samuel Pines

CONTRACT NAS1-15116
JANUARY 1982

NASA

NASA Contractor Report 3511

Terminal Area Automatic Navigation, Guidance, and Control Research Using the Microwave Landing System (MLS)

Part 2 – RNAV/MLS Transition Problems for Aircraft

Samuel Pines
Analytical Mechanics Associates, Inc.
Hampton, Virginia

Prepared for
Langley Research Center
under Contract NAS1-15116

National Aeronautics
and Space Administration

**Scientific and Technical
Information Branch**

1982

CONTENTS

CONTENTS

LIST OF FIGURES

LIST OF FIGURES

LIST OF FIGURES

LIST OF TABLES

SUMMARY

This report contains the results of an investigation carried out for the NASA Langley Research Center TCV B-737 program to study the problems in navigation and guidance encountered by aircraft in the initial transition period in changing from DME, VORTAC, and barometric instruments to the more precise MLS data type navaids in the terminal area. The report investigates the effects of the resulting discontinuities on the estimates of position and velocity for both optimal (Kalman type navigation schemes) and fixed gain (complementary type) navigation filters, and the effects of the errors in cross track, track angle, and altitude on the guidance equations and control commands during the critical landing phase. A method is presented to remove the discontinuities from the navigation loop and to reconstruct an RNAV path designed to land the aircraft with minimal turns and altitude changes.

Areas for additional study are recommended to cover special problems encountered in the study. Smooth transition performance is shown to be possible and feasible for aircraft utilizing MLS navaids in the terminal area.

INTRODUCTION

During the noncritical phases of automated aircraft flight, navaids such as VORTAC, TACAN, and baro-altimeter are considered sufficiently accurate for navigation, guidance, and control. Range bias errors of the order of magnitude of 500 meters are not uncommon, heading bias errors of 1^{o} are often encountered, and corresponding altitude bias errors of 40 meters are ordinarily met. With the introduction of MLS in the terminal area, these instrument biases are abruptly reduced to 30 meters in range, $.05^{o}$ in azimuth and elevation, and 5 meters in altitude.

The effect of this sudden realization of the true error is to present the navigation and guidance system with a large deviation in cross track, track angle and altitude. These command the control system to execute large roll angles to wipe out the cross track and track angle errors, and to call for large elevator and throttle changes to attain the desired altitude and altitude rate. In addition, the navigation filter, in response to the large residuals, causes transient errors in the estimate of the position and velocity. Finally, the guidance gains in the terminal area tend to be somewhat higher than those used during the noncritical flight phase which further aggravates the transition problem.

The purpose of this study is to simulate typical transitions in the terminal area and to investigate what software changes might be undertaken to reduce the severity and perhaps eliminate the navigation guidance and control problems described above without unduly changing the existing guidance laws or navaids.

Simulation programs (ALERT, BANKTURN) of the TCV B737 aircraft are described in Reference 1.* In order to simulate the transition problem it was necessary to add a simulation of the RNAV waypoint path design equations, the noncritical navaids such as VORTAC, and the baro altimeter and to duplicate

---

1. *Pines, S.; Schmidt, S. F.; and Mann, F.: Automated Landing, Rollout, and Turnoff Using MLS and Magnetic Cable Sensors. NASA CR-2907, Oct. 1977.

the guidance equations for the lateral and vertical path control. Finally, it was necessary to include a simulation of both the Kalman and complementary navigation filters in a single program in order to be able to illustrate the relative estimation performance of a given filter when the alternate filter was being used in the guidance loop. The program containing these changes is named FILCOMP. Only those items that are new and not contained in Ref. 1 are described herein. The analytical work is contained in four Appendices. Appendix A contains an introduction into vector and matrix operations which are extensively used in the waypoint path equations and in the guidance formulation. Appendix B contains the derivation of the waypoint path equations and guidance. Appendix C contains the derivation of the third order complementary filter in discrete form (i. e., without internal numerical integration loops) which is not used in the TCV B737 flight control computer. Appendix D contains the derivation of navigation filter equations for estimating the wind direction and speed.

The main body of the report contains the results of the simulation study carried out using the FILCOMP program.

I. RNAV GUIDANCE EQUATIONS

(a) Coordinate Frames

The RNAV path equations are defined and derived in Appendix B. The desired horizontal path consists of a series of straight lines (great circles) connected by circular turns of constant radius. The vertical path is a piecewise linear function of the ground track distance between the consecutive midpoints of the circular turns. The entire path is fixed in the Earth and rotates rigidly with the Earth about the North Pole. The guidance equations are designed to null out the cross track, track angle and altitude errors between the aircraft position and heading with respect to this rotating path. In order to accomplish this, the navigation system must provide estimates of these errors from knowledge of the desired position and velocity and the best estimate of the aircraft actual position and velocity.

Several coordinate systems are required to accomplish this task. The primary inertial coordinate system is illustrated in Fig. 1a where $\hat{x}_{1I}$ is directed along the Earth North Pole. $\hat{x}_{3I}$ is fixed at the intersection of the Greenwich Meridian and the Earth equator. The $\hat{x}_{2I}$ coordinate forms a right hand orthogonal system defined by

$$\{ \hat{x}_{2I} \} = \{ \hat{x}_{3I} \} \times \{ \hat{x}_{1I} \} \tag{1}$$

The second coordinate frame of interest is the Earth fixed coordinate system. In this reference frame, $\hat{x}_{1E}$ is along the Earth North Pole, $\hat{x}_{3E}$ is fixed along the intersection of the Greenwich Meridian and the Earth equator and rotates with the Earth at the earth rotation rate, w_E ; $\hat{x}_{2E}$ forms a right hand system. The transformation from the E frame to the I frame is given by

$$T_{IE} = T (w_E (t-t_o) , \hat{x}_1) \tag{2a}$$

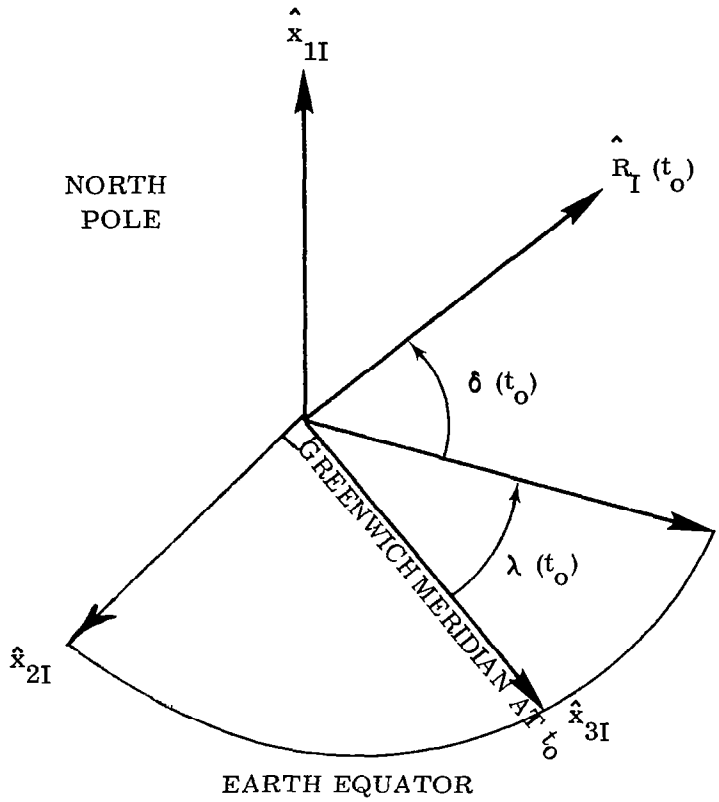

Figure 1(a).-Primary Inertial Coordinate System

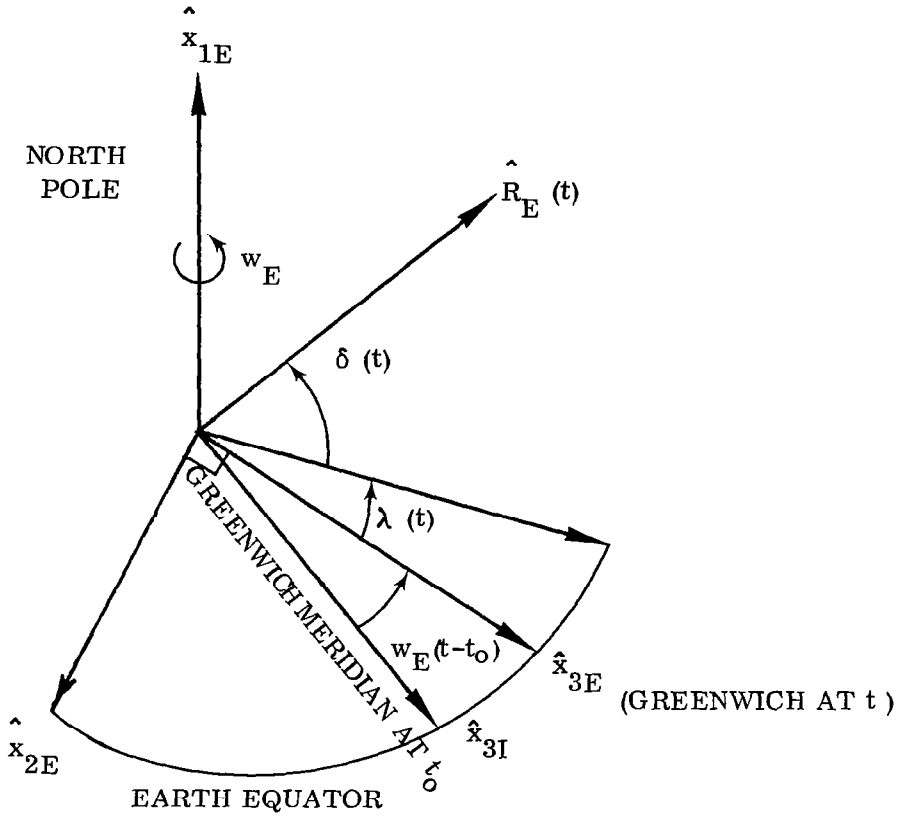

(b) Earth Fixed Inertial Coordinate System

Figure 1.-Concluded.

The transformation matrix, $T(\alpha, \hat{x})$ is defined in Appendix A. The coordinate system is illustrated in Fig. 1(b). We have

$$T_{IE} = \begin{bmatrix} 1 & 0 & 0 \\ 0 & \cos(w_E(t-t_o)) & -\sin(w_E(t-t_o)) \\ 0 & \sin(w_E(t-t_o)) & \cos(w_E(t-t_o)) \end{bmatrix} \quad (2b)$$

The value of w_E is given in Table I.

To obtain the vector velocity and acceleration of a point in Earth fixed coordinates in terms of inertial coordinates, we have

$$\{\dot{R}_E\} = \{\dot{R}_I\} - w_E \{\hat{x}_1\} \times \{R_I\} \quad (2c)$$

$$\{\ddot{R}_E\} = \{\ddot{R}_I\} + w_E^2 \{R_I\} \quad (2d)$$

The third coordinate frame used in the guidance equations is the local level coordinate frame. In this system the x_{1L} coordinate points due north, the x_{2L} coordinate points due west, and the x_{3L} coordinate is positive up away from the Earth center through the center of gravity of the aircraft. The origin of the system is at the center of gravity of the aircraft. The transformation from local level to inertial coordinates, T_{IL}, is given by

$$T_{IL} = T(\alpha_1, \hat{x}_1)\ T\ (\alpha_2, \hat{x}_2) \quad (3a)$$

where

$$\alpha_1 = w_E (t-t_o) + \lambda$$

$$\alpha_2 = \delta$$

λ is the longitude of the aircraft

δ is the latitude of the aircraft

The coordinate system is illustrated in Figure 2(a). The transformation, T_{IL}, is given by

$$T_{IL} = \begin{bmatrix} \cos\delta & 0 & \sin\delta \\ \sin\delta \sin\alpha_1 & \cos\alpha_1 & -\cos\delta \sin\alpha_1 \\ -\sin\delta \cos\alpha_1 & \sin\alpha_1 & \cos\delta \cos\alpha_1 \end{bmatrix} \tag{3b}$$

Given the inertial coordinates of the aircraft (x_{1I} , x_{2I} , x_{3I}) we have the unit north vector,

$$\hat{N} = \begin{Bmatrix} \cos\delta \\ \sin\delta \sin\alpha_1 \\ -\sin\delta \cos\alpha_1 \end{Bmatrix} \tag{4a}$$

the unit west vector,

$$\hat{W} = \begin{Bmatrix} 0 \\ \cos\alpha_1 \\ \sin\alpha_1 \end{Bmatrix} \tag{4b}$$

and the unit radius vector,

$$\hat{R} = \begin{Bmatrix} \sin\delta \\ -\cos\delta \sin\alpha_1 \\ \cos\delta \cos\alpha_1 \end{Bmatrix} \tag{4c}$$

where

$$\begin{aligned} \delta &= \sin^{-1}\left(\frac{x_{1I}}{r_E}\right) \\ \alpha_1 &= \tan^{-1}\left(\frac{-x_{2I}}{x_{3I}}\right) \end{aligned} \tag{4d}$$

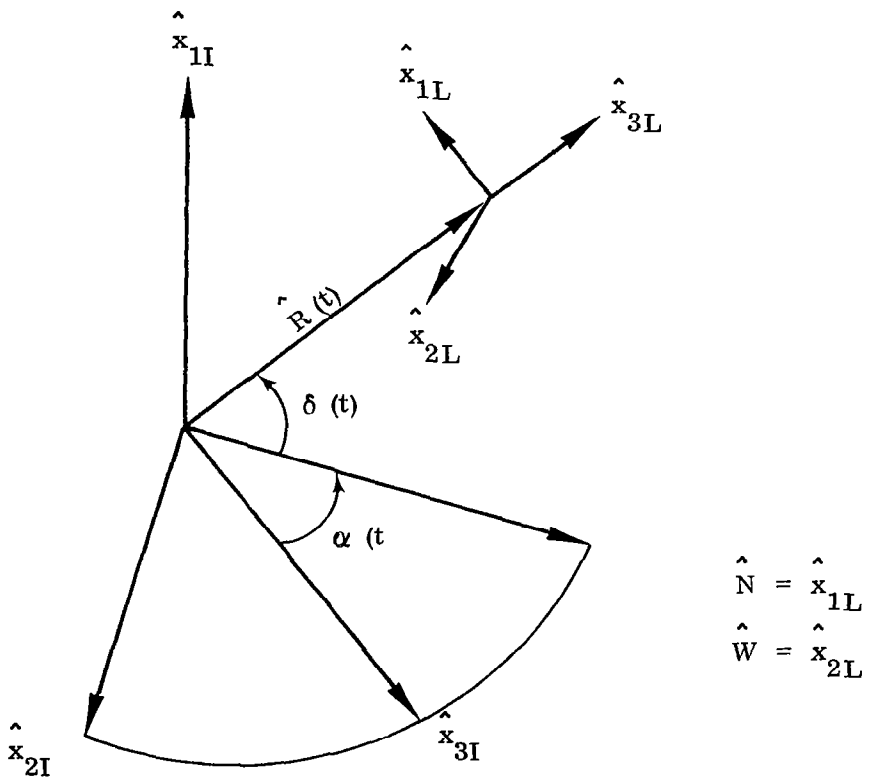

Figure 2(a).- Local Level Coordinate System

The aircraft longitude is given by

$$\lambda(t) = \alpha_1 - w_E (t-t_o) \tag{4e}$$

A fourth coordinate system is the level ground coordinate which is a rotation of the local level system about the north pointing axis through 180^o (see Fig. 2b). Thus, x_{1G} is north, x_{2G} is east, and x_{3G} is down. We have

$$T_{IG} = T(\alpha_1, \hat{x}_1)\ T(\delta, \hat{x}_2)\ T(\pi, \hat{x}_1) \tag{5}$$

To find the aircraft track angle we first obtain the relative velocity vector with respect to the Earth, $\dot{R}_{REL}$, expressed in the inertial frame and then rotate this relative velocity vector into the local ground system.

$$\{\dot{R}_G\} = (T_{GI})\{\dot{R}_{REL}\} \tag{6a}$$

where $\dot{R}_{REL} = \dot{R}_I - w_E \hat{i} \times R_I$

Finally,

$$\psi_T = \tan^{-1}\left(\frac{\dot{R}_G(1)}{\dot{R}_G(2)}\right) \tag{6b}$$

The aircraft altitude rate, $\dot{h}$, with respect to the ground is given by

$$\dot{h} = -\dot{R}_G(3) \tag{6c}$$

Similarly for the vertical acceleration in the local ground system we have

$$\{\ddot{R}_G\} = T_{GI}\{\ddot{R}_{REL}\} \tag{7a}$$

where $\ddot{R}_{REL} = \ddot{R}_I - w_E^2 R_I$

and $\ddot{h} = -\ddot{R}_G(3)$ (7b)

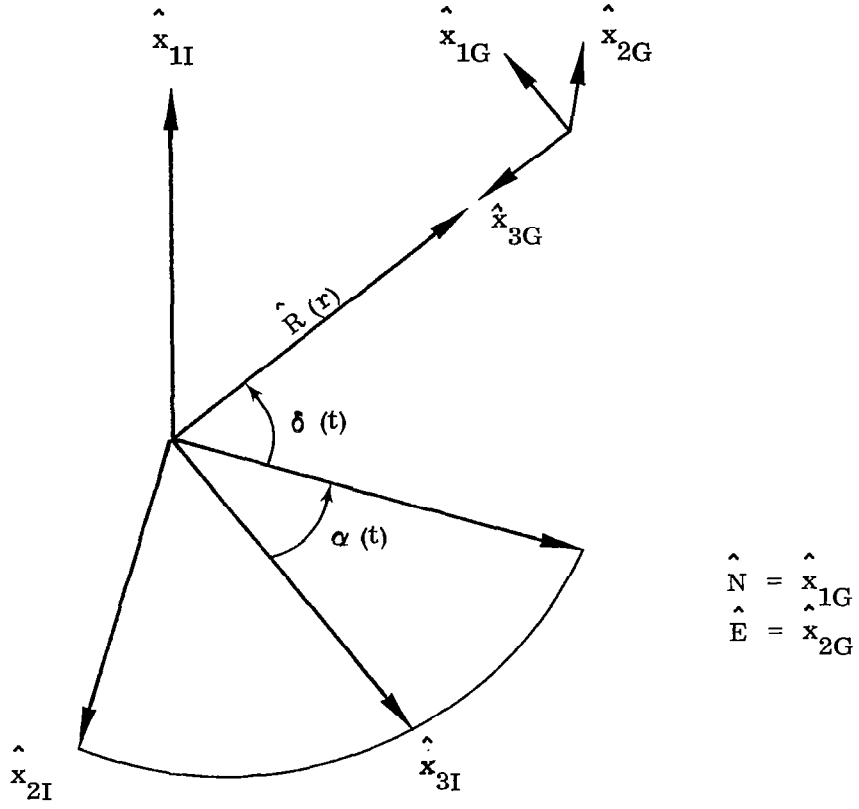

(b) Local Ground Coordinate System

Figure 2. - Concluded

The aircraft altitude is given by

$$h = \sqrt{x_{1I}^2 + x_{2I}^2 + x_{3I}^2} - r_E \tag{8}$$

The final coordinate system used in the guidance equations is the body system. The x_{1B} coordinate is along the fuselage pointing forward, the x_{3B} coordinate vertically down toward the level ground, and the x_{2B} coordinate is positive out along the right wing forming a right hand system. See Fig. 3. The transformation from body axis to inertial is given by

$$T_{IB} = T_{IG}\, T(\psi, \hat{x}_3)\, T(\theta, \hat{x}_2)\, T(\varphi, \hat{x}_1) \tag{9}$$

(b) RNAV Guidance Parameters

The desired path is divided into segments. Each leg is either a straight line (great circle) terminating at the intersection with an arc of a circle, or a portion of a circular turn terminating at either the second half of the same circular turn or at the intersection with a straight line (great circle). The end of each leg is defined by a fixed vector waypoint whose coordinates are generated in the fixed Earth coordinate system in Appendix B. Along each segment we are required to generate the following RNAV parameters required for guidance:

(1) Cross track error
(2) Track angle error
(3) Distance to go to the end of the leg
(4) Time to go to the end of the leg
(5) Desired altitude and altitude rate
(6) Desired airspeed
(7) Desired flight path angle
(8) Desired bank angle in the turn

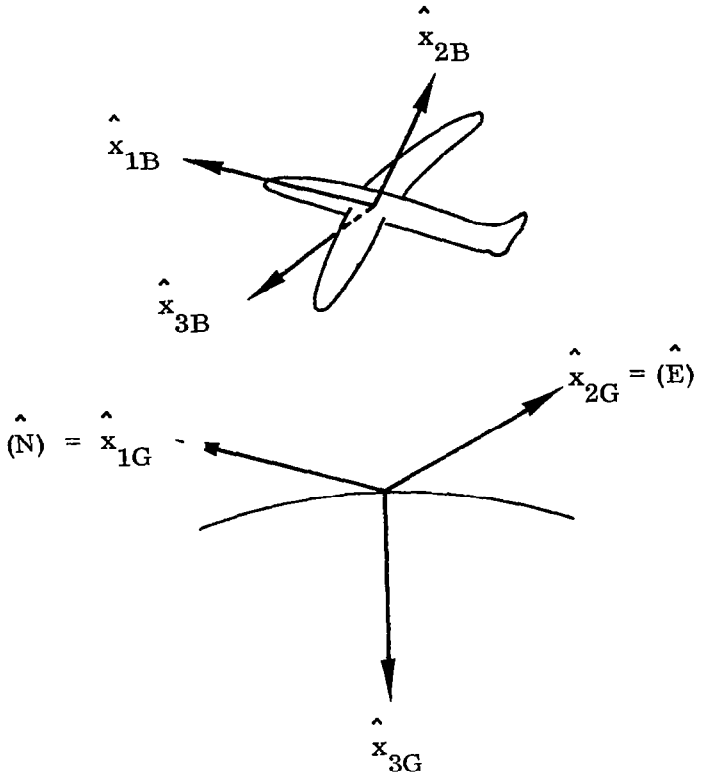

Figure 3(a).- Body Coordinate System Relative To Level Ground

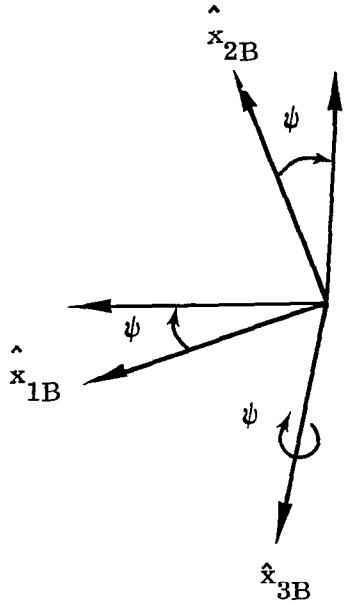

(b) ψ Rotation About $\hat{x}_{3B}$

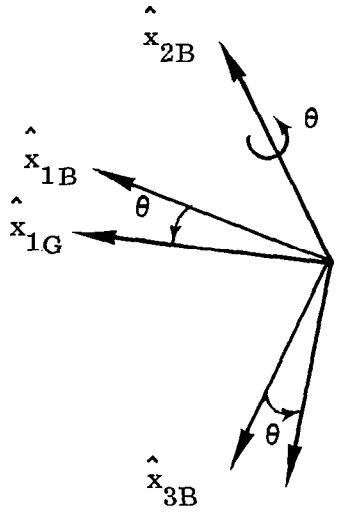

(c) θ Rotation About Rotated $\hat{x}_{2B}$

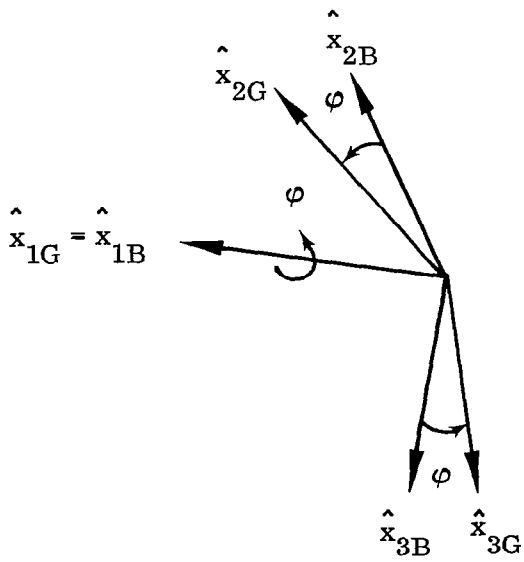

(d) φ Rotation About Rotated $\hat{x}_{1B}$

Figure 3. - Concluded

The equations for these quantities are different on a straight line than they are along a circular turn. The equations will be derived separately for each segment type. We may assume that we have available from the Inertial Navigation Unit the position, velocity and acceleration vectors in the inertial coordinate system.

(1) Great Circle Guidance Parameters

The desired position on a great circle, $\hat{WD}$, lies in a plane which contains the unit radius vector to the aircraft, $\hat{R}_E$, and the normal to the plane containing the great circle, $\hat{WN}$. $\hat{WN}$ is generated for each great circle by means of the equations given in Appendix B. Since every line in a plane is perpendicular to the normal of that plane, it follows that

$$\hat{WD} = \frac{1}{\cos\beta}\,\hat{R}_E + \frac{\sin\beta}{\cos\beta}\,\hat{WN} \tag{10a}$$

where

$$\sin\beta = -\hat{WN} \cdot \hat{R}_E = -\cos(\pi/2 + \beta) \tag{10b}$$

$$\cos\beta = \sqrt{1 - \sin^2\beta}$$

See Fig. 4.

The cross track error is given in terms of the angle between $\hat{R}_E$ and $\hat{WD}$. Since the normal, $\hat{WN}$, is perpendicular to $\hat{WD}$, we have

$$CRTE = -r_E \sin^{-1}(\hat{R}_E \cdot \hat{WN}) \tag{11}$$

The distance to go to the end of the segment is given in terms of the angle between $\hat{WD}$ and the waypoint at the terminus of the great circle segment, $\hat{PI}(J)$, which is computed in Appendix B.

$$DISTGO = r_E \sin^{-1}(|\,\hat{WD} \times PI(J)\,|) \tag{12}$$

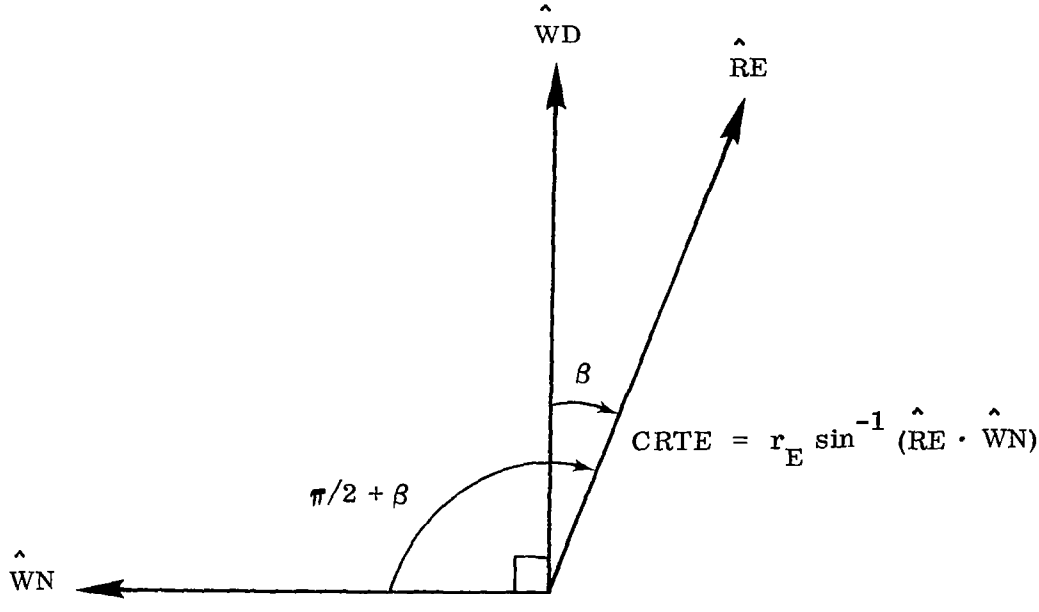

Figure 4.- Cross Track Error Along A Great Circle Segment

To obtain the desired heading along the ground track at the desired path position vector, $\hat{WD}$, we note that the unit vector, $\hat{WD}$, is perpendicular to the plane which contains the unit north vector, $\hat{N}$, the unit west vector, $\hat{W}$, and the unit normal, $\hat{WN}$. (See Fig. 5).

The desired heading, ψ_D , is the negative of the angle through which we must rotate the unit normal vector, $\hat{WN}$, about the desired unit position vector, $\hat{WD}$, to have it coincide with the unit west vector $\hat{W}$. Thus

$$\hat{W} = \cos\psi_D \, \hat{WN} - \sin\psi_D \, \hat{WD} \times \hat{WN} \tag{13a}$$

It follows that

$$\psi_D = \tan^{-1} \frac{\hat{WN} \cdot \hat{N}}{\hat{WN} \cdot \hat{W}} \tag{13b}$$

The track angle error is defined as $\psi_T - \psi_D$. Since this angle is small it is more accurate to use the tangent of the difference of the two angles rather than take the difference of two arc tangents. We have

$$TAGE = \tan^{-1} \frac{\tan\psi_T - \tan\psi_D}{1 + \tan\psi_T \tan\psi_D} \tag{14a}$$

The recommended equation is given by

$$TAGE = \tan^{-1} \left(\frac{\dot{R}_G(2) \, (\hat{WN} \cdot W) - \dot{R}_G(1) \, (\hat{WN} \cdot N)}{\dot{R}_G(1) \, (\hat{WN} \cdot W) + \dot{R}_G(2) \, (\hat{WN} \cdot N)} \right) \tag{14b}$$

To obtain the time to go to the end point of the great circle segment we divide the distance to go by the ground speed and obtain

$$TMTGO = DISTGO/VG \tag{15a}$$

where

$$VG = \left(\dot{R}_G^{\,2}(1) + \dot{R}_G^{\,2}(2) \right)^{\frac{1}{2}} \tag{15b}$$

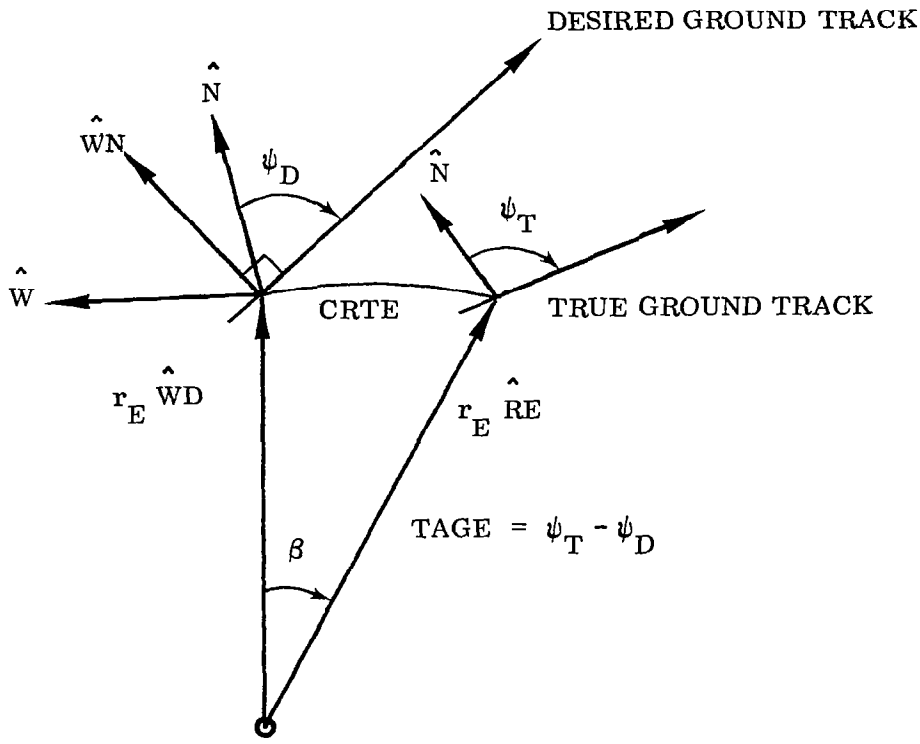

Figure 5. - Track Angle Error Along A Great Circle Segment

The RNAV equations for desired height, HC , the desired altitude rate, HDC , and the desired airspeed are given by

$$HC(t) = HEND - GRAD \cdot DISTGO(t) \tag{16a}$$

$$HDC(t) = VG(t) \cdot \tan(GRAD) \tag{16b}$$

$$VDESIR(t) = VGE - DVG \cdot DISTGO(t) \tag{16c}$$

where,

HEND is the desired height at the end point of the segment and is computed in Appendix B

GRAD is the desired altitude gradient and is computed in Appendix B

DVG is the desired airspeed gradient (change in airspeed per unit of ground track distance) and is computed in Appendix B.

VGE is the desired airspeed at the end of the segment aircraft is tracking.

The bank angle command for the great circle is zero since we desire a straight line path,

$$BANK = 0. \tag{17a}$$

In order to provide lead time to execute the bank command at the onset of the turn, the bank command is switched to the value it would have in the turn, namely,

$$BANK = \text{sign}(\Delta\psi) \tan^{-1}\left(VG^2 / R_T / G\right) \tag{17b}$$

as soon as the time to go to the end of the great circle is less than the bank command divided by the maximum bank rate, $\dot{\Phi}_{MAX}$. We switch from Eq. (17a) to Eq. (17b) whenever

$$TMTGO \leq \tan^{-1}\left(VG^2 / R_T / G\right) / \dot{\Phi}_{MAX} \tag{17c}$$

where

R_T is the turn radius of the oncoming turn, and G is the constant of gravity.

and

$\Delta\psi$ is the change in heading to be executed by the turn. $\Delta\psi$ and its sign are computed in Appendix B.

(2) Guidance Parameters in the Turn

The logic for defining the unit desired vector, $\hat{W}D$, on the turn circle and the unit normal to the path at the turn circle, $\hat{W}N$, is based on the concept that they both lie in the plane defined by the unit aircraft position vector, $\hat{R}_E$, and the unit center of the turn vector, $\hat{C}R$. See Fig. 6. The vector equation for $\hat{W}D$ and $\hat{W}N$ are given by

$$\hat{W}D = \frac{1}{\sin\beta}\left(\sin\alpha\ \hat{R}E - \sin(\alpha-\beta)\ \hat{C}R\right) \tag{18a}$$

and

$$\hat{W}N = -\frac{\text{sign}(\Delta\psi)}{\sin\beta}\left(-\cos\alpha\ \hat{R}E + \cos(\alpha-\beta)\ \hat{C}R\right) \tag{18b}$$

where

$$\alpha = \frac{R_T}{r_E}$$

and (18c)

$$\beta = \sin^{-1}\left|\hat{R}E \times \hat{C}R\right|$$

Having obtained the desired unit vector position on the turn and the normal to the desired path, the equations for the guidance parameters for the cross track error, CTRE, and the track angle error, TAGE, are identical to those given in Eq's. (11) and (14b).

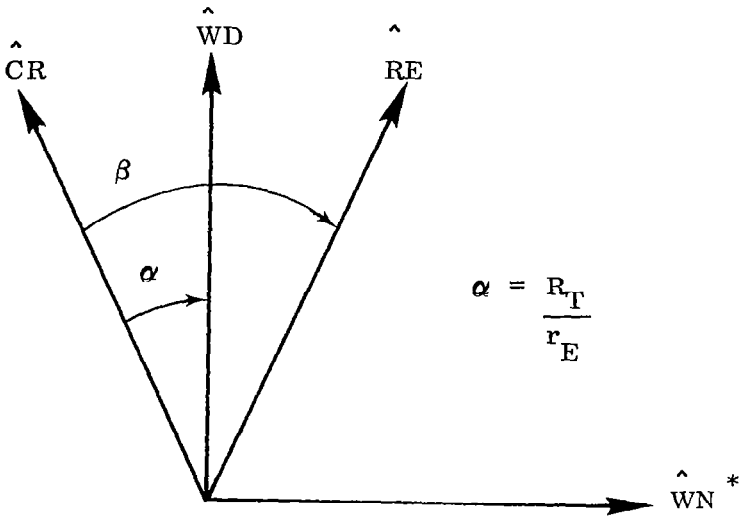

*If sign ($\Delta\psi$) is negative, $\hat{WN}$ points inward toward $\hat{CR}$

Figure 6. -Normal, Desired Position, and Center of Turn Circle Along a Turn Segment

The distance to go equation to the end of the turn segment differs from the straight line DISTGO in two respects. First the ground track length of the turn is the arc of a circle whose radius is R_T and not r_E; second, the turn is divided into two segments in order to provide a mechanism for introducing changes in the altitude and airspeed gradients which may occur at the midpoint of the turn.

To solve for the distance to go on a turn we compute the angle between the unit normal at $\hat{WD}$ and the unit normal at the end of the circular segment, $\hat{WNE}$. The normal at the end of the segment is computed in Appendix B. We have

$$\theta = \sin^{-1}\left(\left|\hat{WN} \times \hat{WNE}\right|\right) \tag{19a}$$

where WNE is the normal at the end of the circular segment

Since the $\sin\theta = \sin(\pi - \theta)$ we must test to see if $\theta \gtrless \pi/2$. To accomplish this we compute

$$\cos\theta = \hat{WN} \cdot \hat{WNE} \tag{19b}$$

If $\cos\theta$ is negative, we set

$$\theta = \pi - \sin^{-1}\left(\left|\hat{WN} \times \hat{WNE}\right|\right) \tag{19c}$$

The final result yields

$$DISTGO = R_T \cdot \theta \tag{20}$$

The equations for the time to the end of the segment, TMTGO , HC(t), HDC(t) and VDESIR(t) are all computed in a manner identical to Eq's. (15a), (15b), (16a), (16b), and (16c).

The bank angle command logic along the turn is given by

$$\text{BANK} = \text{sign}(\Delta\psi)\tan^{-1}\left(VG^2/G/R_T\right) \tag{21}$$

The lead command for anticipated return to the straight line is exercised only at the end of the second half of the turn. The bank angle command is continuous across the middle of the turn. Toward the end of the second half turn we test to see if the time to go is less than the time to return the bank angle to zero at the maximum bank rate. Whenever

$$\text{TMTGO} \leq \tan^{-1}\left(VG^2/R_T/G\right)/\dot{\Phi}_{MAX} \tag{22}$$

we switch the bank command from Eq. (21) to BANK = 0.

(3) Switching Logic

The segments are arranged in groups of three. A great circle followed by a half turn, followed by another half turn. Only the final leg terminating at a touchdown waypoint is treated separately. Each leg is numbered in sequence with the first leg initialized as segment number 1. This is always a straight line segment. The guidance information common to a given segment, such as the unit end waypoint, the desired height, airspeed and gradient, etc. are stored in an array for that segment. These data are computed once for the entire flight following the equations outlined in Appendix B.

If the segment number, modulo 3, is 1 we are on a great circle straight line segment and enter the data block for active guidance computations for a great circle arc. This arc is terminated whenever

$$\text{TMTGO} < .075 \text{ seconds} \tag{23}$$

A logical trigger defining a great circle arc as being TRUE is set to FALSE and remains FALSE until the segment number, modulo 3, is equal to 0. The segment number is advanced by unity at the end of each segment and the block storage for the segment parameters is brought into the active guidance loop.

On the final leg a test is made on the last segment number and if the leg segment is equal to the last integer no further call to the block storage is made.

II. NAVIGATION AND FILTERING FOR WAYPOINT GUIDANCE

(a) The Estimate of the Inertial State

The aircraft is equipped with an inertial navigation system (INS) consisting of body mounted accelerometers for measuring the specific forces acting on the aircraft, plus a stabilized platform containing rate gyros for integration of the aircraft attitude and attitude rates. In the absence of instrument errors the inertial position and velocity may be obtained by integrating the inertial equations of motion

$$\frac{d^2}{dt^2}\{R_I\} = -\frac{\mu}{r_I^3}\{R_I\} + T_{IB}\{f_{SFB}\} \tag{24a}$$

where

$$\mu = G r_E^2 \tag{24b}$$

$$r_I = |R_I| \tag{24c}$$

$$T_{IB} = T(\alpha_1, \hat{x}_1)\, T(\alpha_2, \hat{x}_2)\, T(\pi, \hat{x}_1)\, T(\psi, \hat{x}_3)\, T(\theta, \hat{x}_2)\, T(\varphi, \hat{x}_1) \tag{24d}$$

$\{f_{SFB}\}$ is the specific force vector in the body system as computed by the IMU from the output of the body mounted accelerometers, $\{a_{cc}\}$,

$$r_I = |R_I|$$

$$\{f_{SFB}\} = \{a_{cc}\} \tag{24e}$$

$$\alpha_1 = \tan^{-1}\left(-R_I(2) \Big/ R_I(3)\right) \tag{24f}$$

$$\alpha_2 = \sin^{-1}\left(R_I(1) \Big/ r_I\right)$$

$$\hat{x}_1 = \begin{Bmatrix} 1 \\ 0 \\ 0 \end{Bmatrix}$$

$$\hat{x}_2 = \begin{Bmatrix} 0 \\ 1 \\ 0 \end{Bmatrix} \qquad (24g)$$

$$\hat{x}_3 = \begin{Bmatrix} 0 \\ 0 \\ 1 \end{Bmatrix}$$

The Euler angles φ , θ , and ψ are computed by the IMU system from the output of the rate gyros mounted on the stable platform.

Since the rate gyros are subject to drift, the accelerometers contain biases and all the measurements are noisy, it is required to design an estimator to filter out the noise and obtain the best estimate of the aircraft state and the instrument biases. In addition, external navaids are required, such as VORTAC range and bearing as well as an aircraft barometer during the non-critical flight phase. For the critical terminal area, MLS range, azimuth, and elevation are used. These navaids are themselves subject to instrument biases.

(b) Filter State Estimators

Two estimators are described here. First, an optimal Kalman filter and second, a fixed gain complementary filter. Both are used in the study in a manner that permits the aircraft guidance equations to utilize the output of one filter with the non-controlling filter operating only in its estimating mode. In this manner both filters provide state estimates for comparison with the true state, and both filters can be compared as guidance state estimators as well.

The two filters are designed to operate in a local flat Earth coordinate frame with the origin set at the navaid site. Thus when the VORTAC mode is in operation, the coordinate system for the error state estimate has its origin at the VORTAC station site

$\hat{x}_{1v}$ is due north

$\hat{x}_{2v}$ is due east

$\hat{x}_{3v}$ is down toward the Earth center

The coordinates of the VORTAC station in the inertial system are given in terms of the station longitude, latitude, and altitude, h_V,

$$\{ R_{IV}(t) \} = T_{IE} \begin{Bmatrix} \sin \delta_V \\ -\sin \lambda_V \cos \delta_V \\ \cos \lambda_V \cos \delta_V \end{Bmatrix} (r_E + h_V) \tag{25}$$

To obtain the local flat Earth coordinates of the aircraft with respect to the VORTAC station, we have

$$\{ R_{FV} \} = T_{FI} \{ R_I - R_{IV} \} \tag{26a}$$

where

$$T_{FI} = T(-\pi, \hat{x}_1)\, T(-\alpha_2, \hat{x}_2)\, T(-\alpha_1, \hat{x}_1) \tag{26b}$$

$$\alpha_1 = w_E (t - t_o) + \lambda_V \tag{26c}$$

$$\alpha_2 = \delta_V \tag{26d}$$

(See Fig. 7)

In the case of the MLS landing site, the local flat Earth coordinate system is oriented so that $\hat{x}_1$ is aligned with the runway and the origin is located at the center line of the runway as shown in Fig. 8.

The inertial coordinates of the runway origin are given by

$$\{ R_{IR}(t) \} = T_{IE} \begin{Bmatrix} \sin \delta_R \\ -\sin \lambda_R \cos \delta_R \\ \cos \lambda_R \cos \delta_R \end{Bmatrix} (r_E + h_R) \tag{27}$$

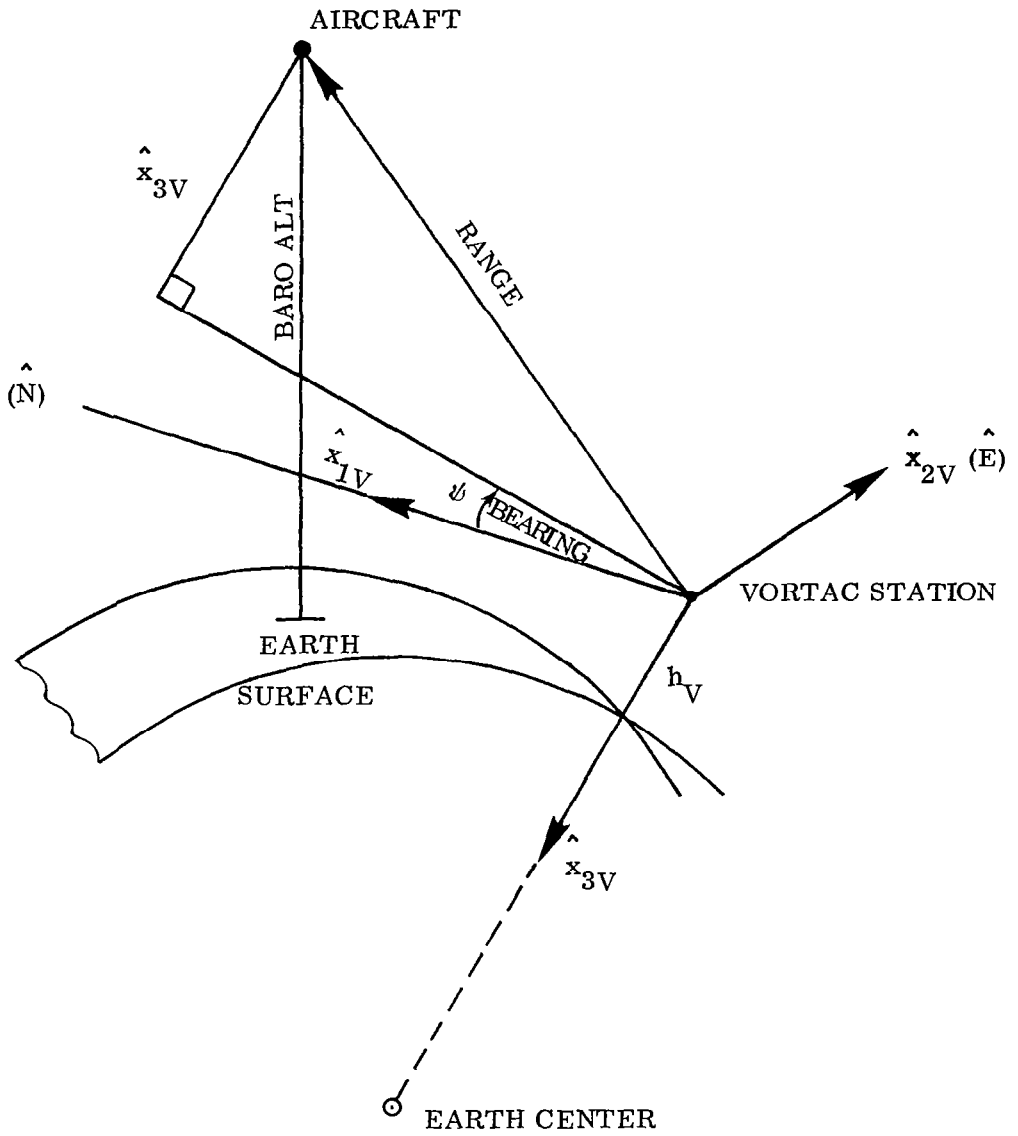

Figure 7.- VORTAC Flat Earth Coordinate System

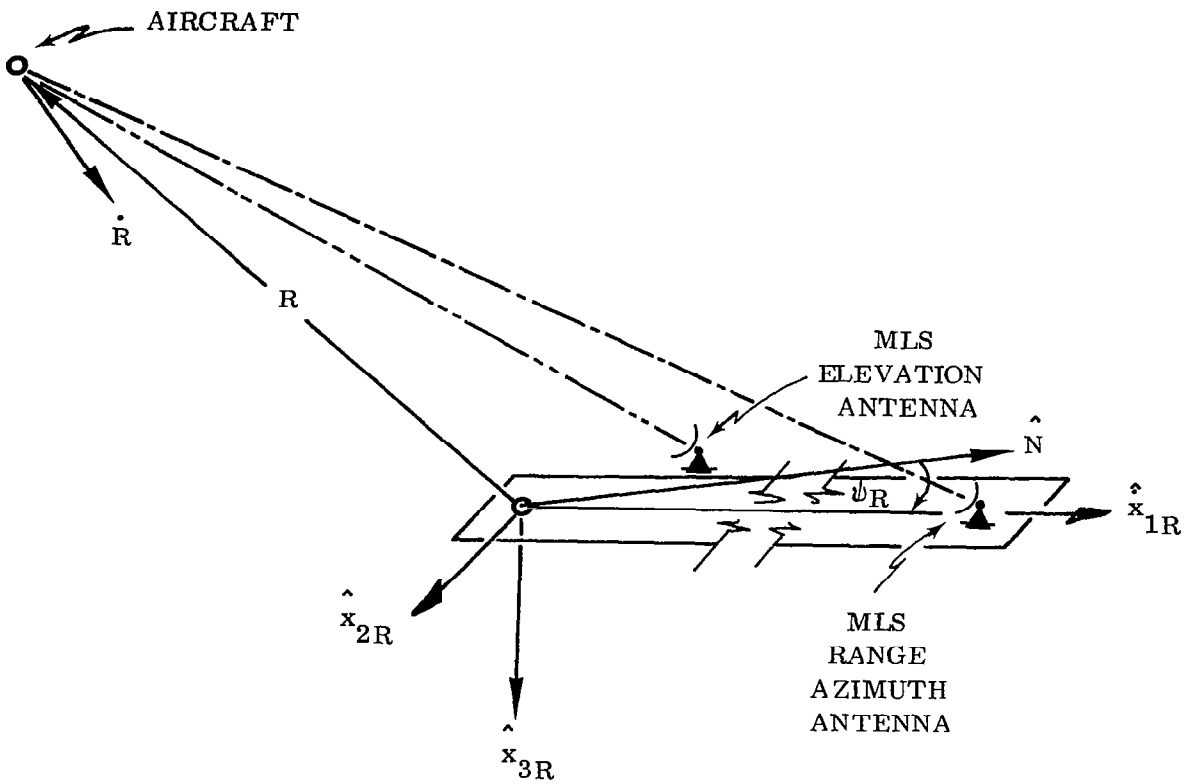

Figure 8. -Runway Flat Earth Coordinate System

To obtain the local flat Earth coordinates of the aircraft in the runway system, we have

$$\{ R_{FR} \} = T_{FI} \{ R_I - R_{IR} \} \tag{28a}$$

where

$$T_{FI} = T(-\psi_R, \hat{x}_3) T (-\pi, \hat{x}_1) T (-\alpha_2, \hat{x}_2) T (-\alpha_1, \hat{x}_1) \tag{28b}$$

$$\begin{aligned} \psi_R &= \text{runway azimuth measured from true north} \\ \alpha_1 &= w_E(t - t_o) + \lambda_R \\ \alpha_2 &= \delta_R \end{aligned} \tag{28c}$$

The Kalman error state is a 15 element vector consisting of

$\tilde{R}$	error in the estimate of the aircraft position vector in the flat Earth coordinate system
$\dot{\tilde{R}}$	error in the aircraft estimate of the aircraft velocity vector in the local flat Earth system
$\tilde{p}$, $\tilde{q}$, $\tilde{r}$	error in the estimate of gyro drift rates
w_x , w_y	error in the estimates of horizontal components of the local wind
b_1 , b_2 , b_3	errors in the estimate of the navaid instrument biases
b_4	error in the estimate of vertical acceleration due to instrument bias.

When the VORTAC navaids are operative, we have

b_1	=	bias in DME (range)
b_2	=	bias in bearing
b_3	=	bias in the baro reading of pressure altitude

When the MLS navaids are operative, we have

b_1 = bias in azimuth

b_2 = bias in elevation

b_3 = bias in range (DME)

Immediately prior to landing, at an altitude of 50 meters, the elevation reading is replaced by a vertical radar and b_2 is the estimate in the bias of radar altitude.

The filter equations for the Kalman optimal estimator for a flat Earth coordinate system are described in Ref. 1 and are not repeated here.

The error state for the fixed gain complementary filter consists of the following:

$\tilde{R}$ Three components in the error of the position vector in the flat Earth coordinate system

$\dot{\tilde{R}}$ Three components in the error of the velocity vector in the flat Earth coordinate system

$\ddot{\tilde{R}}$ Three components in the error of the estimate of acceleration in the flat Earth coordinate system

$\tilde{w}_x, \tilde{w}_y$ errors in the estimates of the horizontal components of the winds

Thus the complementary filter is a nine state filter for the aircraft position, velocity, and acceleration. This is amply described in Ref. 1 and is not repeated here. The derivation of the complementary filter in discrete explicit form is derived in Appendix C since the derivation was not included in Ref. 1.

The navigation equations for the two filters are different and are described herein.

(1) Kalman Navigation Equations

When using the optimal Kalman filter, the navigation system estimates the expected bias errors in the gyro drifts. These are converted into corrections in the Euler angles and added to the output of the IMU estimate of the Euler angles as described in Ref. 1.

$$\begin{aligned} \hat{\varphi} &= \varphi_{IMU} + \Delta\varphi \\ \hat{\theta} &= \theta_{IMU} + \Delta\theta \\ \hat{\psi} &= \psi_{IMU} + \Delta\psi \end{aligned} \tag{29}$$

The Kalman filter also estimates the bias error in the vertical accelerometer. This is treated as a correction to the estimate of the vertical specific force in the body system.

$$\hat{f}_{SFB}(3) = f_{SFB}(3) - b_4 \tag{30a}$$

and

$$\hat{f}_{SFB}(1) = f_{SFB}(1) \tag{30b}$$

$$\hat{f}_{SFB}(2) = f_{SFB}(2) \tag{30c}$$

The Kalman navigation equations integrate Eq. (24a) in the inertial reference frame using an Euler integration formula.

$$\{ \hat{\dot{R}}_2(t) \} = \{ \hat{\dot{R}}_I(t - \Delta t) \} + \frac{\Delta t}{2} \{ \hat{\ddot{R}}_I(t) + \hat{\ddot{R}}_I(t - \Delta t) \} \tag{31a}$$

where

$$\{ \ddot{\hat{R}}_I (t) \} = - \frac{\mu}{\hat{r}_I(t-\Delta t)} \{ \hat{R}_I (t - \Delta t) \} + T_{IB} \{ \hat{f}_{SFB} \} \tag{31b}$$

and the angles used in computing the transformation T_{IB} are

$$\alpha_1 = \tan^{-1} \left(- \hat{R}_{I2}(t - \Delta t) / \hat{R}_{I3} (t - \Delta t) \right)$$

$$\alpha_2 = \sin^{-1} \left(\hat{R}_{I1} (t - \Delta t) / \hat{r}_I (t - \Delta t) \right)$$

$$\psi = \hat{\psi} (t) \tag{31c}$$

$$\theta = \hat{\theta} (t)$$

$$\varphi = \hat{\varphi} (t)$$

The Kalman filter velocity correction is "eased in" in an exponential manner so as not to present the control command with abrupt discontinuities as described in Ref. 1.

$$\{ \dot{\hat{R}}_I (t) \} = \{ \dot{\hat{R}}_I (t) \} + e^{- \frac{t-t_k}{t_k}} \left(T_{IF} \{ \dot{\tilde{R}} (t_k) \} \right) \tag{32}$$

where the angles used in computing the transformation T_{IF}, are given by Eq's. (26b) - (26d) or Eq's. (28b), (28c) depending on the station coordinates.

The time, t_k, is the last Kalman update time prior to the present time, t. The Kalman filter equations are processed only once every 10 normal time steps as described in Ref. 1.

The integration of the velocity in the inertial reference frame to obtain the position vector is accomplished in a similar fashion.

$$\{ \hat{R}_I (t) \} = \{ \hat{R}_I (t) \} + \frac{\Delta t}{2} \{ \dot{\hat{R}}_I (t) + \dot{\hat{R}}_I (t - \Delta t) \} \tag{33}$$

The Kalman correction to the position is given by

$$\{ \hat{R}_I(t) \} = \{ \hat{R}_I(t) \} + e^{-\frac{t-t_k}{t_k}} \left\{ T_{IF} \{ \tilde{R}(t_k) \} \right\} \tag{34}$$

The best estimate of the inertial state is presented to the RNAV Guidance and Display routines. A block diagram of the Kalman filter navigation logic is shown in Fig. 9.

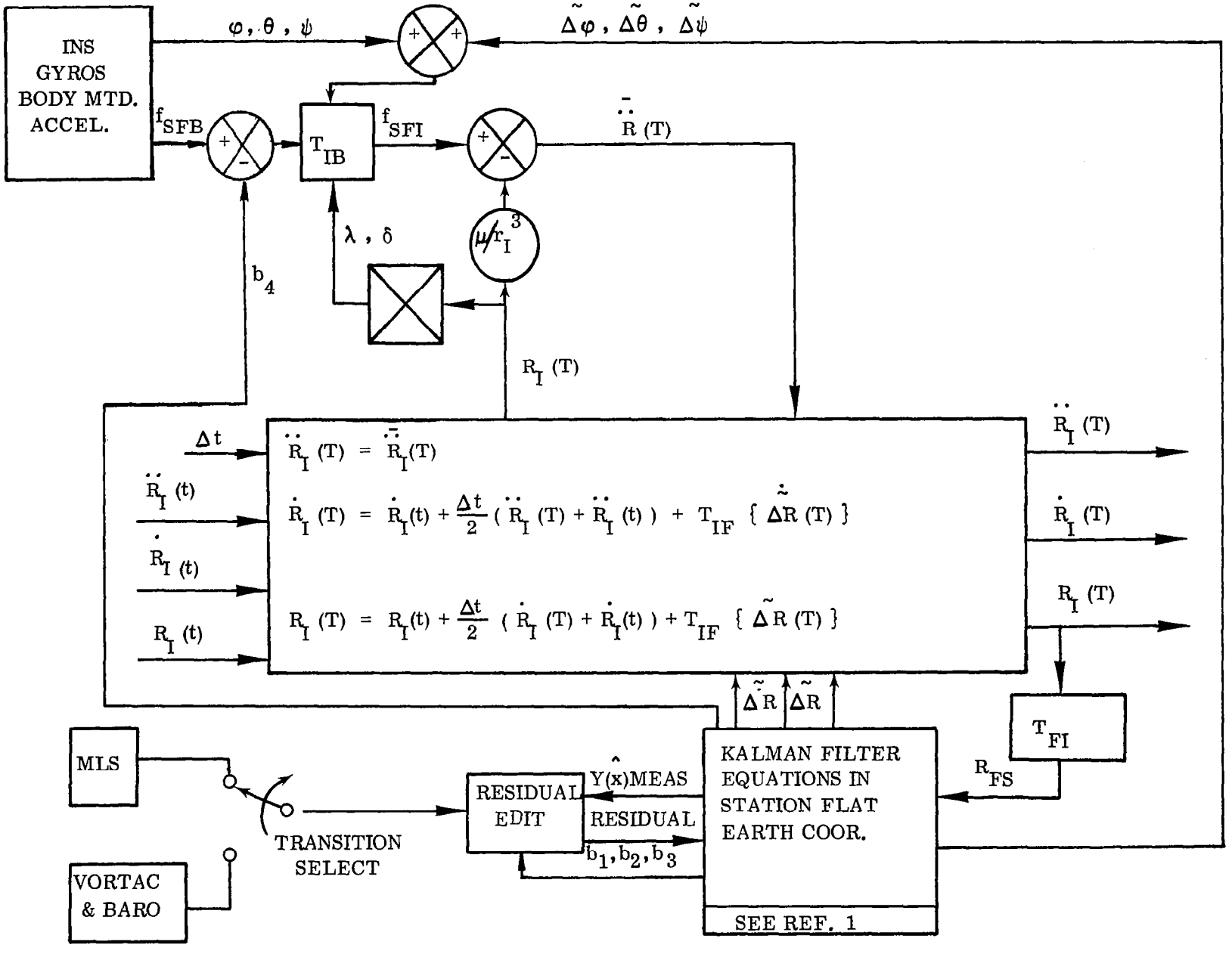

Figure 9.—Navigation Equations for Kalman Filter

(2) Complementary Filter Navigation Equations

The complementary filter navigation equations are described in Appendix C. A prediction of the aircraft position in inertial coordinates is made using the assumption that the acceleration is constant over the start time interval, Δt. The Euler angles, φ, θ and ψ are accepted without correction directly from the IMU. We have

$$\{ \ddot{\hat{R}}_I(t) \} = - \frac{\mu}{r_I^3(t-\Delta t)} \{ \hat{R}_I(t-\Delta t) \} + T_{IB} \{ f_{SFB}(t) \} + T_{IF} \{ \ddot{\tilde{R}}(t-\Delta t) \} \quad (35a)$$

the angles used in computing when the transformation T_{IB} are

$$\alpha_1 = \tan^{-1} \left(- \hat{R}_{I2}(t - \Delta t) / \hat{R}_{I3}(t - \Delta t) \right)$$

$$\alpha_2 = \sin^{-1} \left(R_{I1}(t - \Delta t) / \hat{r}_I(t - \Delta t) \right) \quad (35b)$$

φ, θ and ψ

and angles for computing the transformation T_{IF} are either Eq's. (26b) - (26d), or Eq's. (28b), (28c) depending on the station coordinates. The vector $\{ \ddot{\tilde{R}}(t - \Delta t) \}$ is the previous estimate of the acceleration random error variable from the complementary filter.

To obtain the uncorrected velocity and position in inertial coordinates, we have

$$\{ \dot{\hat{R}}_I(t) \} = \{ \dot{\hat{R}}_I(t-\Delta t) \} + \Delta t \{ \ddot{\hat{R}}_I(t) \} \quad (36)$$

$$\{ \hat{R}_I(t) \} = \{ \hat{R}_I(t - \Delta t) \} + \Delta t \{ \dot{\hat{R}}_I(t - \Delta t) \} + \frac{(\Delta t)^2}{2} \{ \ddot{\hat{R}}_I(t) \} \quad (37)$$

The complementary filter prediction of the pseudo observation used in the complementary filter is the position of the aircraft relative to the navaid site in the flat Earth coordinate system given by either Eq. (26a) or Eq. (28a).

We have

$$\{ \hat{R}_{FS} \} = T_{FI} \{ \hat{R}_{I}(t) - R_{IS}(t) \} \tag{38}$$

when $\{ R_{IS}(t) \}$ is the inertial position vector of the navaid site.

The computation of the pseudo observation of the relative position in terms of VORTAC range, r_v, VORTAC bearing ψ_v, and baro altitude, z_v, is given by

$$\bar{R}_{FS}(1) = r_v \cos(\psi_v) \tag{39a}$$

$$\bar{R}_{FS}(2) = r_v \sin(\psi_v) \tag{39b}$$

$$\bar{R}_{FS}(3) = -z_v + (r_v^2 - z_v^2)/2\, r_E + h_v \tag{39c}$$

Eq. (39c) yields the height above the plane, tangent to the Earth at navaid site as a function of the altitude above the spherical Earth and the range to the navaid site.

The computation of the pseudo observation in terms of the MLS range, r_{MLS}, the MLS azimuth, α_{MLS}, and elevation, δ_{MLS} is given in Ref. 1.

The complementary filter estimates of the errors in position, velocity, and accelerations are

$$\tilde{R}_{FS}(t) = (G_1 - 1) \{ \hat{R}_{FS}(t) - \bar{R}_{FS}(t) \} \tag{40a}$$

$$\tilde{\dot{R}}_{FS}(t) = G_2 \{ \hat{R}_{FS}(t) - \bar{R}_{FS}(t) \} \tag{40b}$$

$$\tilde{\ddot{R}}_{FS}(t) = \tilde{\ddot{R}}_{FS}(t - \Delta t) + G_3 \{ \hat{R}_{FS}(t) - \bar{R}_{FS}(t) \} \tag{40c}$$

The best estimate of the relative state is given by

$$\begin{aligned} \{\hat{R}_{FS}(t)\} &= \{\hat{R}_{FS}(t)\} + \{\tilde{R}_{FS}(t)\} \\ \{\hat{\dot{R}}_{FS}(t)\} &= \{\hat{\dot{R}}_{FS}(t)\} + \{\tilde{\dot{R}}_{FS}(t)\} \end{aligned} \tag{41}$$

To obtain the inertial state required for guidance and display routines, we have

$$\{\hat{R}_I(t)\} = T_{IF}\{\hat{R}_{FS}(t)\} + \{R_{IS}(t)\} \tag{42a}$$

$$\{\hat{\dot{R}}_I(t)\} = T_{IF}\{\hat{\dot{R}}_{FS}(t)\} + w_E\{x_1\} \times \{\hat{R}_I(t)\} \tag{42b}$$

$$\{\hat{\ddot{R}}_I(t)\} = \frac{\mu}{r_I^3(t)}\{\hat{R}_I(t)\} + T_{IB}\{f_{SFB}(t)\} + T_{IF}\{\tilde{\ddot{R}}_{ES}(t)\} \tag{42c}$$

A block diagram of the complementary filter navigation logic is presented in Fig. 10.

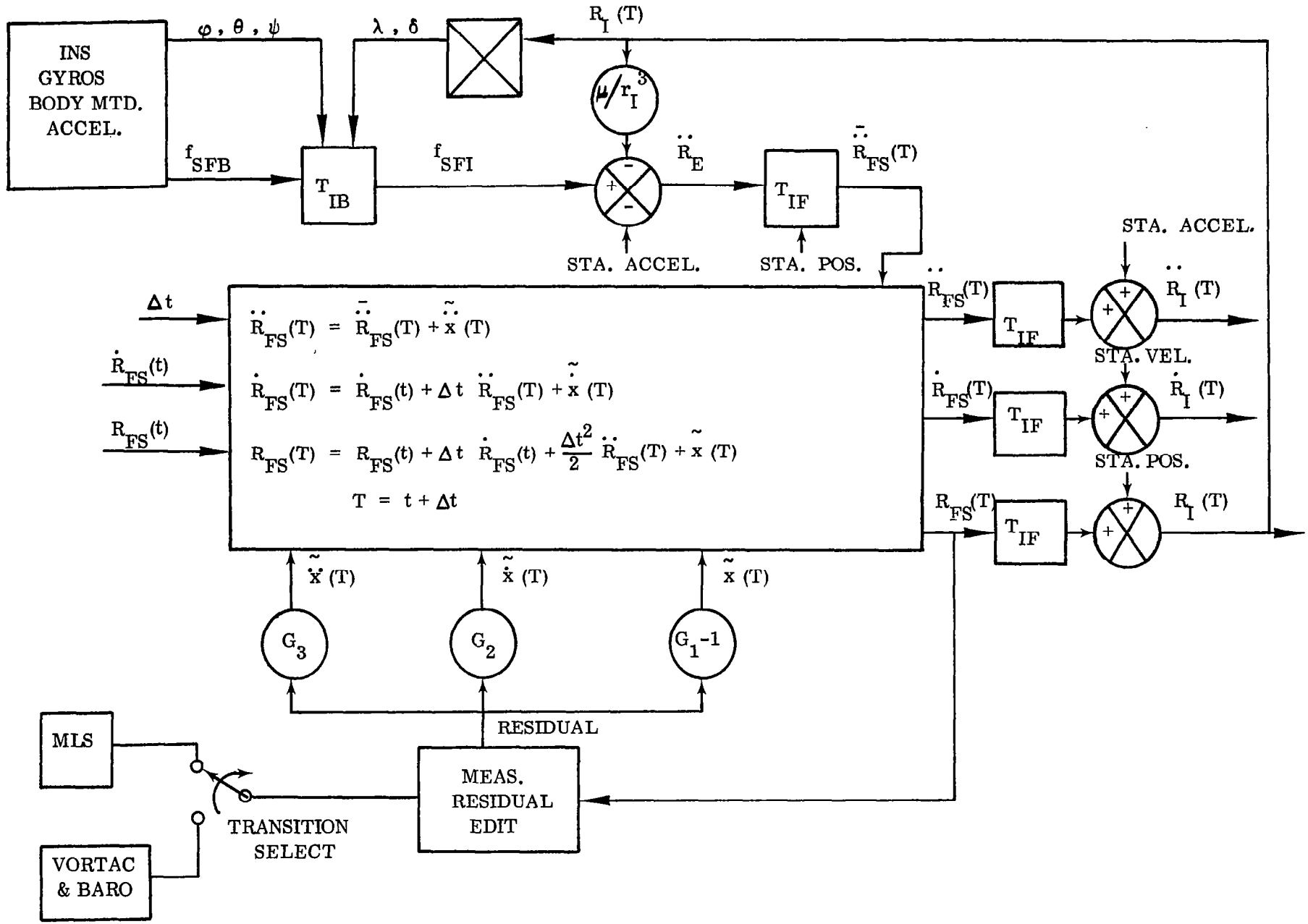

Figure 10.– Navigation Equations for Complementary Filter

III. NAVIGATION AND GUIDANCE AT THE TRANSITION POINT

(a) Filter Update at Transition

Both the optimal Kalman filter and the fixed gain complementary filter require a settling time period when presented with an abrupt change in navaid observation type. As previously discussed, during the transition from VORTAC to the more accurate MLS data, the prediction of the MLS observations, based on the estimates of the aircraft position derived from VORTAC measurements, result in a large residual. In order to avoid undesirable effects of this perturbation, it is most convenient to reinitialize the aircraft estimate of its position from the first valid MLS observation set. The equations necessary to accomplish the change are presented for both filters.

(1) Kalman Filter Update at Transition

Let the coordinates of the range and azimuth antenna, in runway flat Earth coordinates be, $\{ R_{AZ} \}$, and let the coordinates of the elevation antenna relative to the azimuth antenna be $\{ R_{EL} \}$. The position of the aircraft in the runway flat Earth coordinate system computed from the MLS range, r_M, the MLS azimuth, α_M, and the MLS elevation, β_M, is given by

$$\{R_{FS}\} = \{R_{AZ}\} - \begin{Bmatrix} x_{1M} \\ -x_{2M} \\ x_{3M} \end{Bmatrix} \tag{43a}$$

where

$$\begin{aligned}
x_{1M} &= a_1 + (a_1^2 - a_2)^{\frac{1}{2}} \\
x_{2M} &= -r_M \sin(\alpha_M) \\
x_{3M} &= \tan(\beta_M)\left((x_{1M} - x_{1EL})^2 + (x_{2M} - x_{2EL})^2\right)^{\frac{1}{2}} \\
a_1 &= x_{1EL} \sin^2(\beta_M) \\
a_2 &= -r_M^2 \cos^2(\beta_M) + x_{2M}^2 - (2x_{2EL}x_{2M} - x_{2EL}^2 + x_{1EL}^2)\sin^2(\beta_M)
\end{aligned} \tag{43b}$$

Prior to processing the first MLS observation, the Kalman best estimate of the aircraft inertial position is replaced by

$$\{\hat{R}_I(t)\} = T_{IF}\{R_{FS}\} + \{R_{IS}(t)\} \tag{44a}$$

The angles used to generate the transformation T_{IF} are the negative of the angles listed in Eq. (28c) where the transformation T_{FI} is defined.

In addition, the square root of the state covariance matrix, W(t), is reinitialized to diagonal form in order to eliminate undesirable cross correlations that were accumulated during the VORTAC data processing. We have for the diagonal elements of

$$W_{ii} = \left(\sum_{j=1}^{15} W_{ij}^2\right)^{\frac{1}{2}} \qquad i = 1, 9 \text{ and } i = 13$$

$$W_{ij}\ (j \pm i) = 0 \tag{44b}$$

The covariance elements of the expected error in the horizontal wind estimate, $W_{14,14}$, $W_{14,15}$, $W_{15,14}$ and $W_{15,15}$ are retained unaltered.

The elements of covariance matrix for the VORTAC instrument biases are eliminated and replaced by the diagonal elements of the MLS instrument biases

$$\begin{aligned} W_{10,10} &= \sigma_{MLS}\ \text{RANGE} && (30 \text{ meters}) \\ W_{11,11} &= \sigma_{MLS}\ \text{AZIMUTH} && (.05^o) \\ W_{12,12} &= \sigma_{MLS}\ \text{ELEVATION} && (.05^o) \end{aligned} \tag{45}$$

(2) Complementary Filter Update at Transition

In a manner completely similar to the Kalman filter transition Eq's. (43a), (43b) and (44a), the estimate of the inertial aircraft position is given by

$$\hat{R}_I(t) = T_{IF} \{ R_{FS} \} + \{ R_{IS}(t) \} \tag{44a}$$

In this manner the filter equations are no longer presented with abrupt perturbations and the processing of data is smooth. The aircraft guidance equations are now presented with an accurate estimate of the large cross track error, track angle error, and altitude error.

(b) Path Reconstruction at Transition

If the desired path, or the guidance equations remain unaltered at transition, the bank angle command will call for a larger bank correction to recapture the desired path, and the stabilizer and thrust commands will call for large vertical path changes to achieve the desired altitude. In order to avoid these unnecessary maneuvers the method chosen in the study to solve the transition problem is to reconstruct the remainder of the desired path to touch down by eliminating the cross track and altitude errors. This is accomplished by simply accepting the updated valid MLS position as the new first desired way point and retaining the remainder of the data for the initial N way points that have not yet been encountered. By executing the path construction equations, outlined in Appendix B, with this new reduced data set, a path will be constructed which will alter only the following segments of the original path:

(1) The great circle segment from the present MLS position to the incoming tangent way point to the new next turn circle.

(2) The turn segment to the middle of the new turn.

(3) The outgoing segment from the middle of the new turn to the unchanged next great circle.

(4) The vertical path for altitude and airspeed gradients along the three altered horizontal segments.

The consequence of these changes is to eliminate the initial cross track error and to eliminate the error in the desired height at transition. No attempt to zero out the track angle error was undertaken in this study. In addition, in order to reduce the computing work load for an aircraft computer, a trigger was introduced to avoid the path change in the event the cross track error is less than a prescribed amount (say 100 meters).

Let $\hat{R}_E$ be the unit aircraft position vector in the fixed Earth coordinate frame. Then the longitude and latitude of the new first way point is

$$\lambda(1) = \tan^{-1}\left(-\hat{R}_E(2)/\hat{R}_E(3)\right) \tag{47a}$$

$$\delta(1) = \sin^{-1}\left(\hat{R}_E(3)\right) \tag{47b}$$

Let the magnitude of the inertial position vector, R_I, be r_I, then the first desired altitude is given by

$$h(1) = r_I - r_E \tag{47c}$$

and the new first desired airspeed is given by

$$v_D(1) = v_{airspeed}\ (INS) \tag{47d}$$

Let P be integer corresponding to the last middle of the turn, $\hat{WC}(P)$, processed at the time of the MLS transition update. The new number of initial way points to be used in constructing the path is given by

$$M = N - P \tag{48}$$

We have for the remainder of the input data

$$\lambda(I) = \lambda(P + I)$$

$$\delta(I) = \delta(P + I)$$

$$h(I) = h(P + I) \tag{49}$$

$$v_D(I) = v_D(P + I)$$

$$(I) = 2, M$$

The radius of the turn is given by

$$R_T(I) = R_T\,(P - 1 + I) \tag{50}$$

$$(I) = 1,\ M-2$$

Fig. 11 illustrates a typical reconstructed horizontal path.

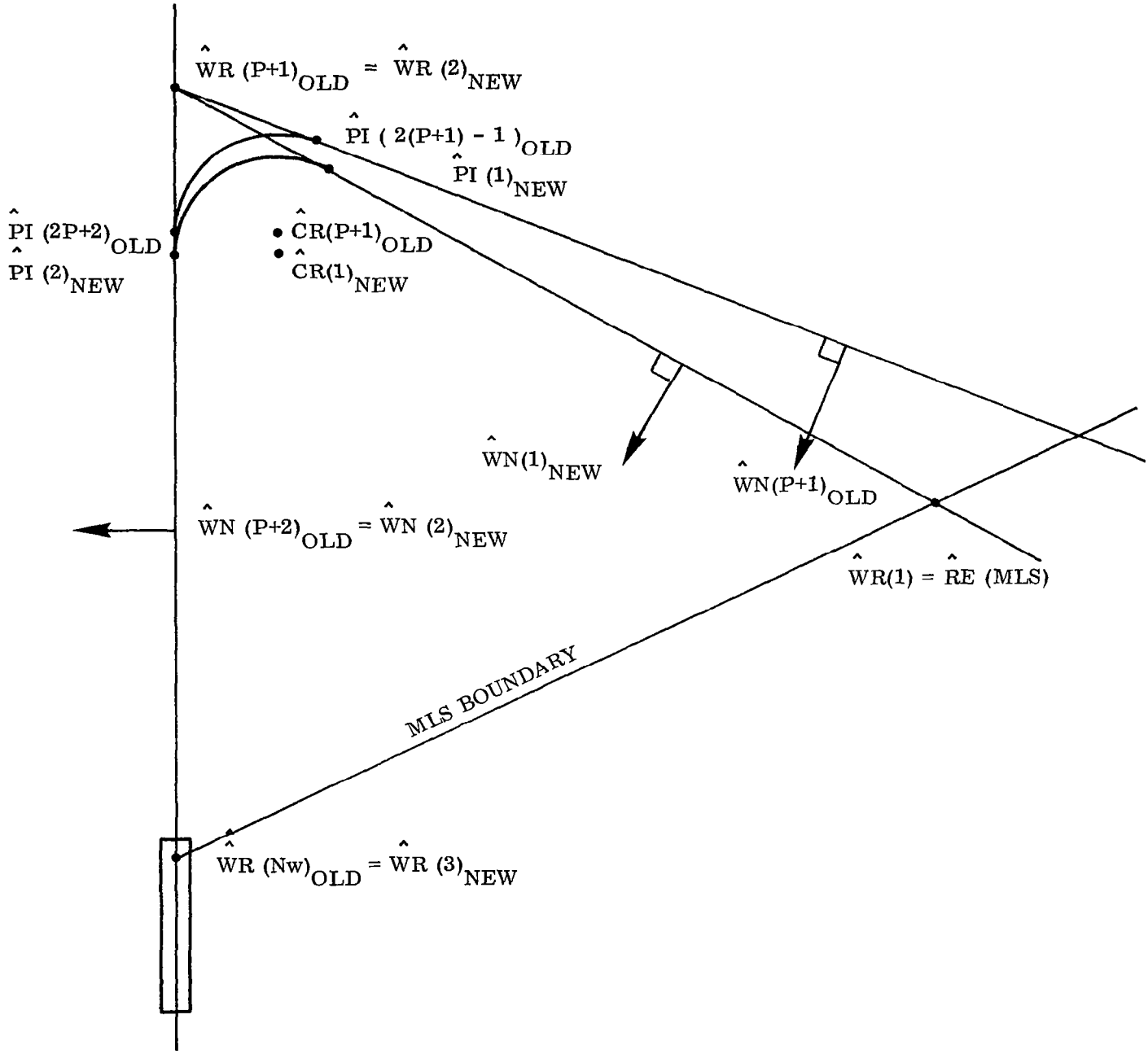

Figure 11.—Reconstructed Path at Transition

IV. RESULTS OF THE SIMULATION STUDY AT TRANSITION

(a) Description of the Simulation Test Data

This section contains the results of the computer runs of the FILCOMP program in the format of plots. Each run consists of three sets of plots. The first contains the input data of the run including the way point path generation information, the magnitude and direction of winds, the filter type used in the navigation, guidance, and control equations, the MLS boundary limits defining the transition point, and a plot of the aircraft true ground track illustrating the reconstruction of the path on transition. The second figure contains seven plots of aircraft performance in the following order:

(1) Glide path deviation in meters for both the true deviation and the estimated deviation for the filter in use in the aircraft control.

(2) Aircraft pitch angle in degrees for the true pitch, the measured pitch output of the IMU (used by the complementary filters) and the measured pitch corrected for the estimated gyro drift bias (used by the Kalman filter).

(3) Aircraft altitude rate, measured in meters per second, for both the true rate of climb and the estimated rate obtained by the filter supplying the control equations.

(4) Error in the estimate of the $\hat{x}_{1R}$ (forward) position in runway coordinates, measured in meters, for both the Kalman and complementary filter.

(5) Error in the estimate of the $\hat{x}_{2R}$ (lateral) position in runway coordinates, measured in meters, for both the Kalman and complementary filter.

(6) Error in the estimate of the $\hat{x}_{3R}$ (vertical) position in runway coordinates, measured in meters, for both the Kalman and complementary filter.

(7) Error in the estimate of the forward velocity ($\hat{\dot{x}}_{1R}$) in runway coordinates, measured in meters per second, for both the Kalman and complementary filter.

The third figure contains eight plots of an aircraft performance in the following order:

(1) Cross track error, measured in meters, for both the true CRTE and the estimated CRTE for the filter used in the control.

(2) Track angle error, converted from degrees to time rate of change of cross track error by multiplying by the ground speed. Both the true track angle error and the estimated track angle error used by the guidance equations are shown, measured in meters per second.

(3) Aircraft roll angle, measured in degrees for the true roll angle, the measured roll angle supplied by the IMU (used in the complementary filter), and the measured roll angle corrected for the gyro drift bias (used in the Kalman filter).

(4) Error in the estimate of the north component of the wind, in meters per second, for both Kalman and complementary filter.

(5) Error in the estimate of the west component of the wind, in meters per second for both the Kalman and complementary filter.

(6) Difference between the true desired airspeed and the true airspeed. A second plot also shows the difference between the true ground speed and the true airspeed. The curves are mirror images of one another if there are no winds, and differ in the presence of winds.

(7) Error in the estimate of the lateral velocity, $\hat{\dot{x}}_{2R}$, in meters per second for both the Kalman and complementary filter.

(8) Error in the estimate of the vertical velocity, $\hat{\dot{x}}_{3R}$, in meters per second for both the Kalman and complementary filter.

(b) Discussion of the Results

The first case, Fig's. (12a), (12b) and (12c), illustrates the performance of the aircraft, following transition, where the VORTAC and baro bias errors have been removed from the estimate of the position through reinitialization, but no path reconstruction has been attempted. Plots 4, 5, and 6 of Fig. (12b) show the effect of the reinitialization at 33 seconds on the errors in the estimate of position. Plot 1 of Fig. (12c) shows the large CRTE presented to the guidance equations with no path reconstruction. Plot 3 of Fig. (12c) shows the large roll angle (20^{o}) at 40 seconds and the overshoot in the opposite direction of 10^{o} at 55 seconds as the aircraft attempts to recapture the original path. Plots 2 and 3

of Fig. (12b) illustrate the excessive pitch change and "roller coaster" effect in the rate of climb that result when the desired vertical path has not been reconstructed. Fig. (12a) illustrates the large shift in ground track as the aircraft attempts to recapture the original path.

Case 2, Fig's. (13a), (13b) and (13c), illustrates the perfect transition that would be possible if the actual vehicle position and velocity information were available to the guidance equations. Since the VORTAC bias errors do not appear in the estimate of the aircraft state, the cross track error, track angle error, and altitude errors are negligible both prior to and following transition and a smooth trajectory results.

Case 3, Fig's. (14a), (14b) and (14c), illustrates the smooth performance at transition, with path reconstruction when the complementary filter supplies the aircraft position and velocity to the guidance equations. Examination of Plot 3, Fig. (14c) shows that no roll is called for during transition indicating that both the cross track error and track angle errors are small at transition (33 seconds). Similarly, Plot 2 and 3, Fig. (14b), show very small activity in the vertical channel as compared with the same plots for Case 1. A vast improvement in aircraft performance with path reconstruction is plainly indicated. Furthermore, a comparison of Fig. (13a) and (14a) shows that the change in ground path is minimal.

Case 4, Fig's. (15a), (15b) and (15c), illustrates similar acceptable transition performance when the Kalman filter is used to supply the guidance equations in conjunction with path reconstruction. The major difference between the Kalman and complementary filter effect on transition performance is illustrated in Plots 2, and 3 of Fig's. (14c) and (15c). The Kalman filter causes a slight aircraft roll (Plot 2) transition due to a non zero track angle error (Plot 3) caused by the error in the Kalman estimate of the lateral velocity. Examination of Plot 7, Fig.(15c), indicates that the Kalman estimate of lateral velocity continues to grow after 25 secs. The complementary filter, lateral velocity error, decreases from 3.5 m/sec at 25 seconds to 2 m/sec at transition (33 sec),

while the Kalman estimate continues to grow to 4.5 m/sec at transition. Following transition, the Kalman estimates of velocity are much better than the complementary filter. Some additional study is recommended to remove this anomaly since it is expected that an optimal filter should be expected to out perform a fixed gain filter. In any case the performance of both filters with path reconstruction does eliminate the objectional features of Case 1 with no path reconstruction.

Case 5 illustrates the effect of winds on the transition performance with path reconstruction. A 10 knot wind at 165^{o} heading is simulated in this run. Comparing this case with Case 3, in which no winds were simulated, shows that the performance at transition, using the complementary filter is unaffected by winds. Even the error in the complementary filter estimate of the winds shown in Plots 4 and 5 of Fig. (16c) are similar to the error in the complementary filter estimate of the winds in Plots 4 and 5 of Fig. (14c) for no winds.

Case 6 illustrates the effect of a 10 knot wind at -15^{o} heading on the transition performance when the Kalman filter information is used in the guidance equations. Case 6 is to be compared to Case 4 in which no winds were acting and the Kalman filter was used in the guidance equations. The performance at transition is seen to be unaffected by winds for both Kalman and complementary filter estimates and both filters produce smooth transition using the path reconstruction method.

Case 7 illustrates the effect of changing the transition point from a 60^{o} to 40^{o} azimuth boundary for the MLS elevation signals. Case 7 is to be compared with Case 5. Both cases differ only in the time and location on the original trajectory that the transition is initiated due to the 40^{o} limit on the MLS elevation antenna. Comparing Fig. (18b) with Fig. (16b) and Fig. (18c) with Fig. (16c) it is apparent that except for the change in the time of transition, the performance is identical.

Case 8 illustrates the effect of a 40^{o} azimuth boundary for the MLS elevation on the performance of Kalman filter. Once again the error in lateral velocity at the

instant of transition is seen to produce a slight track angle error following transition. Comparing Plot 3, Fig. (19c), with Plot 3, Fig. (17c) shows that the slight perturbation in track angle error following transition is moved in time and that smooth transition is possible for both filters and is unaffected by the sweep limits of the MLS elevation antenna.

Case 9 illustrates what happens when the cross track error at transition is not large enough to trigger the path reconstruction. By changing the heading of the incoming leg it is possible to approach the transition point in a direction at right angles to the VORTAC range bias error. In this case the cross track error at the first valid MLS data point is too small to trigger the path reconstruction logic. The vertical error due to the baro bias and along-track error due to range bias now remains as a desired altitude error in the guidance equations and the "roller coaster" search for the proper altitude and altitude rate reoccurs. Plot 3 of Fig. (20b) illustrates the overshoot in altitude and rate of climb at transition. In order to avoid this effect it is deemed necessary to remove the CRTE limit at transition and cause the path redesign logic to occur at transition independent of the magnitude of the cross track error.

Case 10 illustrates a 4 way point trajectory with two turns. Transition occurs after the first turn. The significant feature in this run is the persistence of the track angle error immediately following the transition point (125 secs.). This is illustrated by the roll angle excursion from 125 seconds to 140 seconds in Plot 3, Fig. (21c). It appears that an alternate method in which both the cross track error and the track angle error at transition are nulled out should be investigated.

Case 11 is an illustration of a 6 way point with 4 turns. The entire trajectory takes place within the MLS boundary so that no transition is encountered. It is included here only for the purpose of illustrating the versatility of the way point path construction.

(c) Conclusions and Recommendations

The main result of this study is that a smooth transition to MLS navaids in the terminal area is feasible and possible through the use of path reconstruction and filter reinitialization. The method, investigated in the study, of nulling the cross track error and altitude error with the first valid MLS aircraft position determination is simple and requires very little change in the existing way point trajectory construction software presently existent in the Langley Field TCV B-737 aircraft navigation computer.

The following recommendations are made:

(1) Investigate alternate methods of path reconstruction to null out track angle error as well as cross track and altitude error at transition.

(2) Study the behavior of the Kalman filter at transition to obtain better velocity behavior in the VORTAC navaid area.

(3) Perform path reconstruction when either the cross-track or altitude error exceed specified limits or just always update to eliminate the code required for limit checking.

(4) Investigate the changes that must be made in the existing aircraft software to accommodate the path reconstruction method outlined in this study and flight test the procedure for pilot comments and experience in transition in the terminal area.

(5) Develop a method for path reconstruction for transition occurring during a turn.

TABLE I

CONSTANTS USED IN WAYPOINT TRAJECTORY CONSTRUCTION

w_E (EARTH ROTATION RATE)	$.7292131\ 10^{-4}$	rad/sec
G (GRAVITY CONSTANT)	9.8066	m/sec^2
r_E (RADIUS OF THE EARTH)	6378.156	km

1 knot = .5144434 m/sec

1 radian = 57.2957795^o

TABLE II

INPUT DATA FOR WAYPOINT TRAJECTORY CONSTRUCTION

CASES 1 THROUGH 8

N = 3

I	λ (I) DEG	δ (I) DEG	h(I) m	v_D (I) m/sec
1	-77.1315516	40.2689558	1084.11	74.59
2	-77.0847124	40.1709553	435.16	68.31
3	-77.0232052	40.2523725	0	68.31

R_T = 2286 meters

ψ_{RUNWAY} = 30 ^{o}

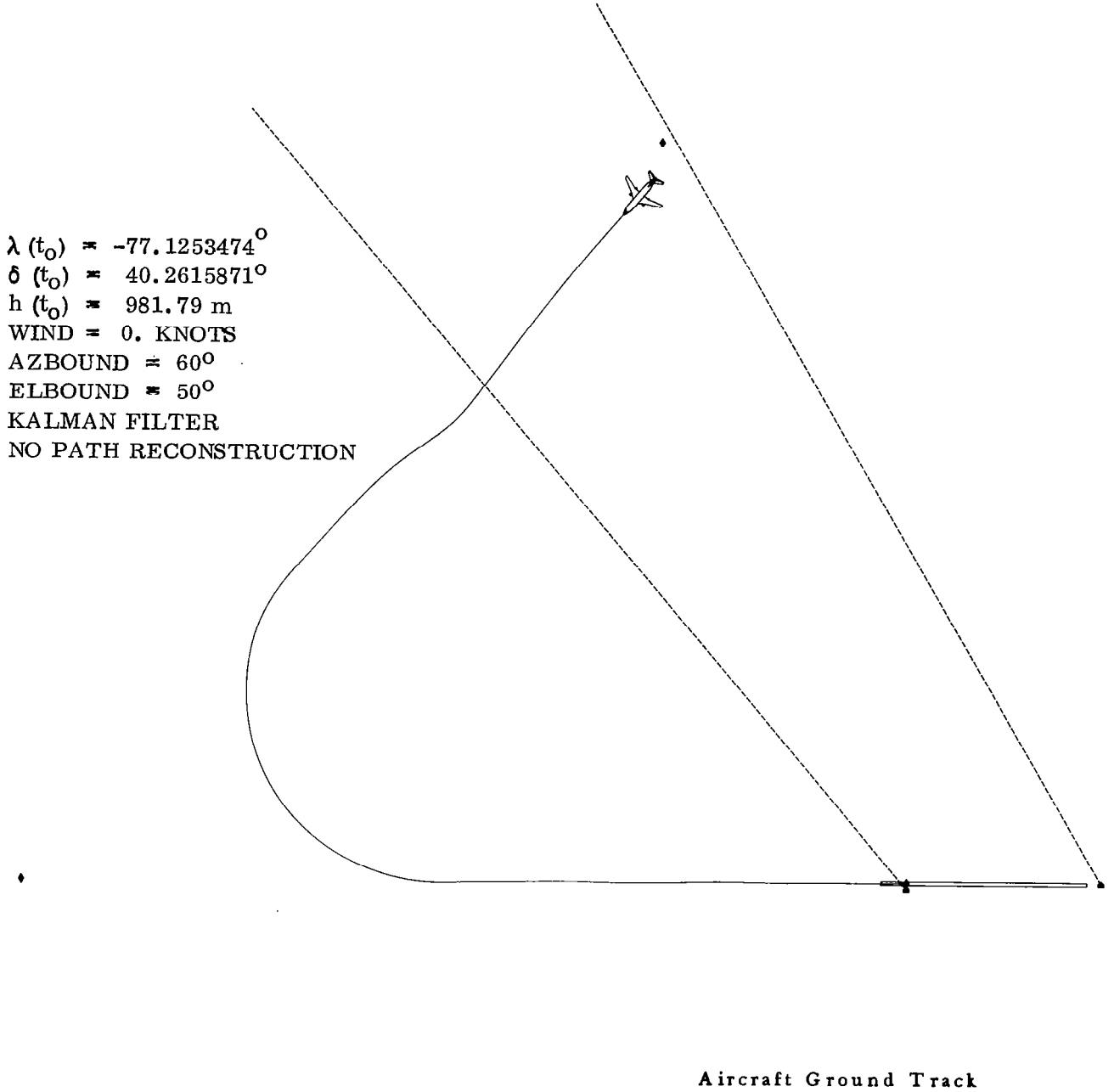

Figure 12(a).-Case 1 MLS Transition Without Path Reconstruction

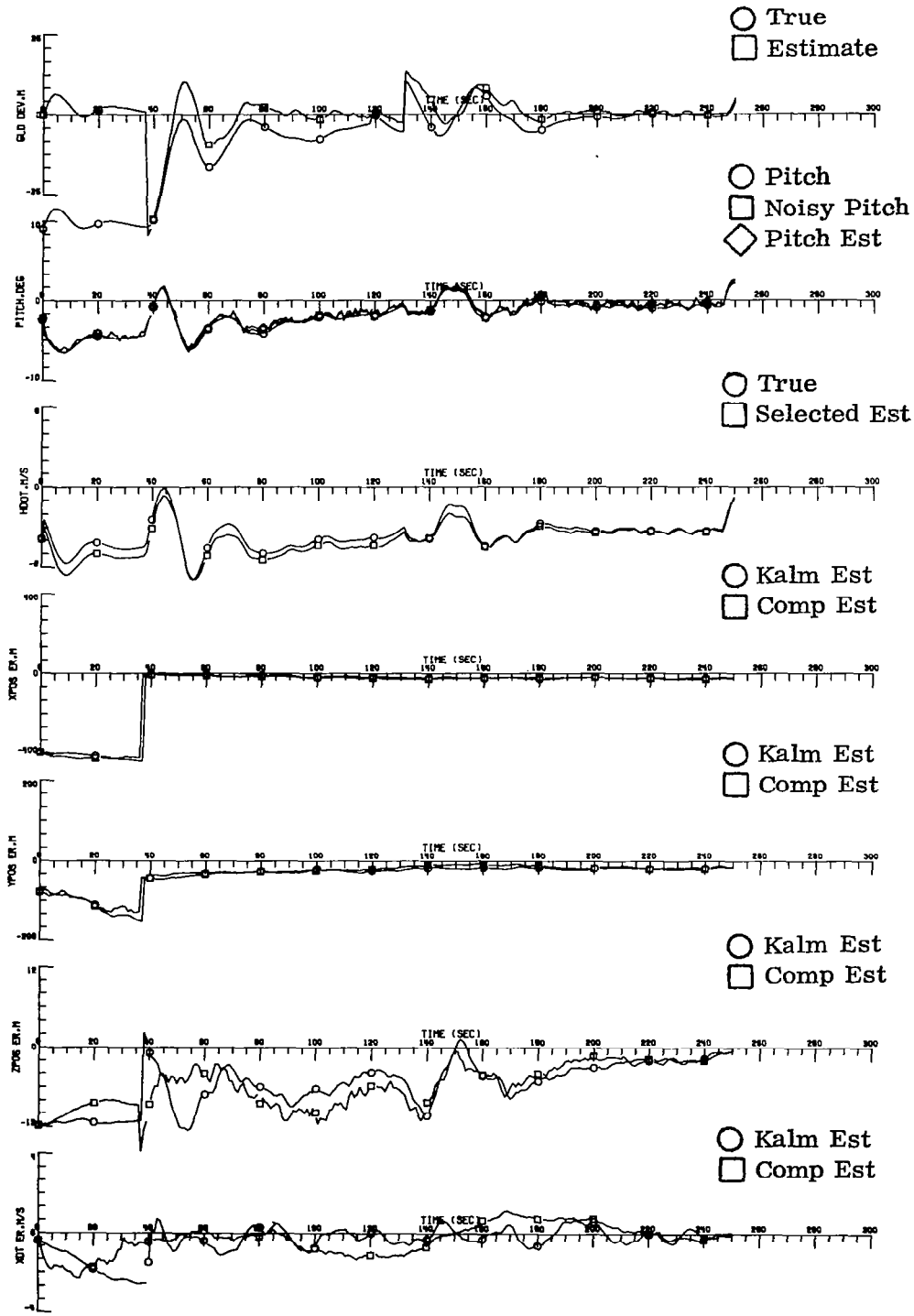

Figure 12(b). - Case 1 Continued

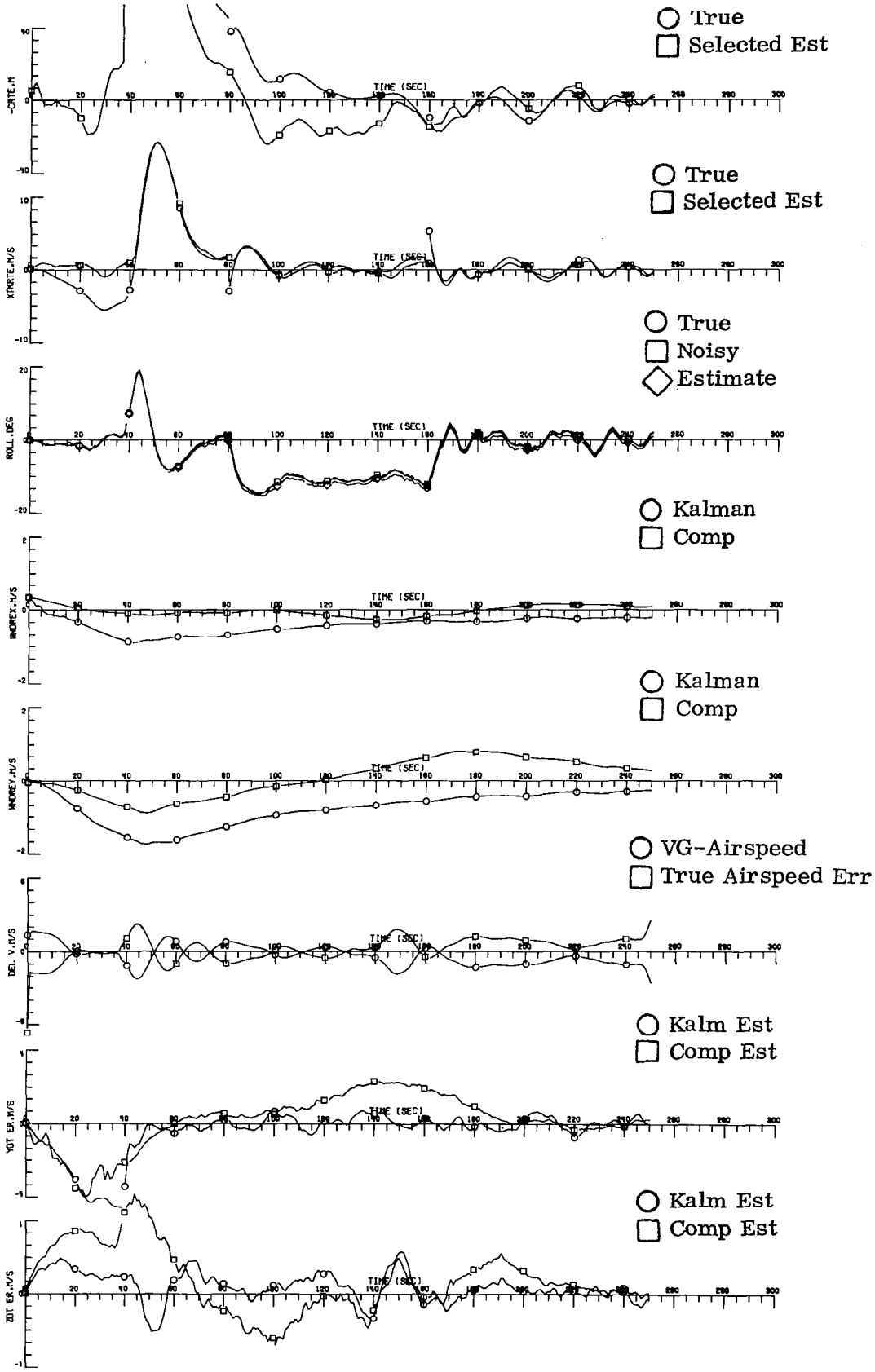

Figure 12(c). - Case 1 Concluded

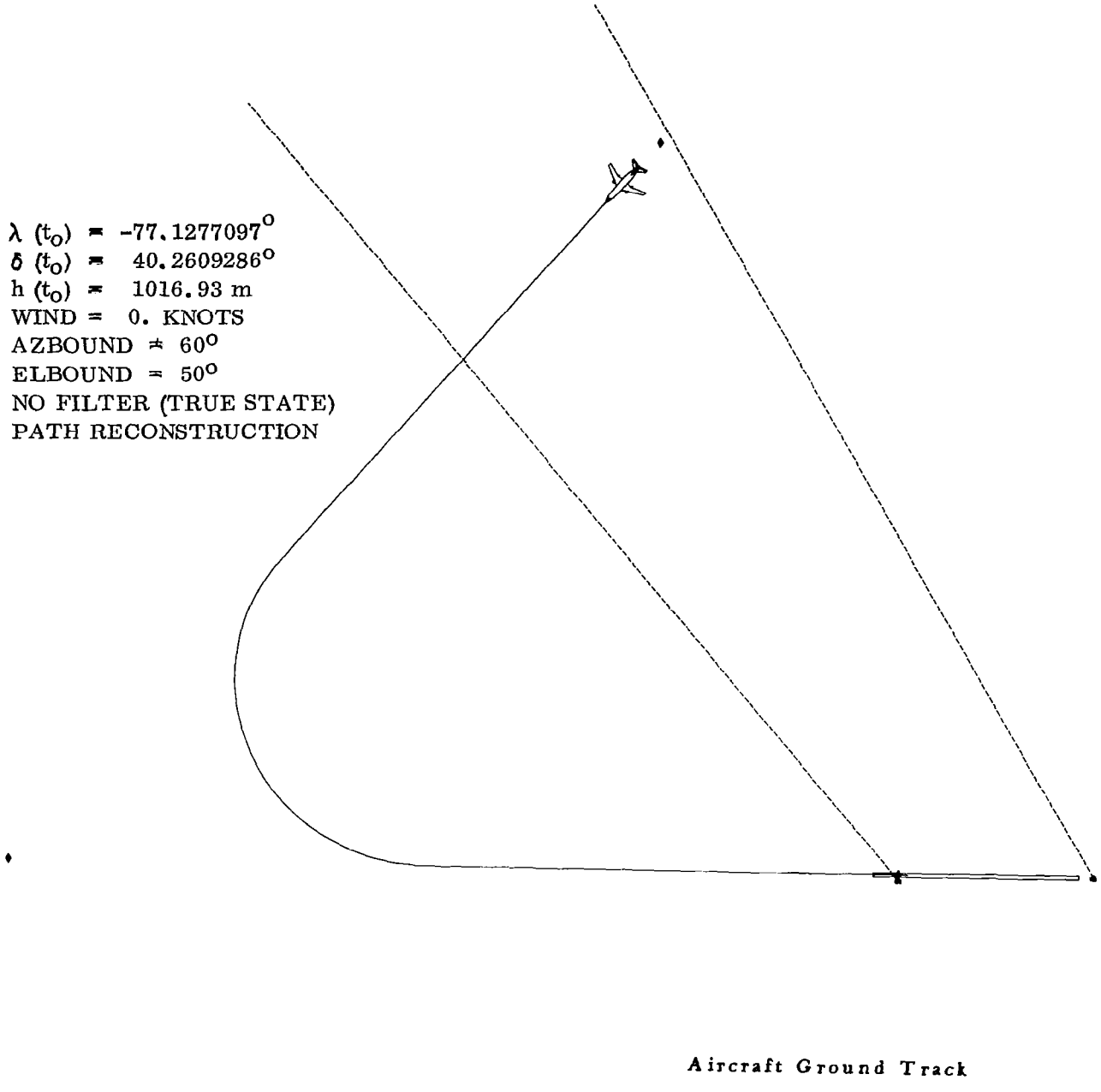

Figure 13(a). - Case 2 MLS Transition With Path Reconstruction and Perfect Navigation Path

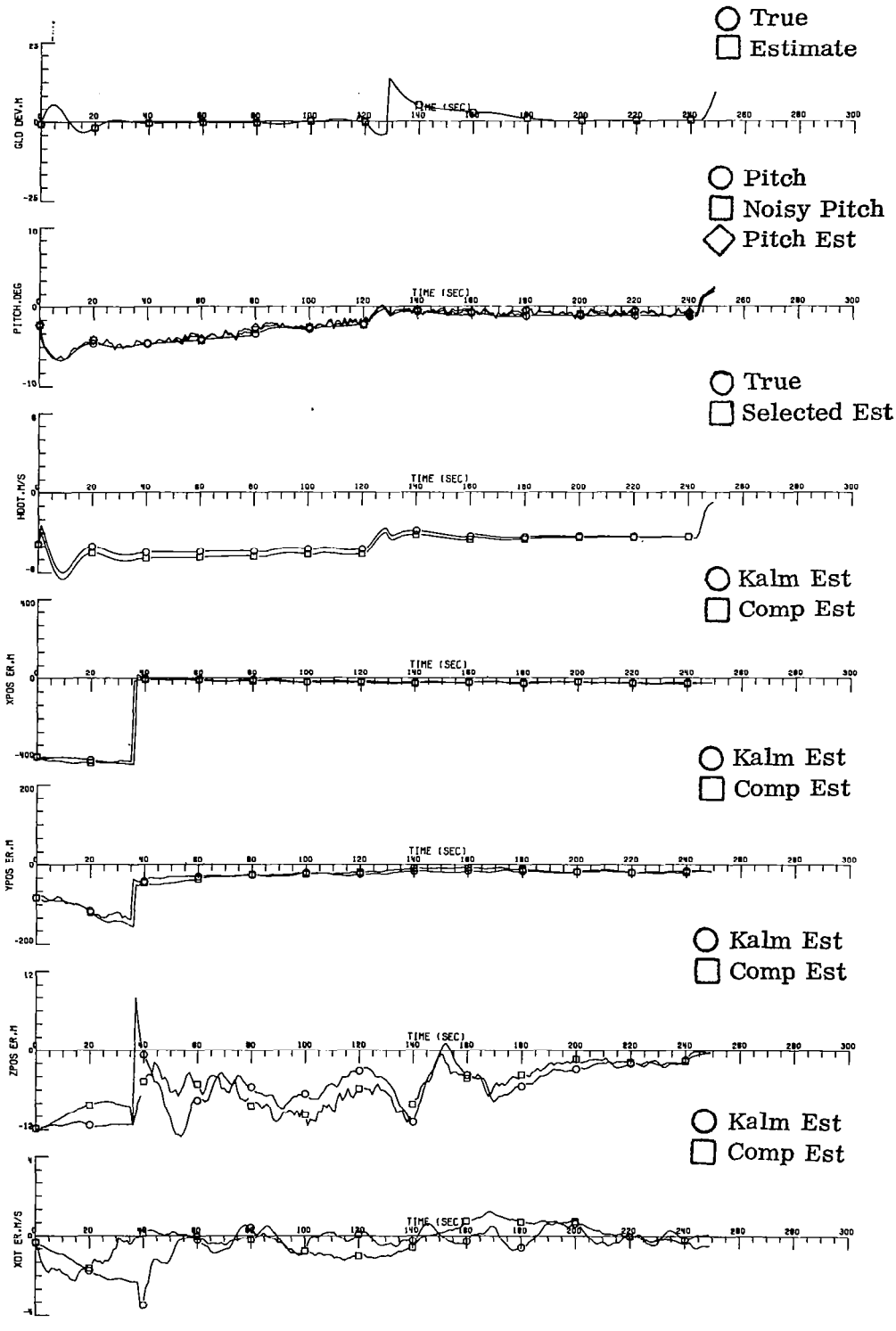

Figure 13(b). - Case 2 Continued

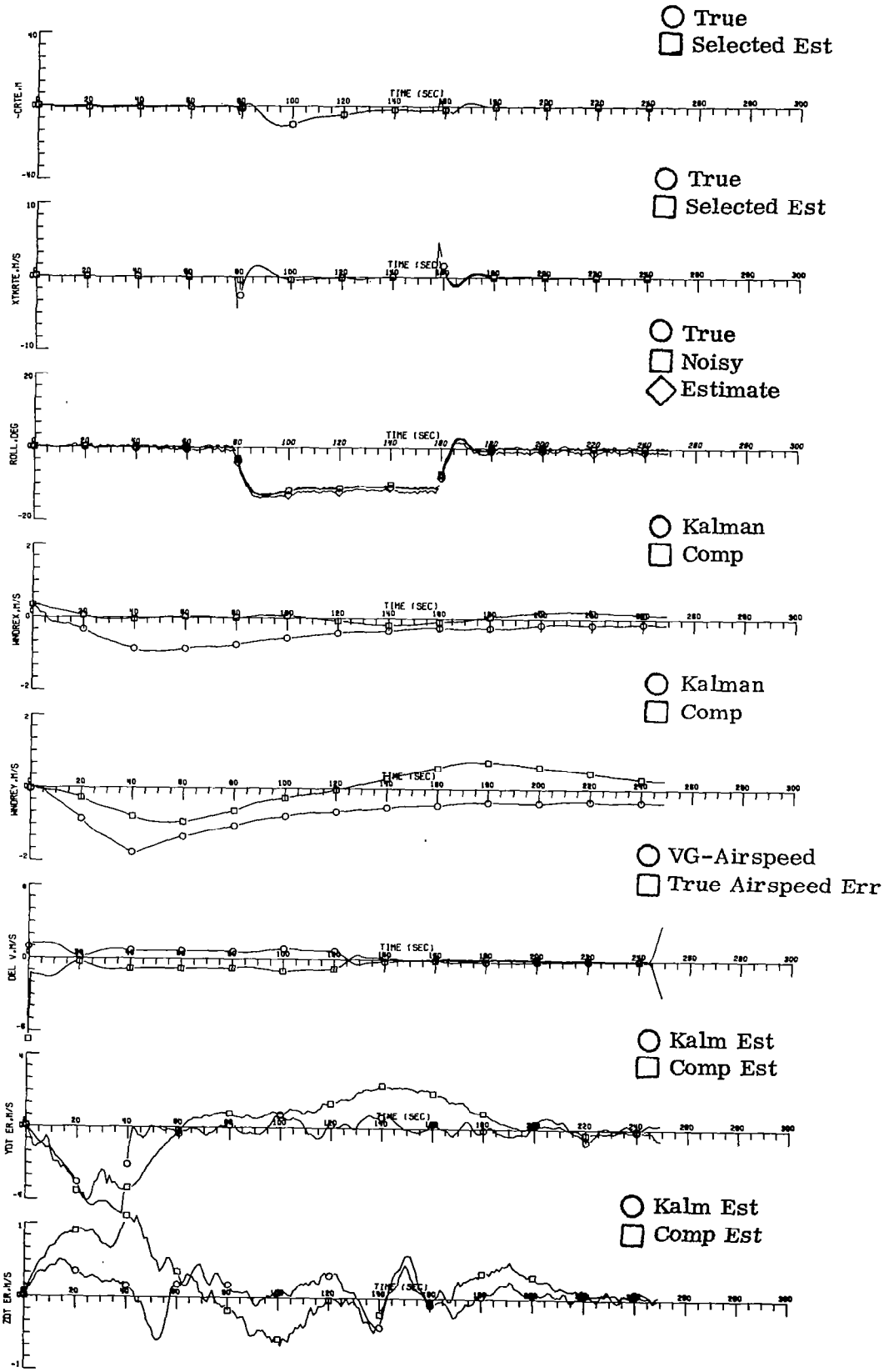

Figure 13(c). - Case 2 Concluded

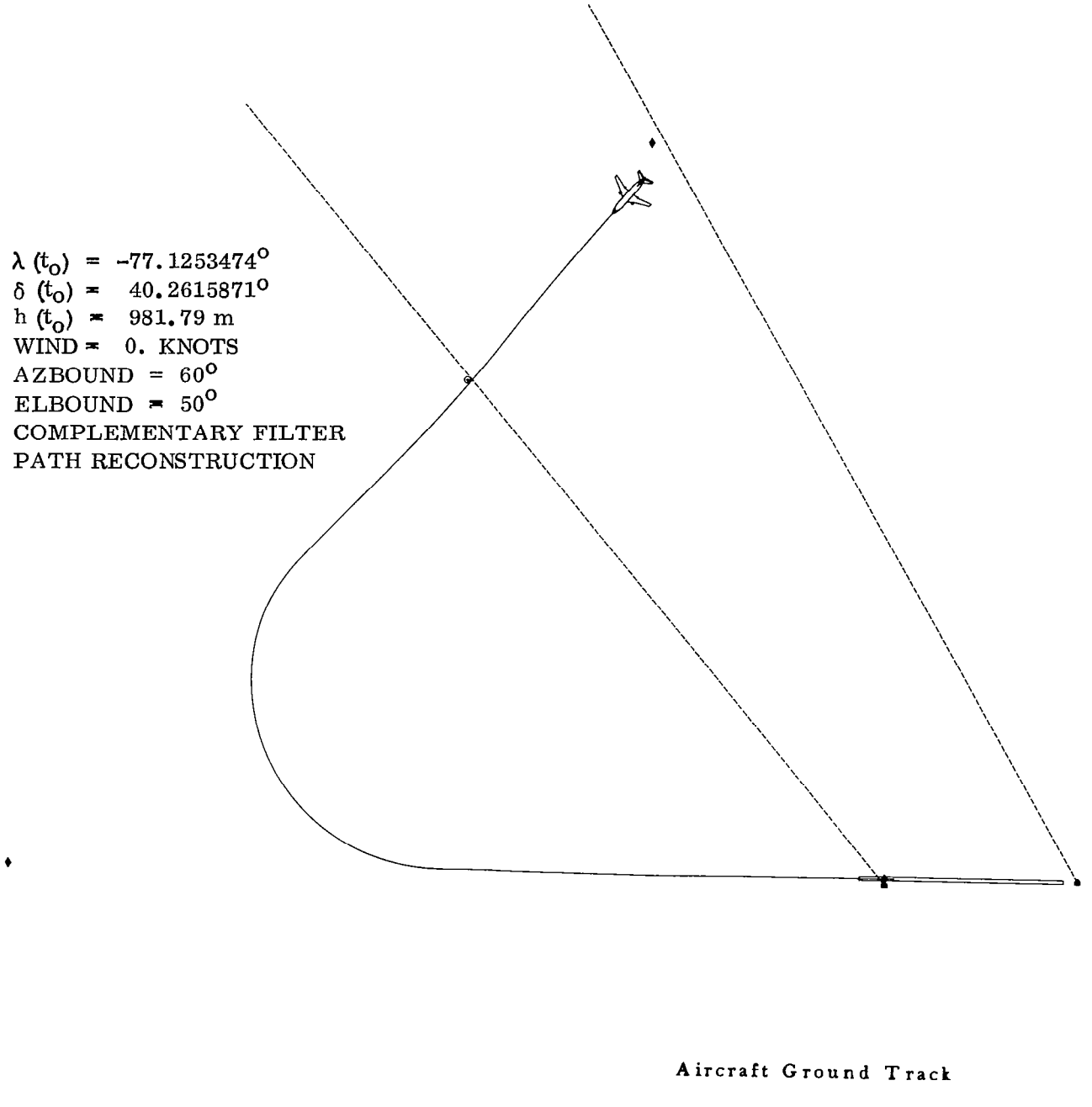

Figure 14(a). - Case 3 MLS Transition With Path Reconstruction With Kalman Filter Navigation

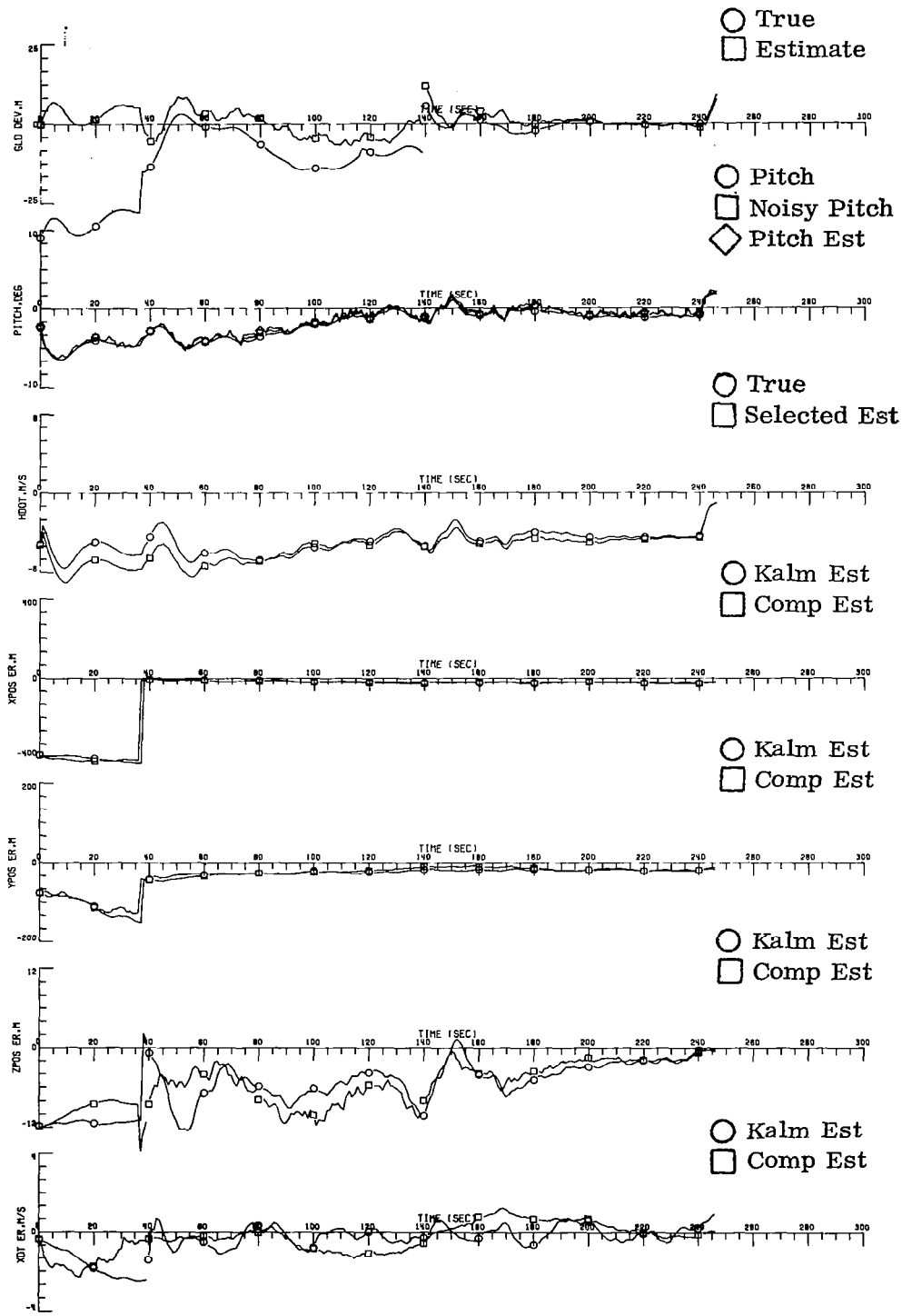

Figure 14(b). - Case 3 Continued

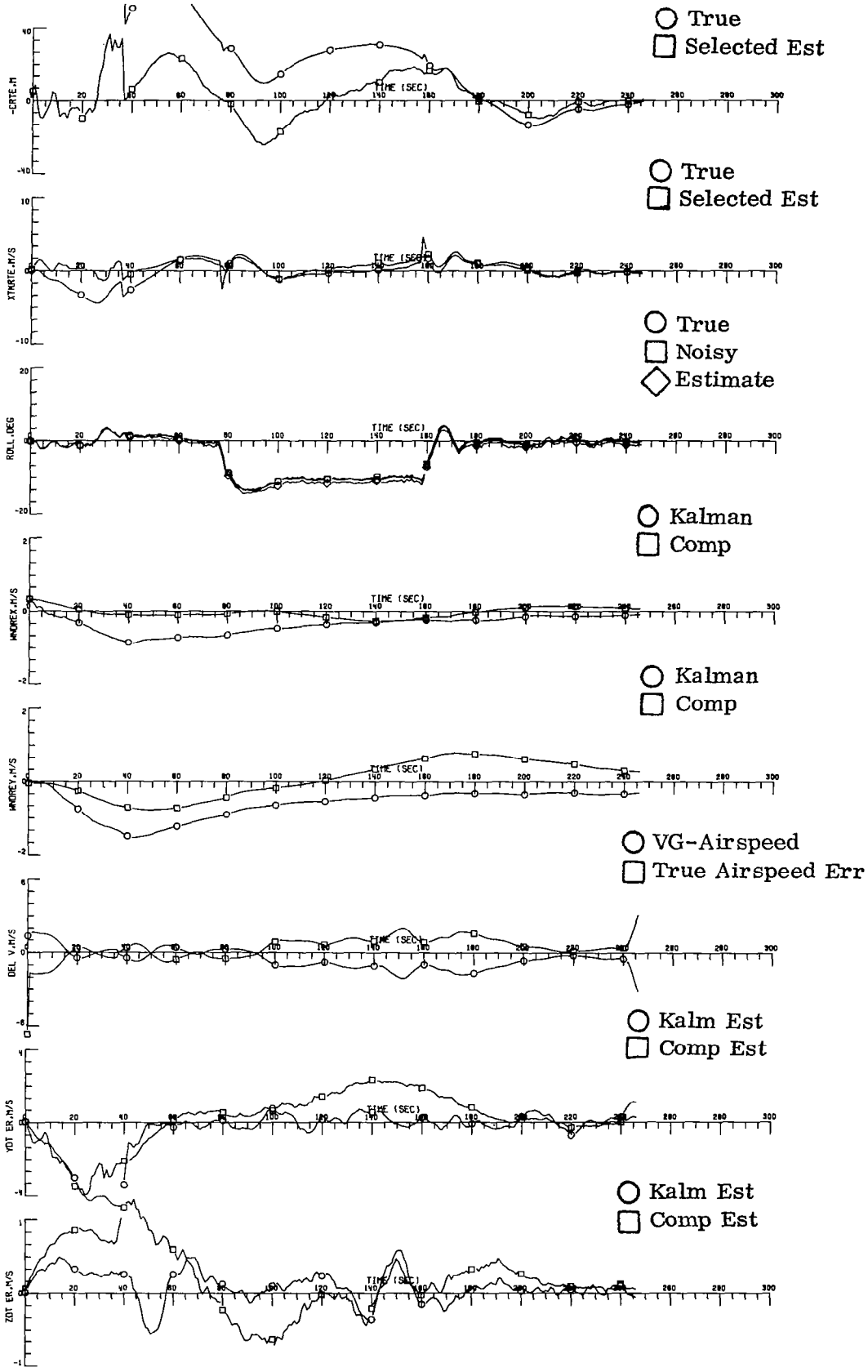

Figure 14(c). - Case 3 Concluded

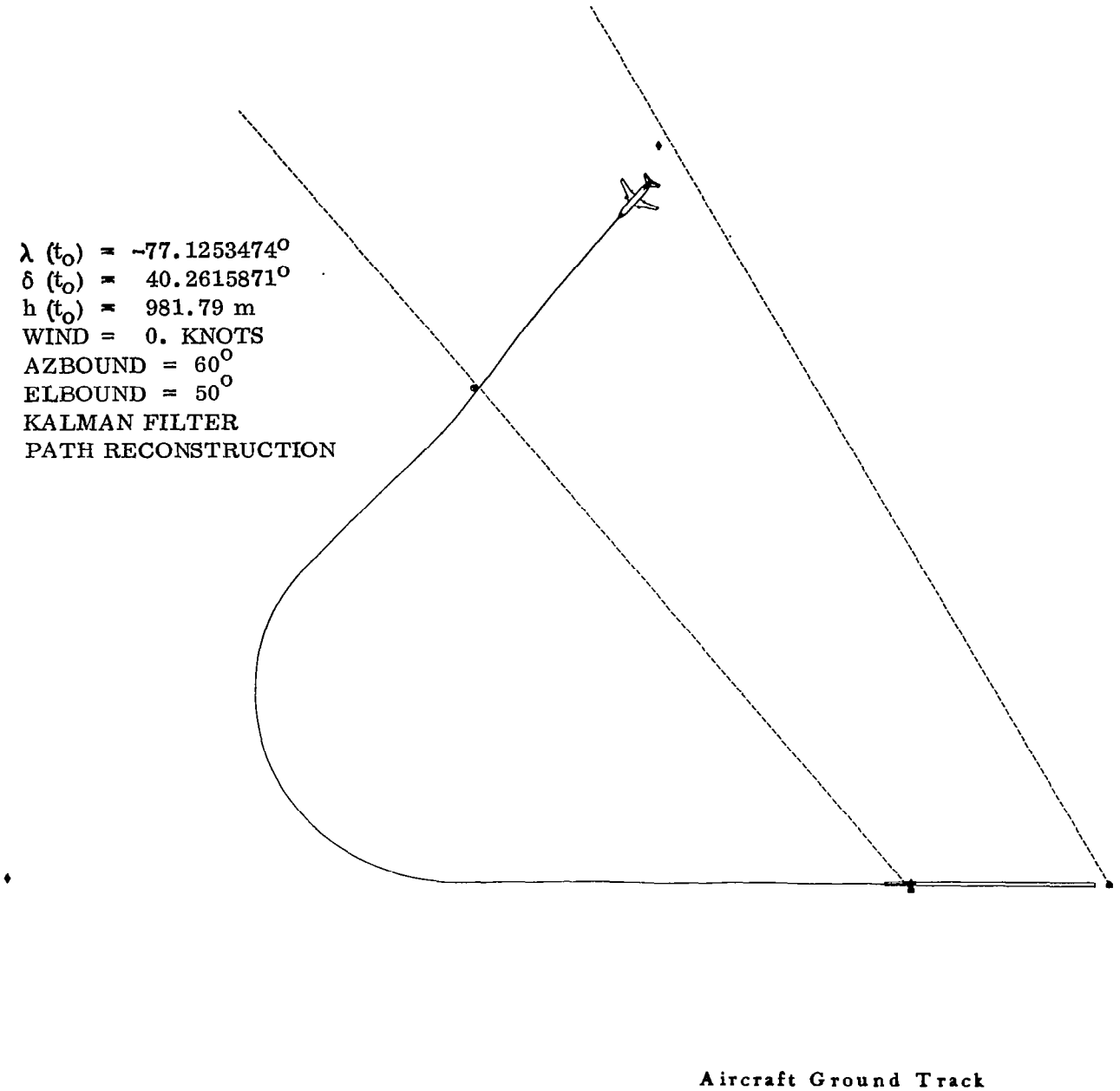

Figure 15(a). - Case 4 MLS Transition With Path Reconstruction With Kalman Filter Navigation

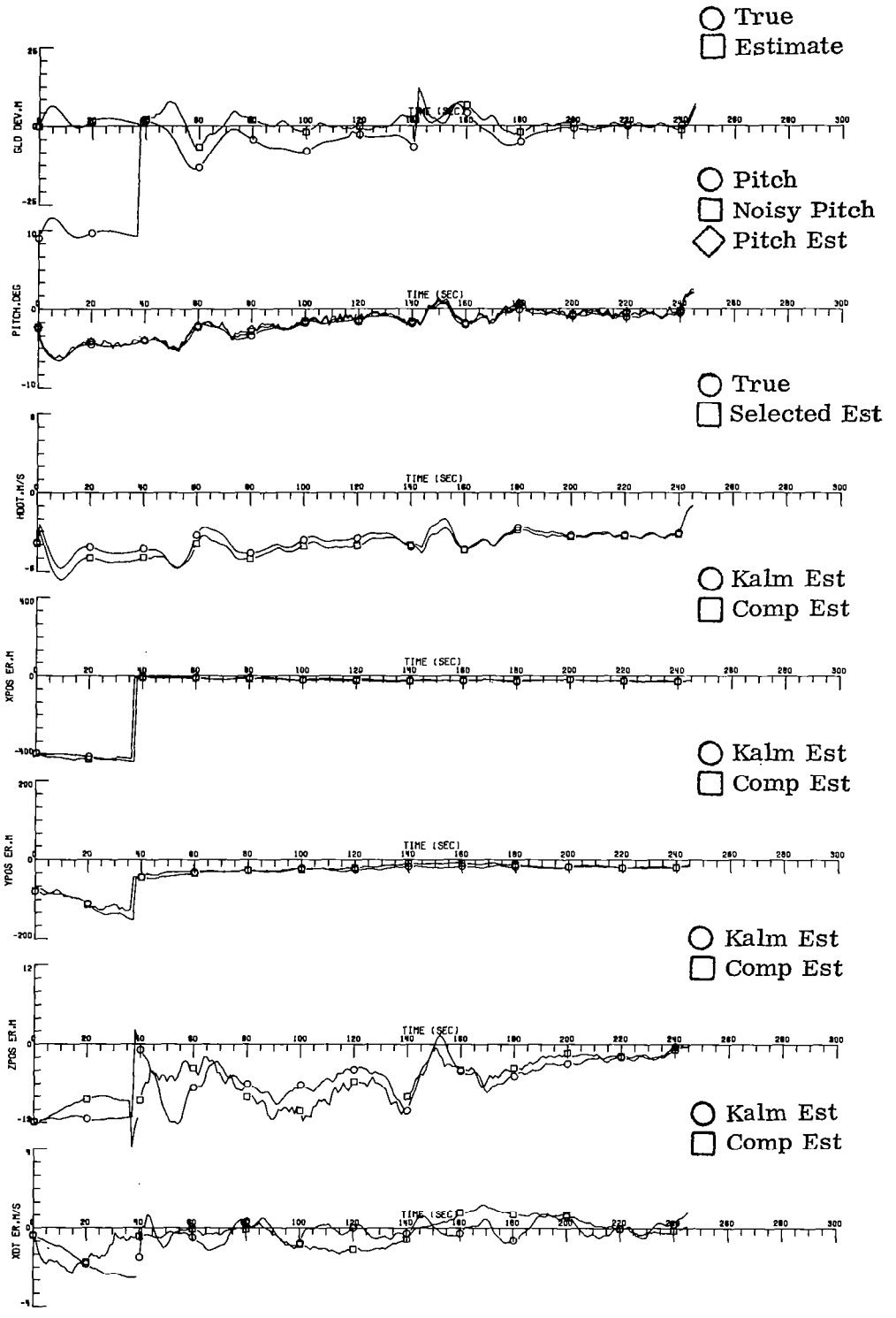

Figure 15(b). - Case 4 Continued

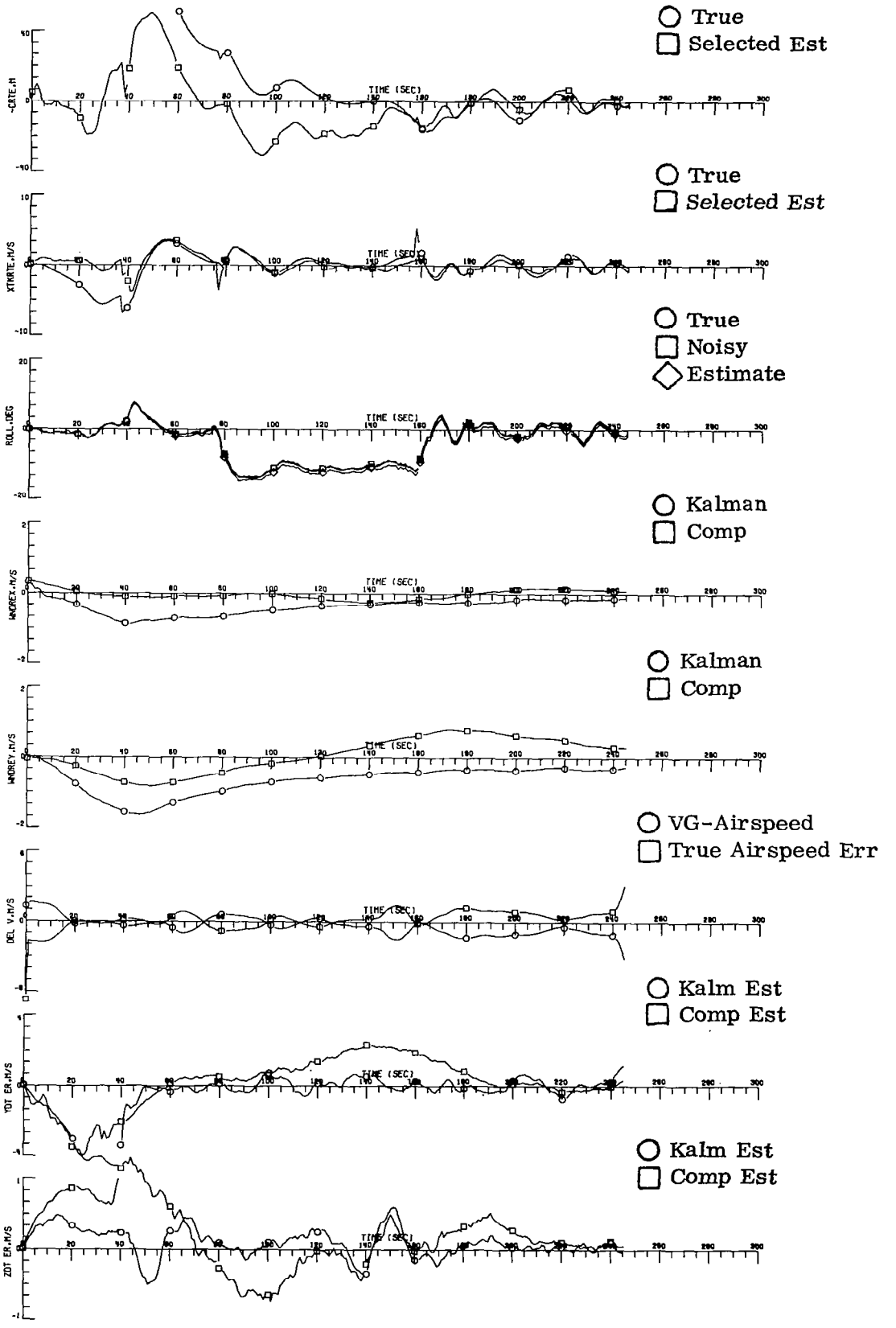

Figure 15(c). – Case 4 Concluded

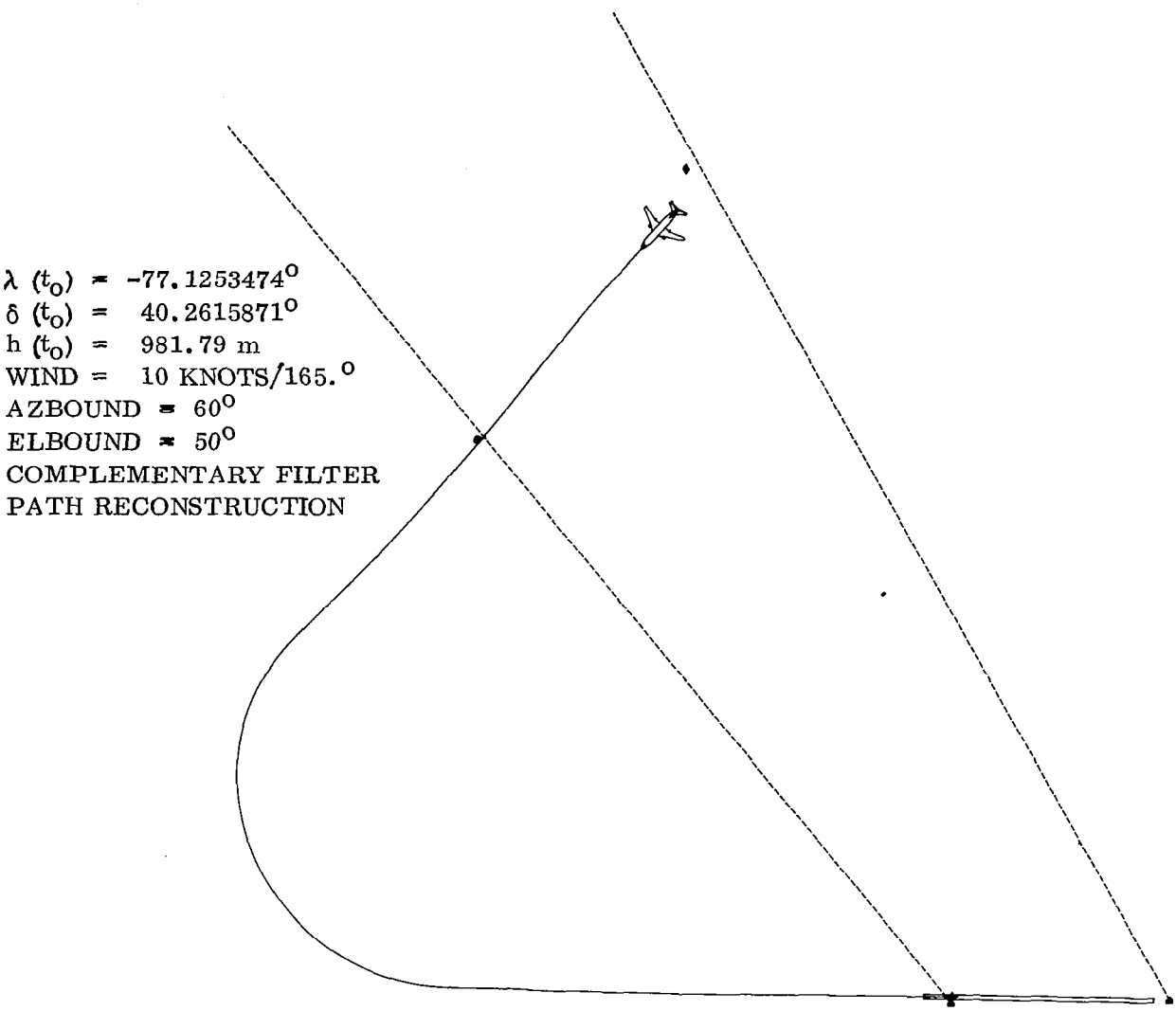

Figure 16(a). – Case 5 MLS Transition With Path Reconstruction in Presence of Winds (10 Knots/165° Heading)

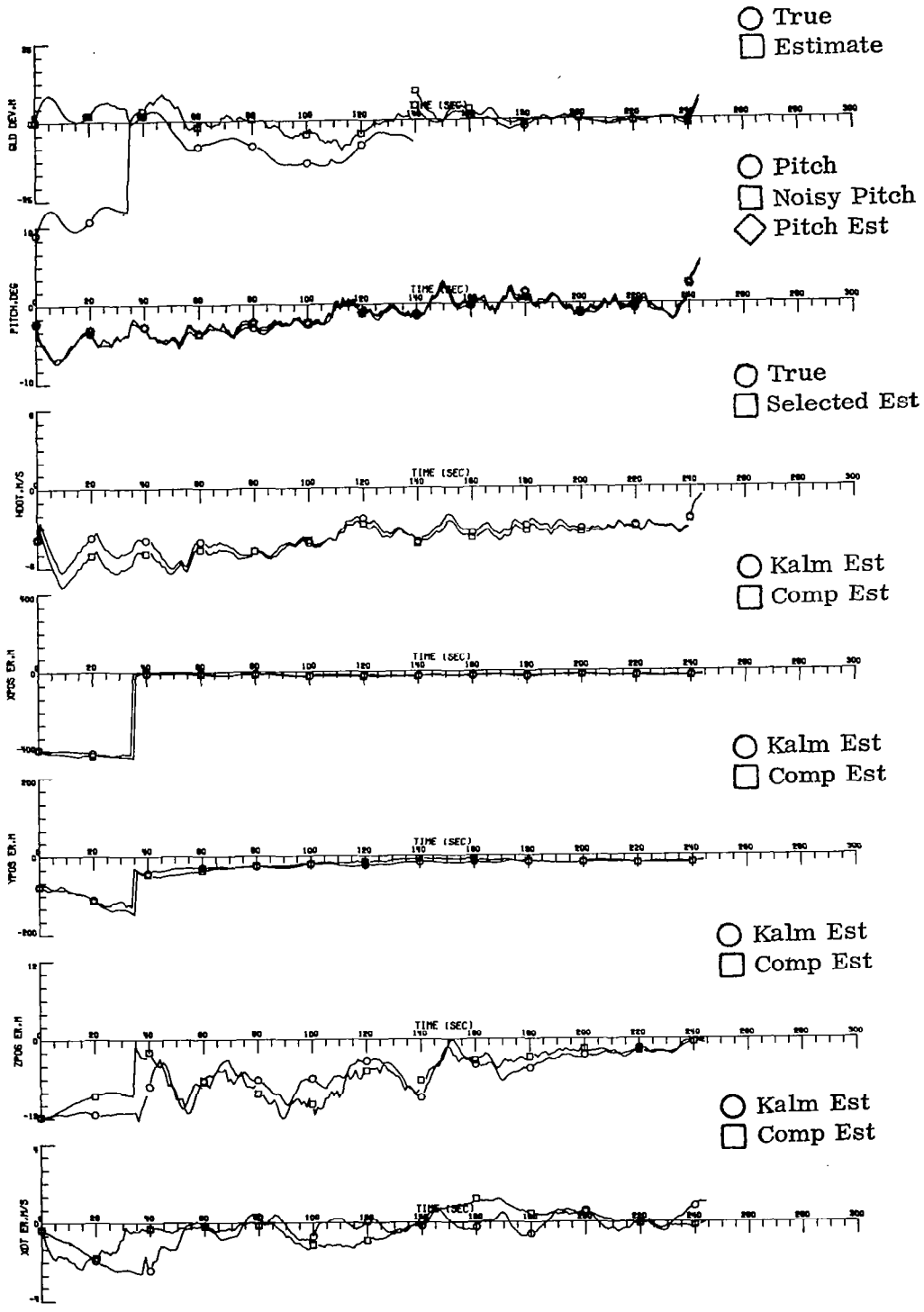

Figure 16(b). – Case 5 Continued

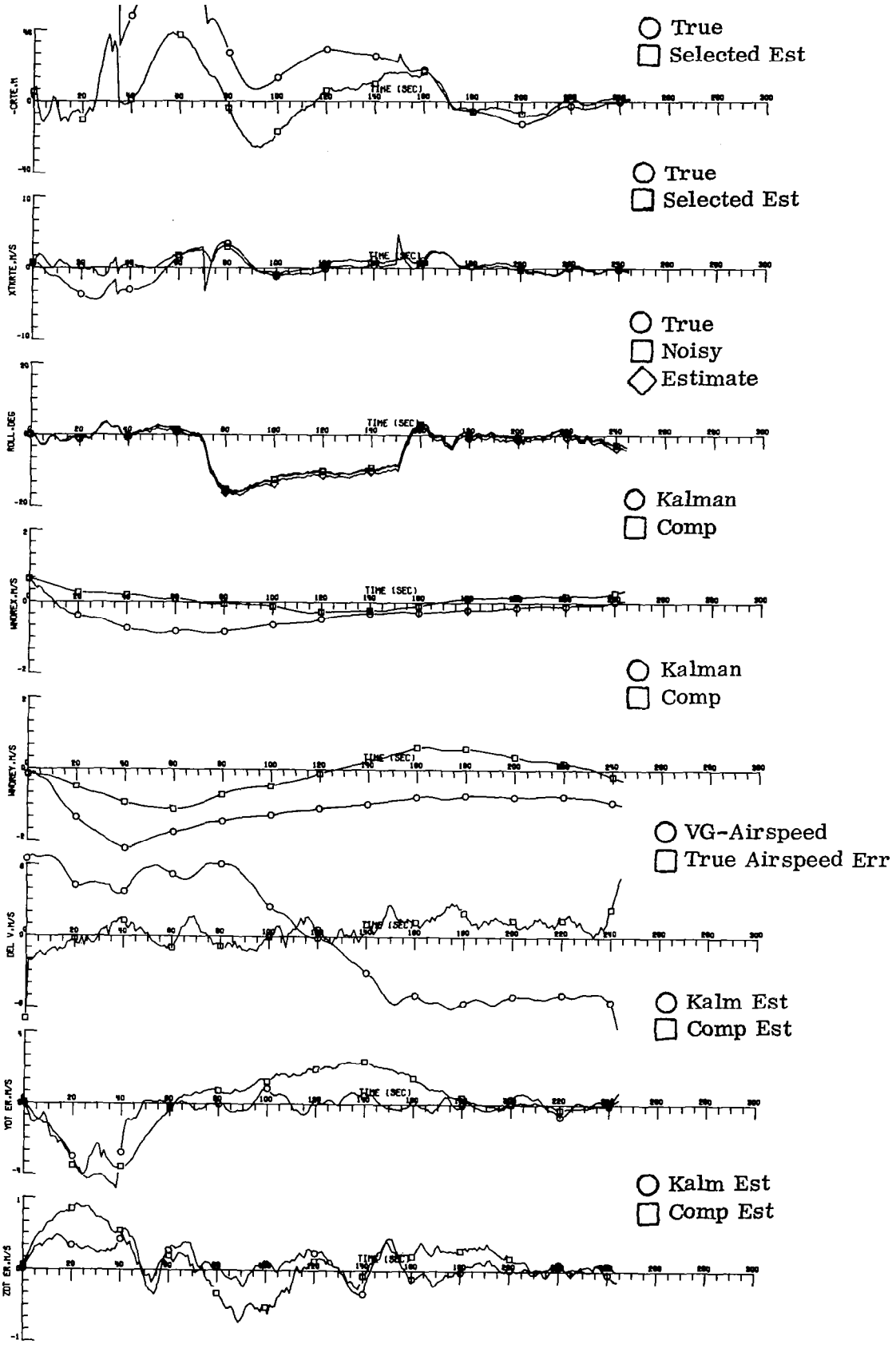

Figure 16(c). – Case 5 Concluded

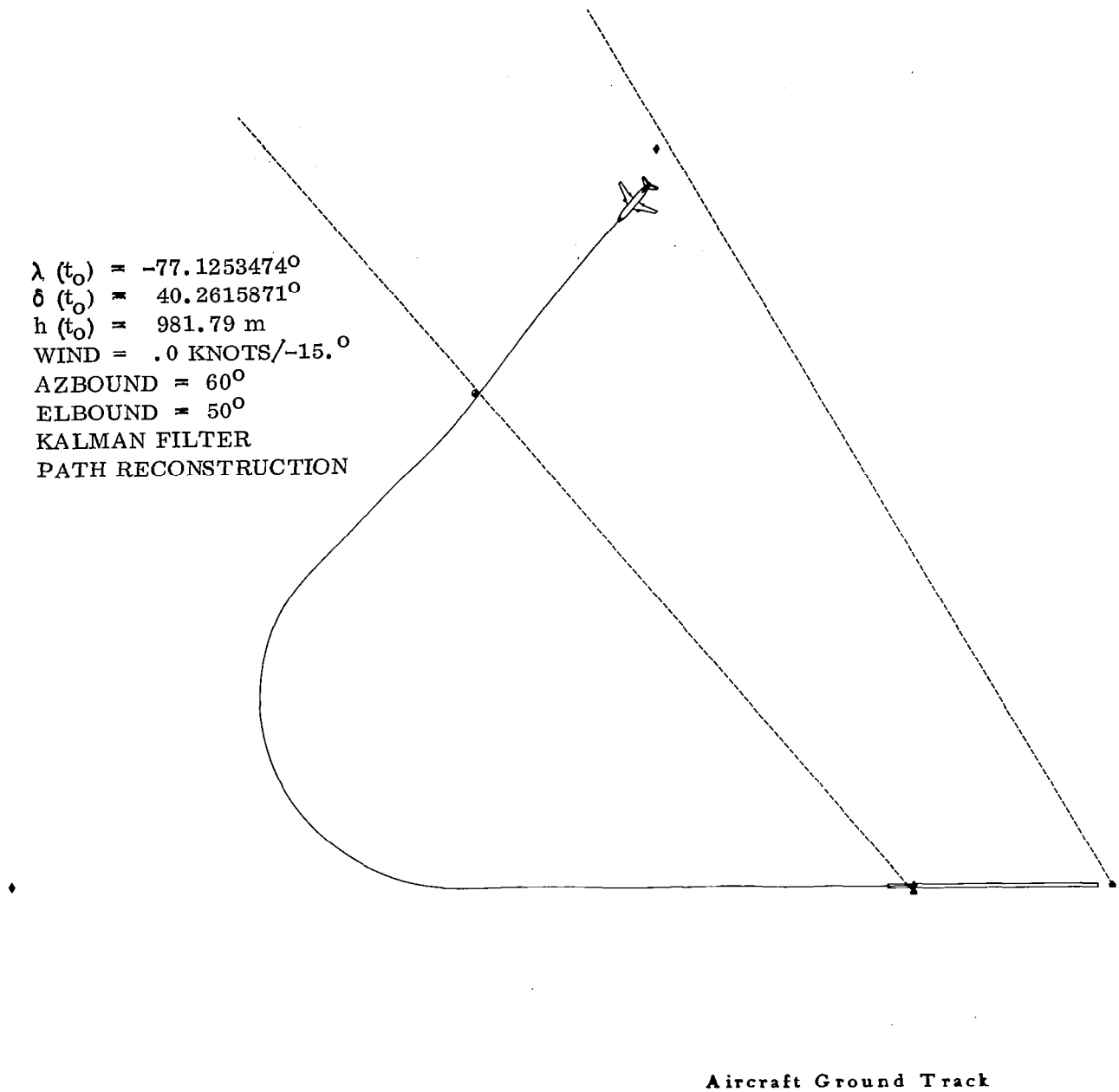

Figure 17(a). – Case 6 MLS Transition With Path Reconstruction in Presence of Winds (10 Knots/-15° Heading)

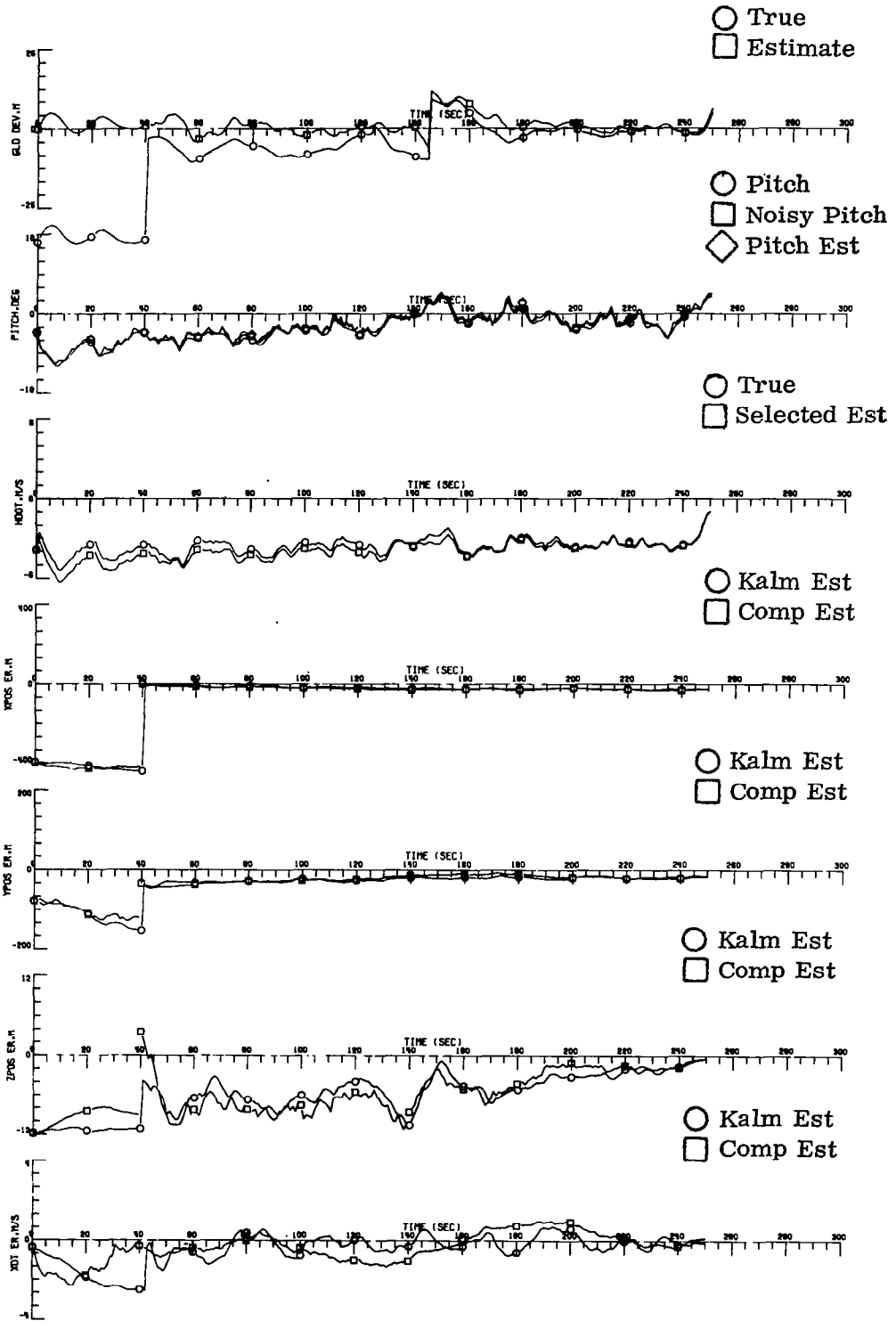

Figure 17(b). – Case 6 Continued

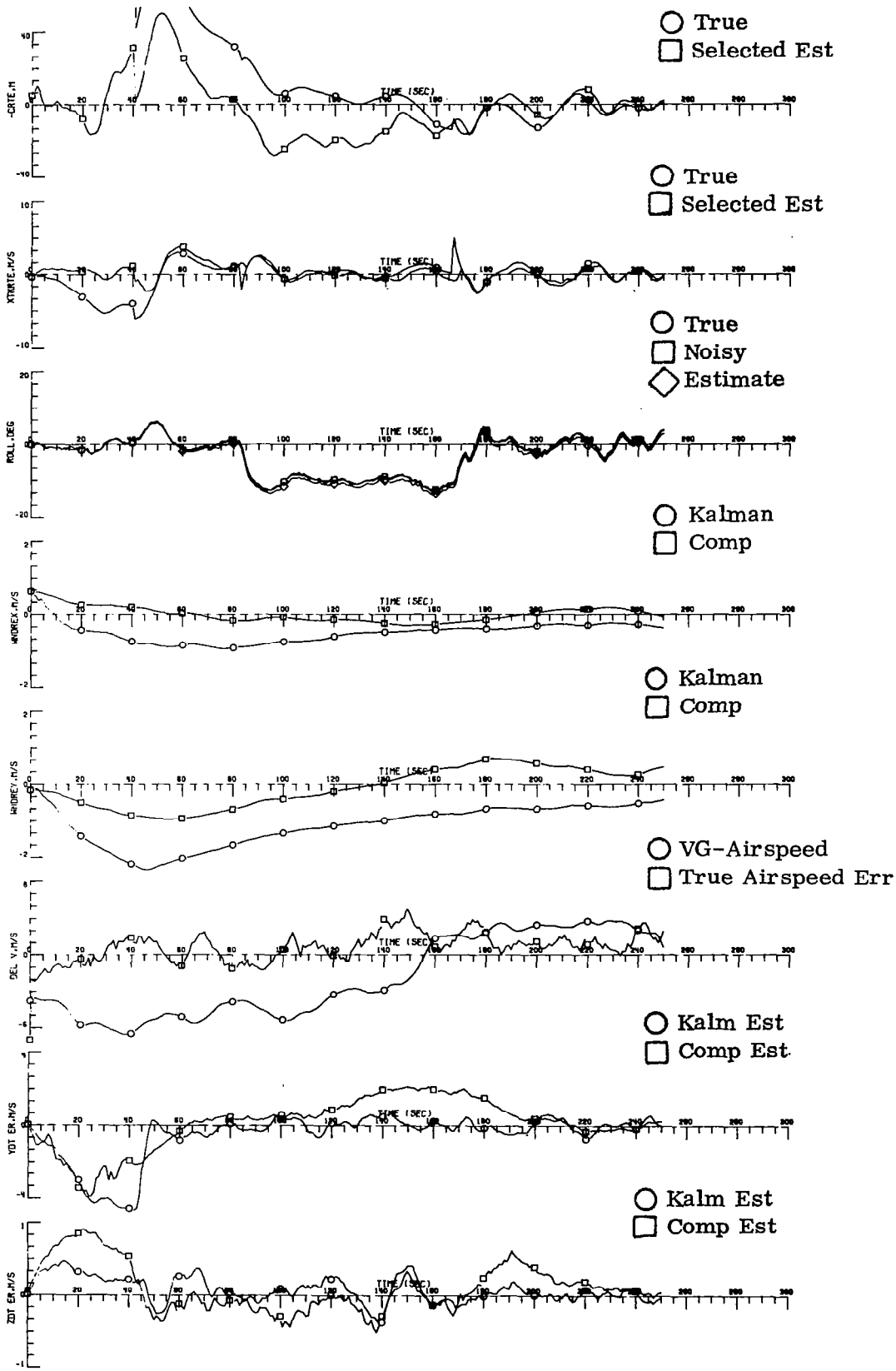

Figure 17(c). - Case 6 Concluded

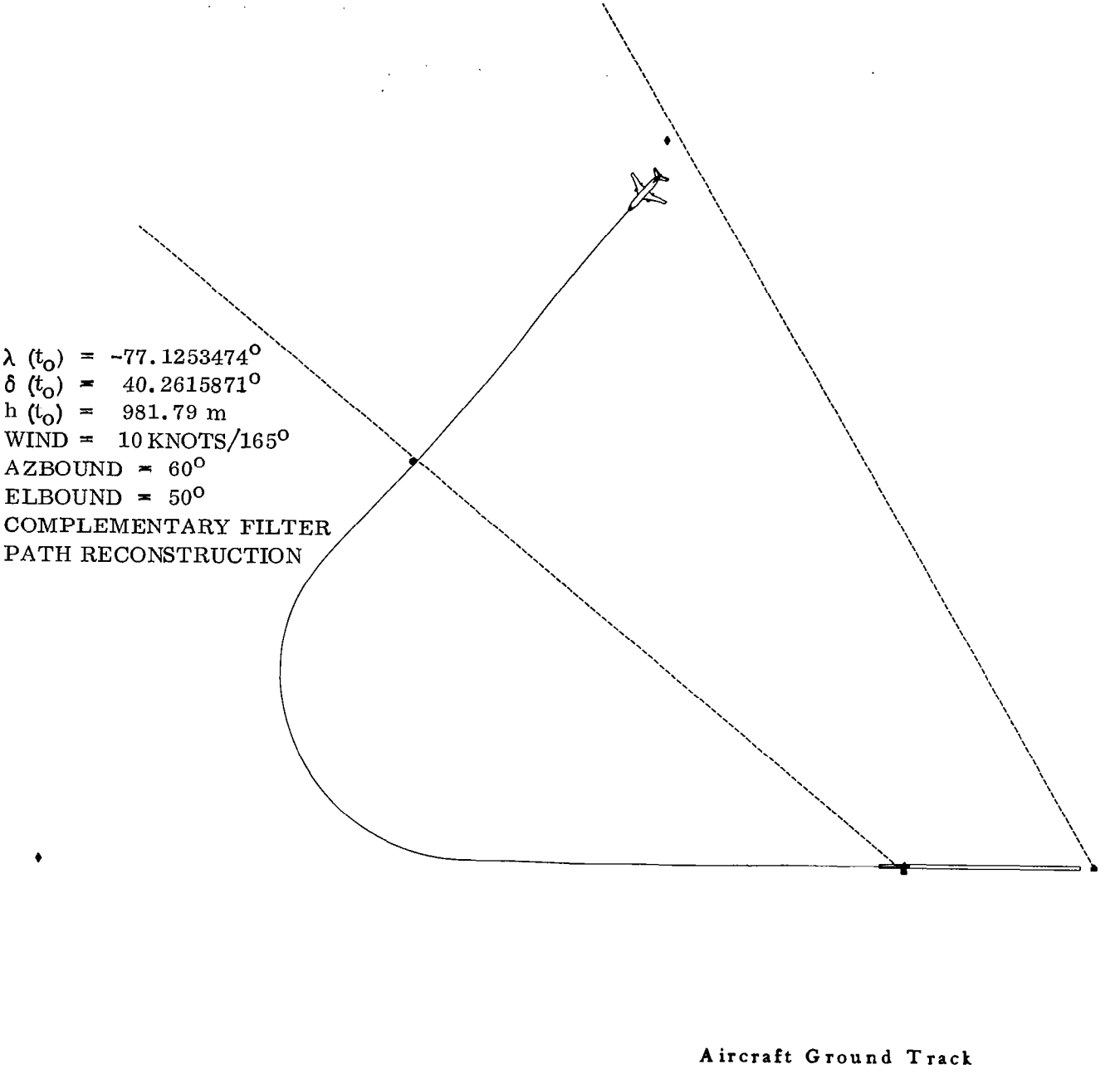

Figure 18(a). – Case 7 MLS Transition With Path Reconstruction at Some Distance From Turn

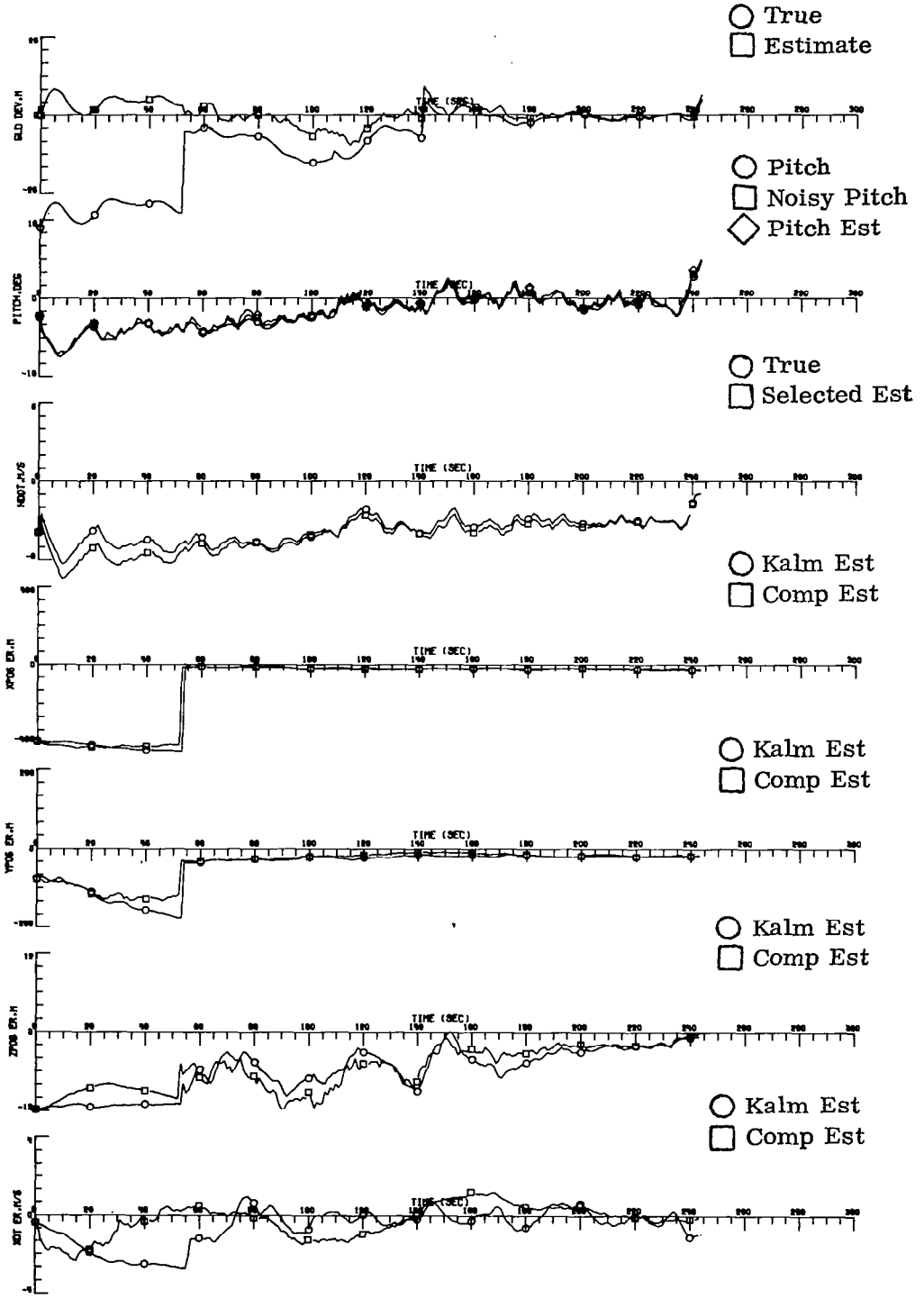

Figure 18(b). – Case 7 Continued

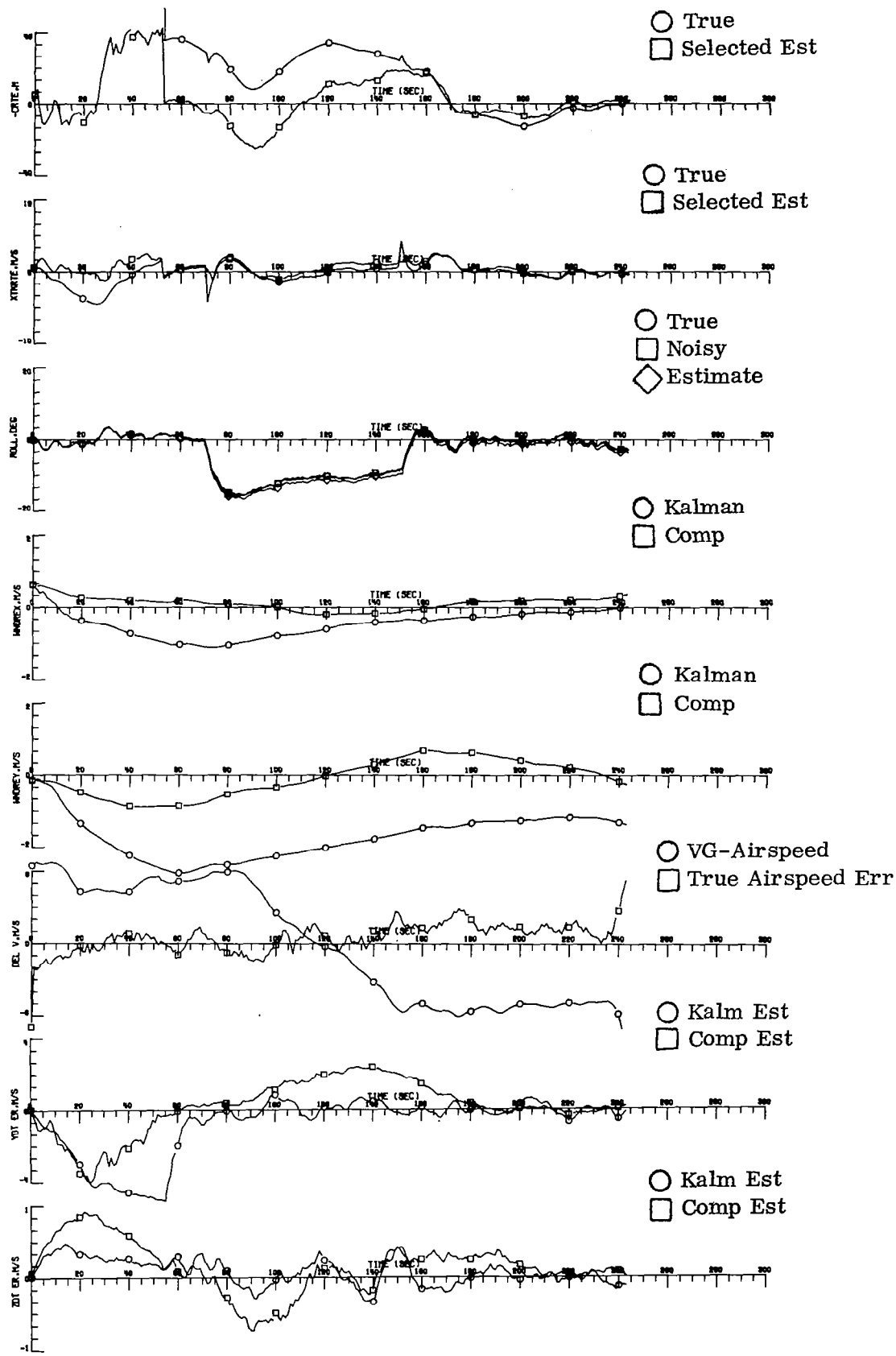

Figure 18(c). - Case 7 Concluded

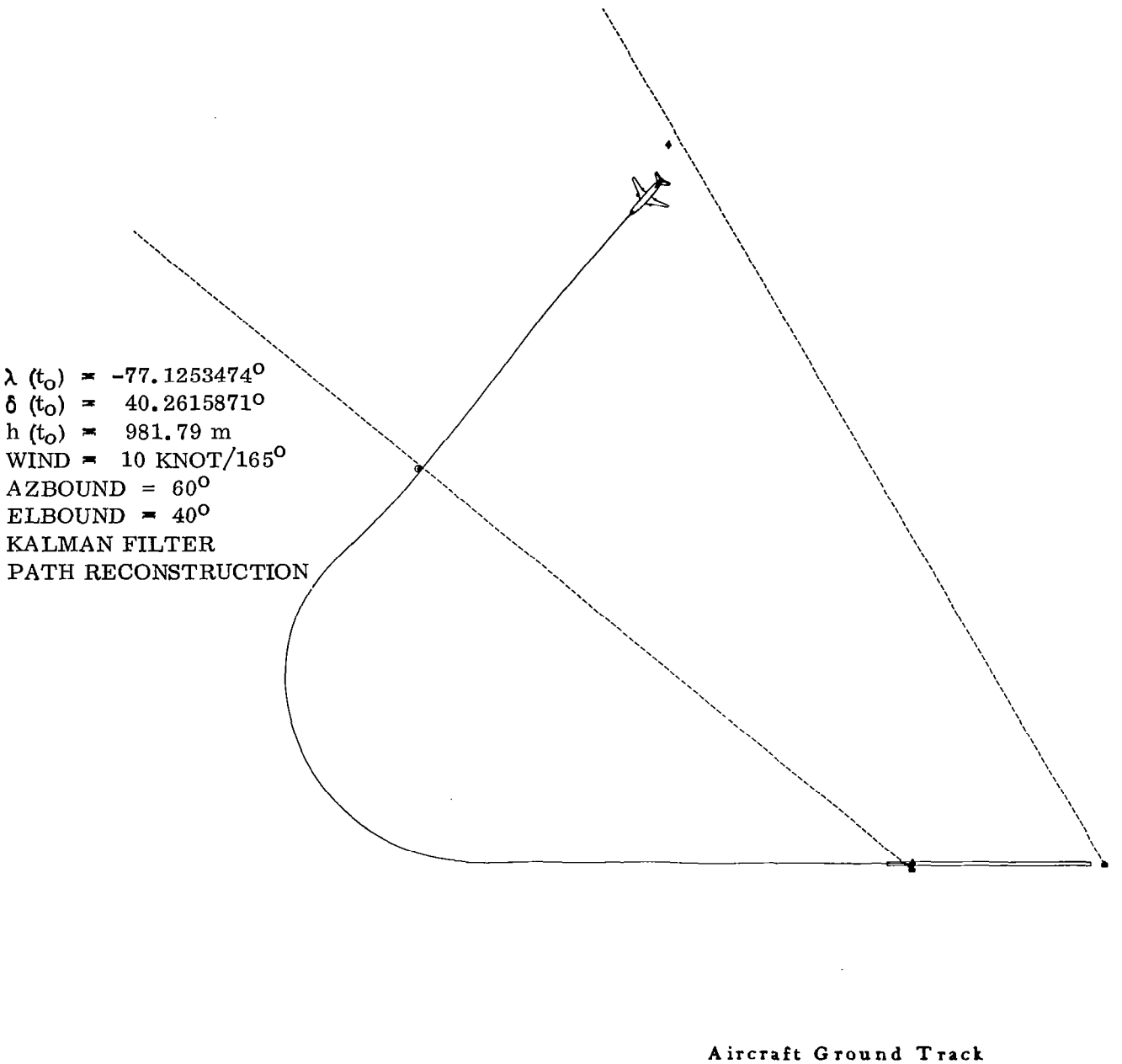

Figure 19(a). – Case 8 MLS Transition With Path Reconstruction Close to Turn

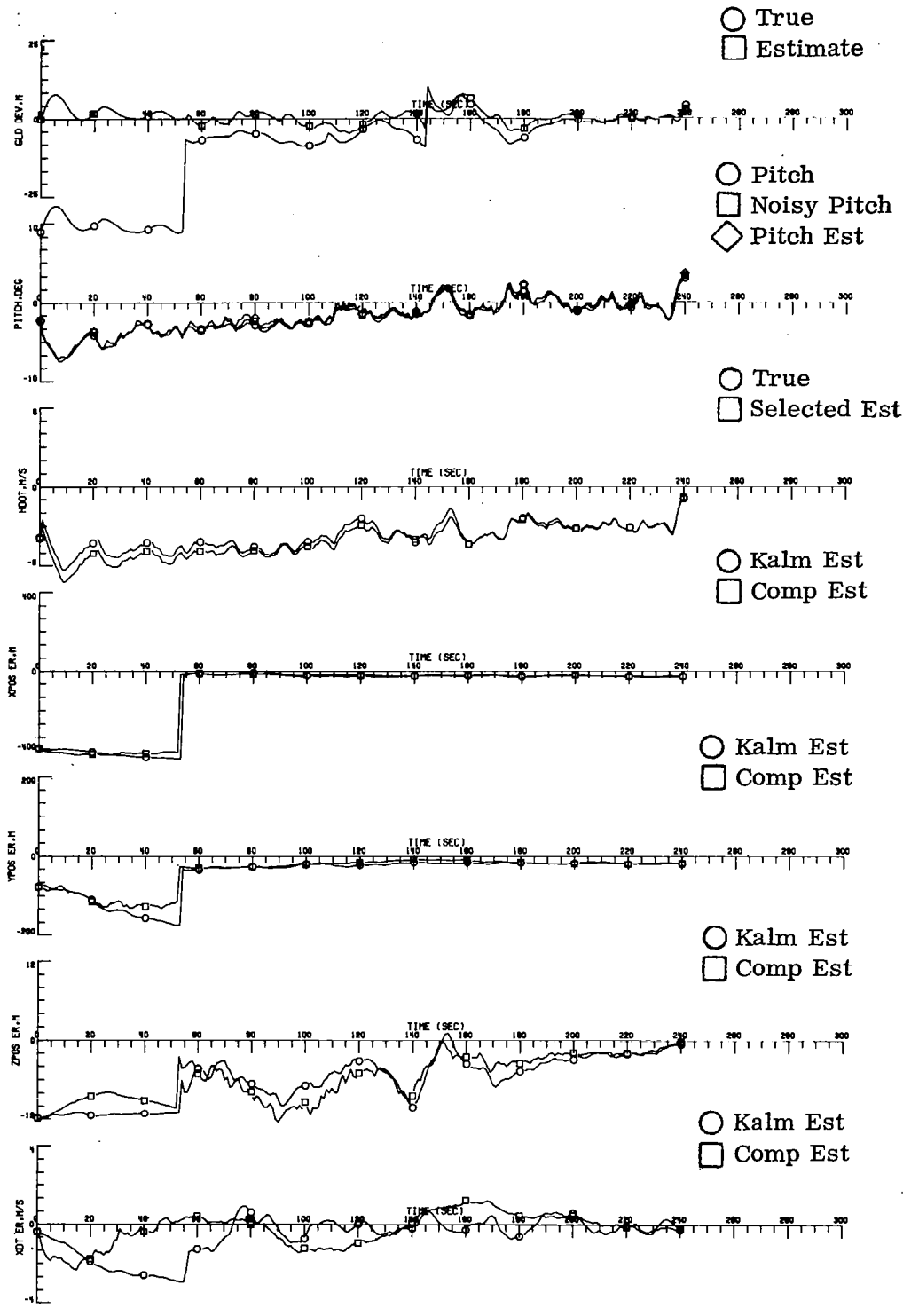

Figure 19(b). – Case 8 Continued

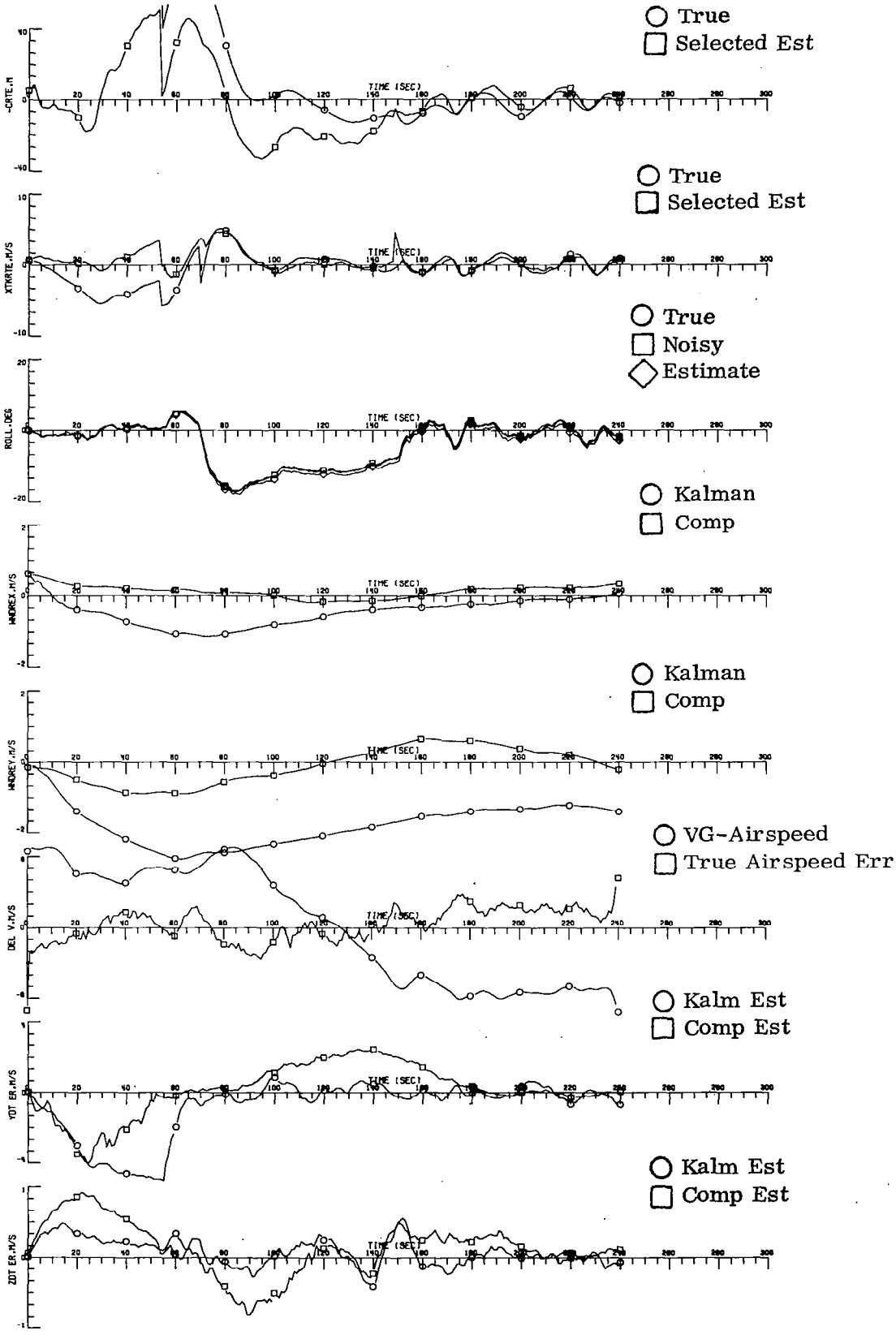

Figure 19(c). – Case 8 Concluded

TABLE III

INPUT DATA FOR WAYPOINT TRAJECTORY CONSTRUCTION

CASE 9

N = 3

I	λ (I) DEG	δ (I) DEG	h (I) m	v_D (I) m/sec
1	-77.0742769	40.2101441	873.25	74.59
2	-77.1152352	40.1298037	331.56	64.31
3	-77.0232052	40.2523725	0	64.31

$R_T(1)$ = 2286 meters

$\psi_{RUNWAY} = 30^{o}$

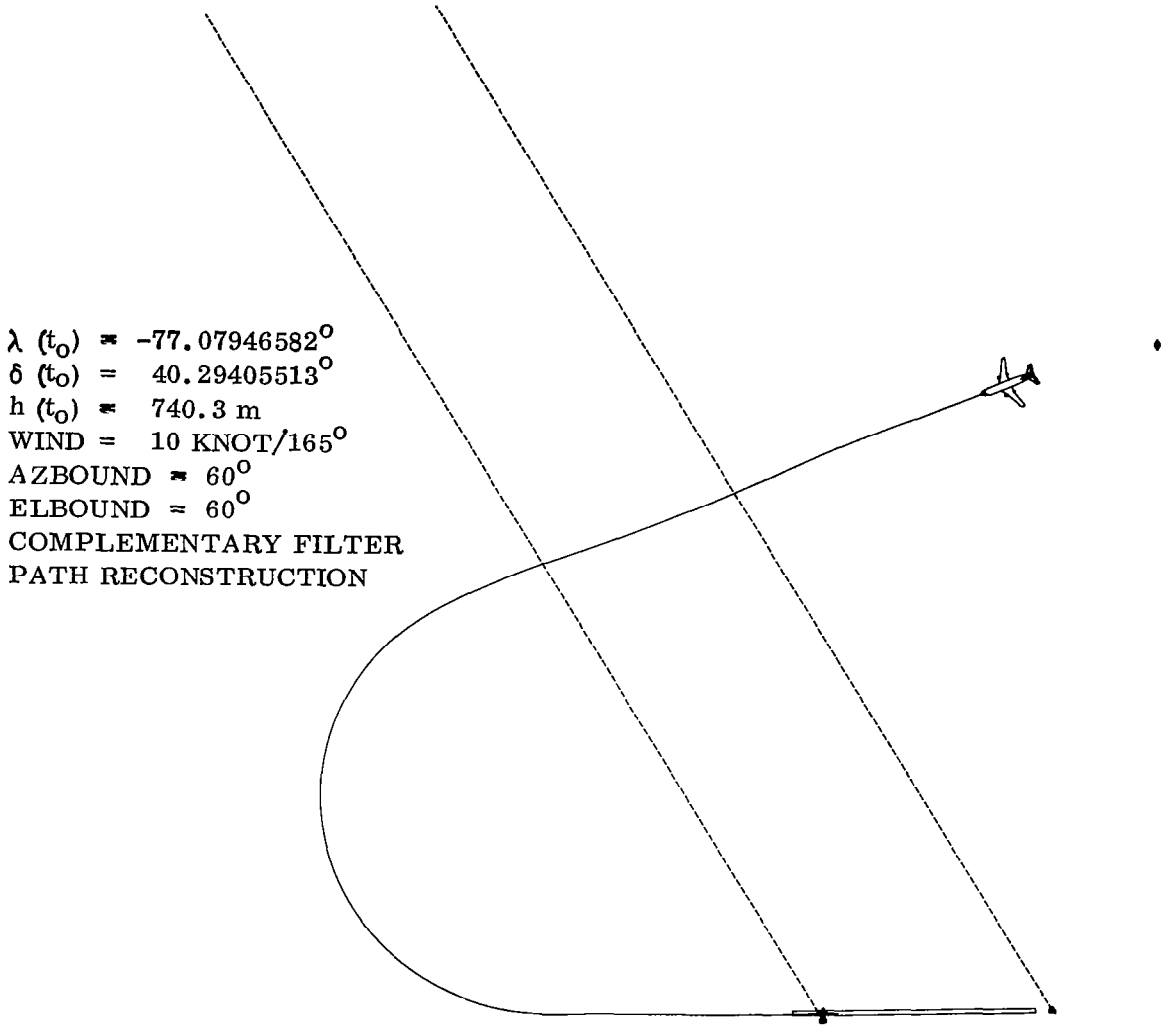

Figure 20(a). – Case 9 MLS Transition When Cross Track Error Does Not Trigger Path Reconstruction

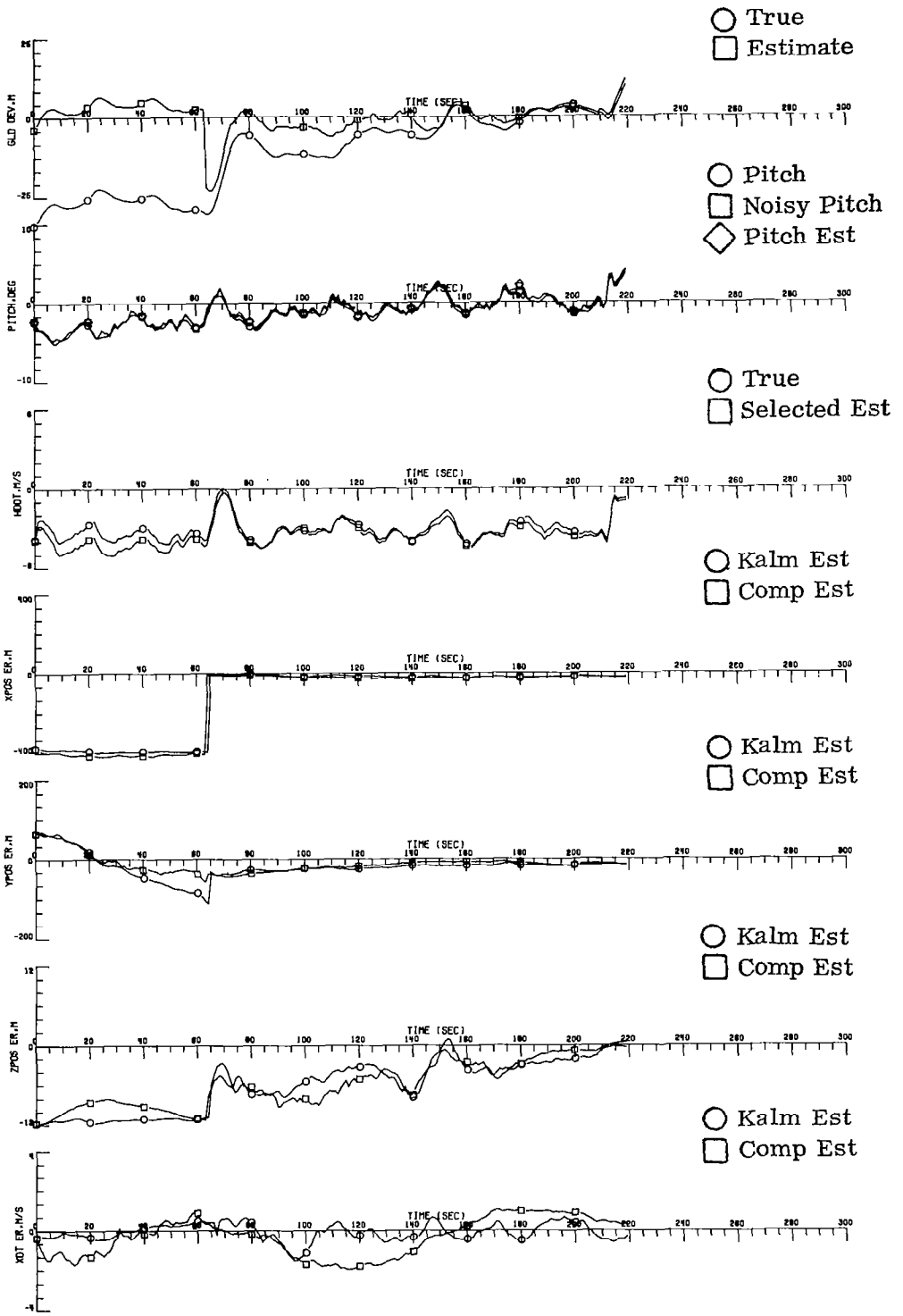

Figure 20(b). – Case 9 Continued

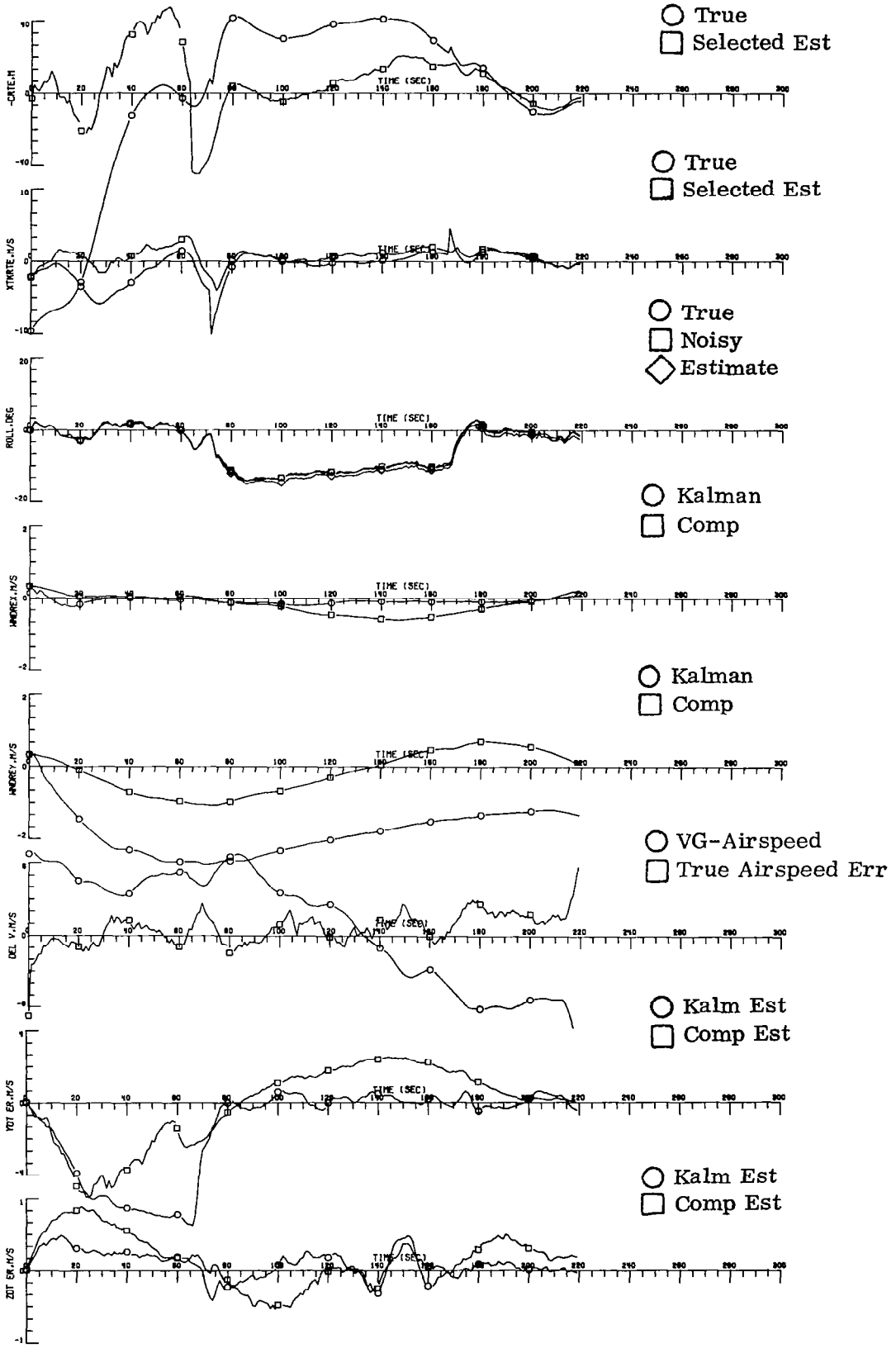

Figure 20(c). - Case 9 Concluded

TABLE IV

INPUT DATA FOR WAYPOINT TRAJECTORY CONSTRUCTION

CASE 10

N = 4

I	λ (I) DEG	δ (I) DEG	h (I) m	v_D (I) m/sec
1	-77.1276539	40.1986043	643.30	74.59
2	-77.1384963	40.25056842	643.87	69.45
3	-77.0530063	40.21295326	241.46	64.31
4	-77.02320524	40.2523725	0	64.31

R_T (1) = 2286 meters

R_T (2) = 2286 meters

$\psi_{RUNWAY} = 30^{o}$

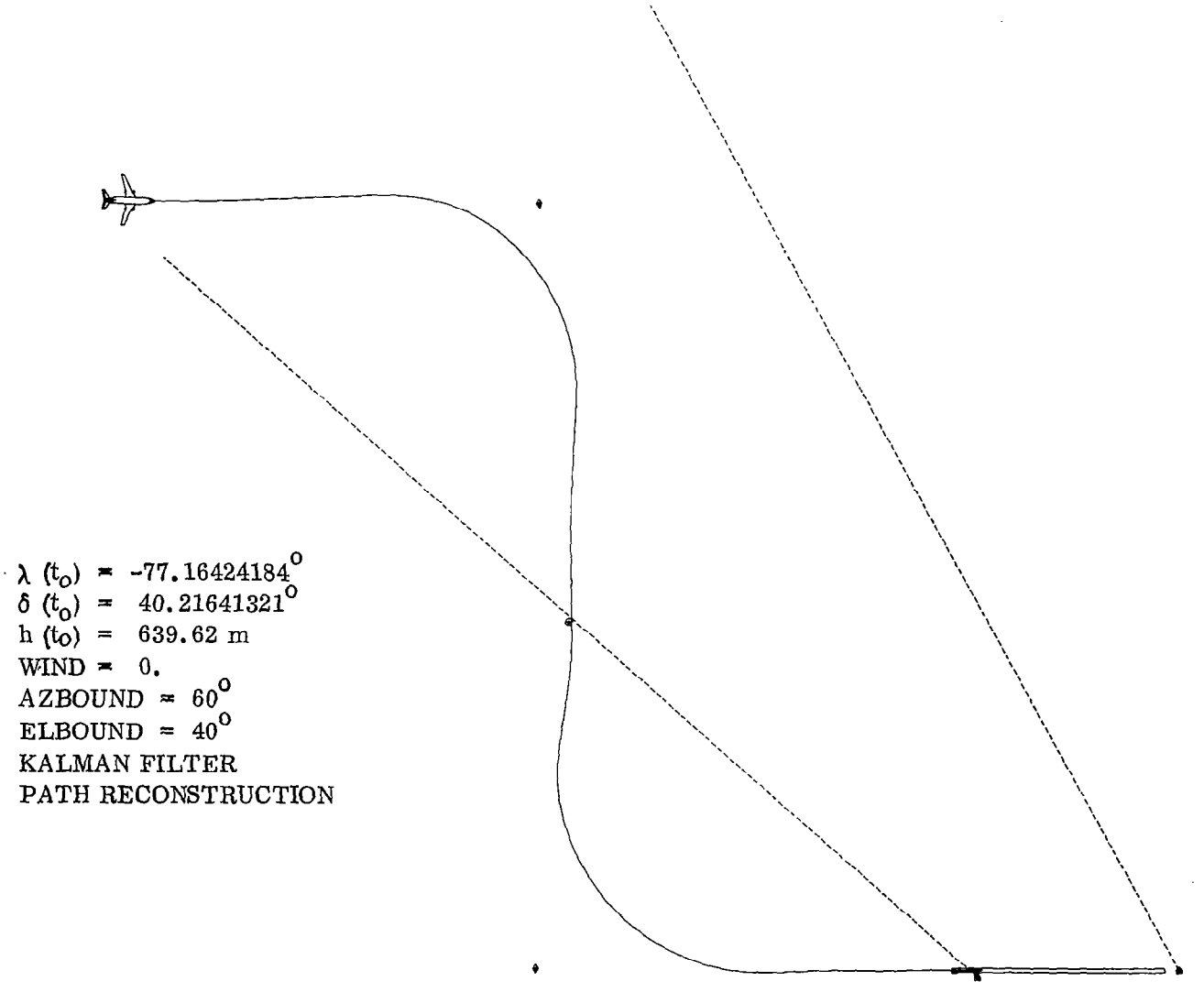

Figure 21(a). – Case 10 MLS Transition With Path Reconstruction and Multiple Turn Capability

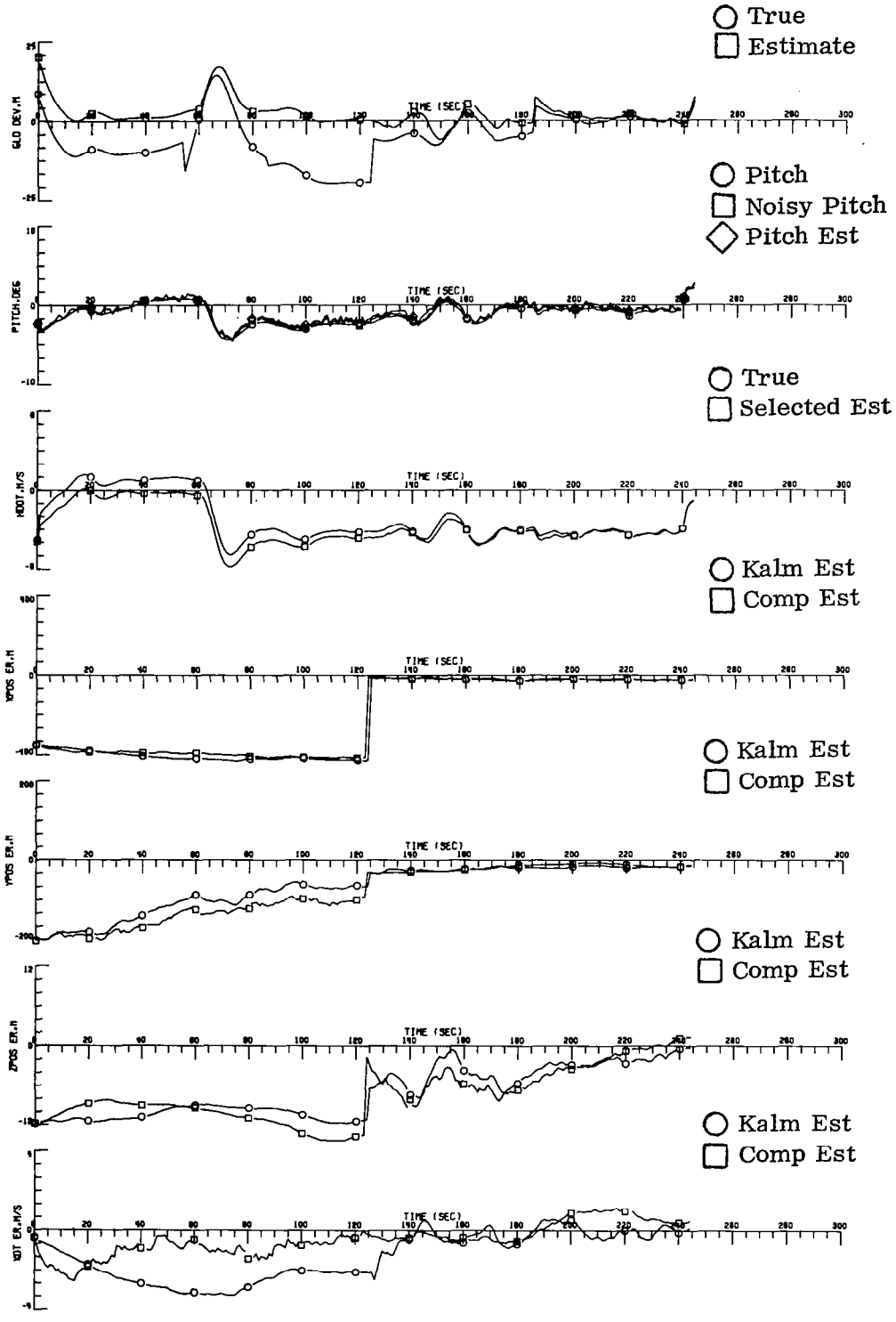

Figure 21(b). – Case 10 Continued

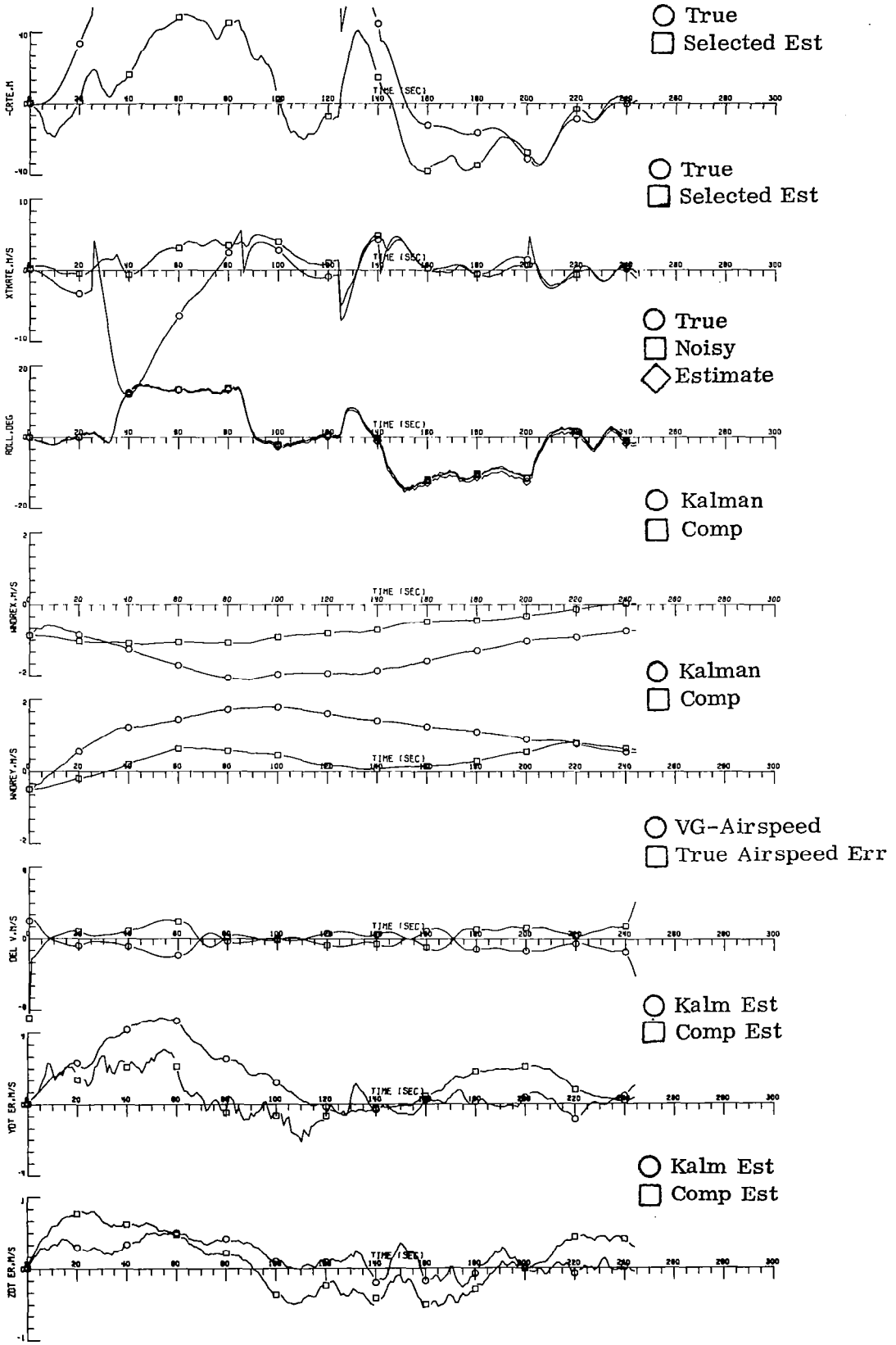

Figure 21(c). – Case 10 Concluded

TABLE V

INPUT DATA FOR WAYPOINT TRAJECTORY CONSTRUCTION

CASE 11

N = 6

I	λ (I) DEG	δ (I) DEG	h (I) m	v_D (I) m/sec
1	-77.04768972	40.2599459	1720.29	77.16
2	-77.09841711	40.192883238	989.38	77.16
3	-77.05699524	40.16107542	650.11	77.16
4	-77.02892824	40.19823274	378.26	72.02
5	-77.04632437	40.22179639	202.60	64.31
6	-77.02320521	40.25237254	0	64.31

R_T (1) = 1828.8 meters

R_T (2) = 2286 meters

R_T (3) = 1524 meters

$\psi_{RUNWAY} = 30^o$

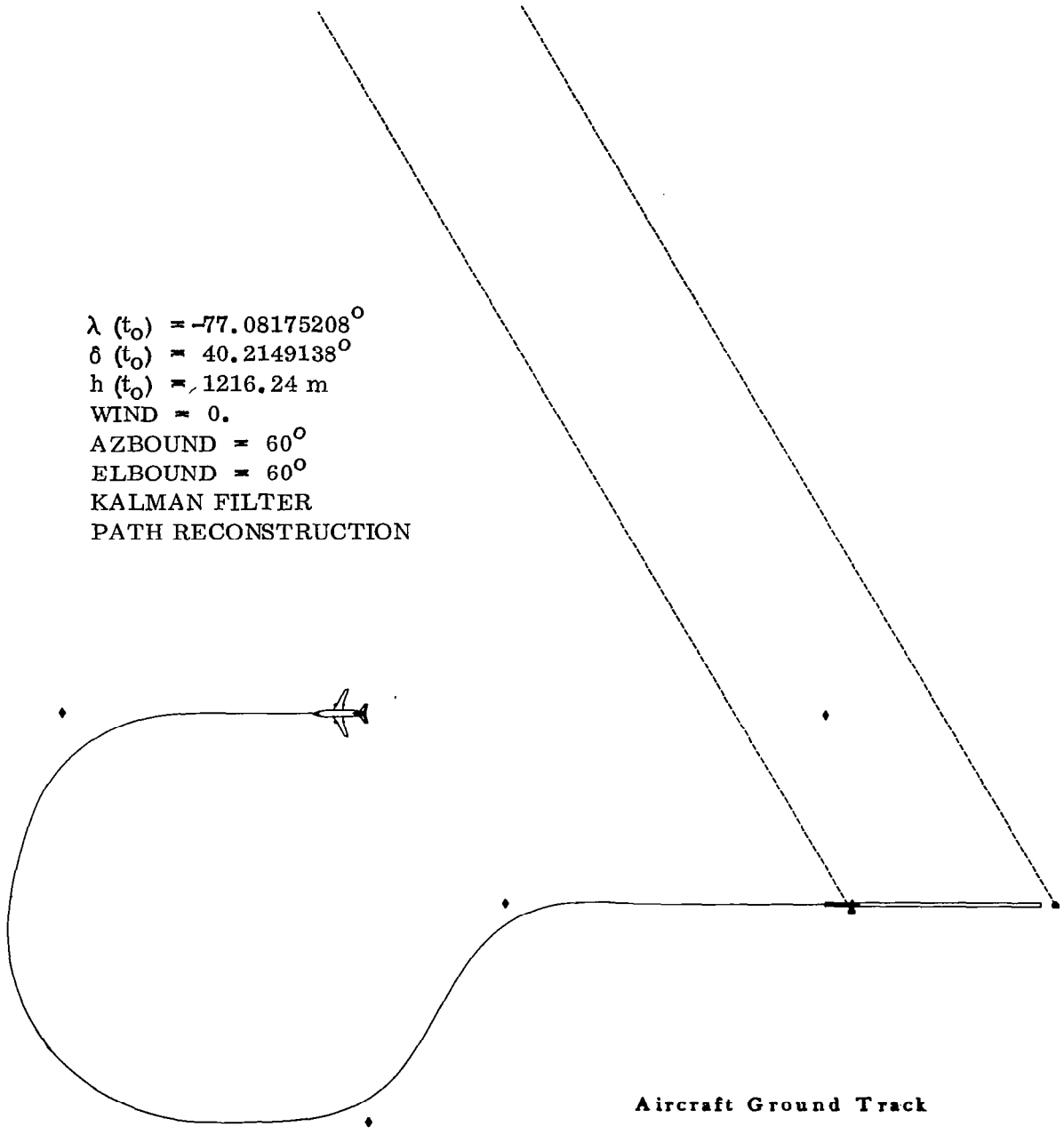

Figure 22(a). – Case 11 MLS Transition With Path Reconstruction and Multiple Turn Capability

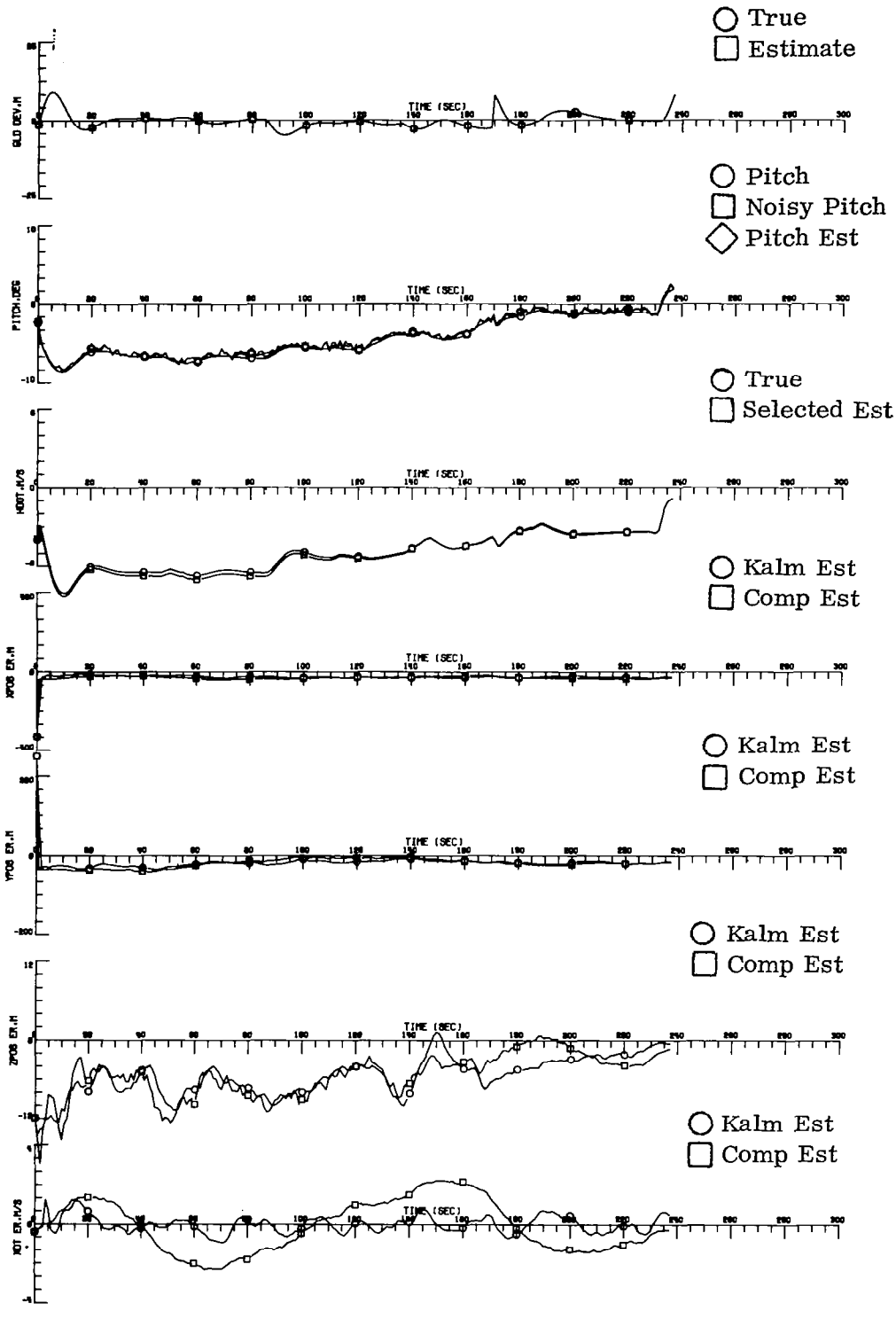

Figure 22(b). - Case 11 Continued

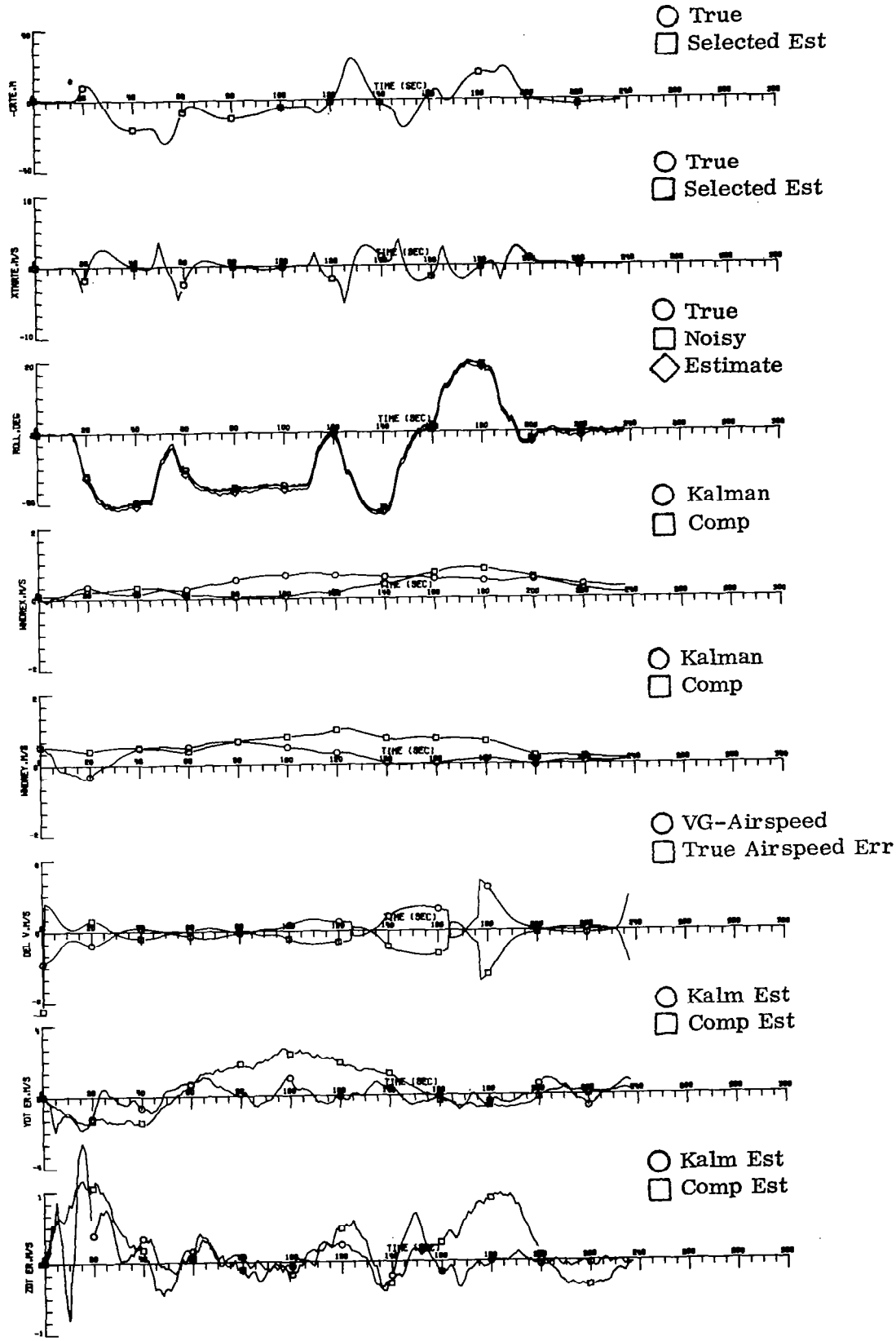

Figure 22(c). - Case 11 Concluded

TABLE VI

VORTAC AND BARO SIMULATION DATA

VORTAC SIMULATION DATA

$\lambda_v = -77.164894^o$

$\delta_v = 40.403016^o$

$h_v = 45.72$ m

VORTAC BIAS

Range bias = 365.76 m

Bearing bias = $.6^o$

VORTAC RANDOM NOISE

$\sigma_v = 48.77$ m

$\sigma_b = .3^o$

BAROMETER SIMULATION DATA

BARO BIAS = 12.19 m

$\sigma_{baro} = 1.524$ m

APPENDIX A

Vectors and Matrices

This appendix derives the equation for rotating a given vector about a fixed unit vector, through a given angle in Cartesian three space. The resulting transformation is used to describe the rotation of one Cartesian coordinate system into another. Rules for vector addition, dot products, and cross products are reviewed. Finally, a vector matrix equation is derived which describes the instantaneous rotation rate vector in the transformed coordinate system in terms of the rotation rates in the component systems comprising the transformation.

A. Elementary Operations on a Vector

A vector is an array of quantities. In this appendix we restrict ourselves to a Cartesian three space. Given a point in the coordinate system (x_1, x_2, x_3), the vector, R, is most easily visualized as the directed line segment from the origin (0., 0., 0.) to the point. Thus the vector R, arranged as a column, is given by

$$R = \begin{Bmatrix} x_1 \\ x_2 \\ x_3 \end{Bmatrix} \tag{A1}$$

The sum of two vectors, $A + B$, is a vector C, whose components are given by the sum of the corresponding components of A and B.

$$C = \begin{Bmatrix} a_1 + b_1 \\ a_2 + b_2 \\ a_3 + b_3 \end{Bmatrix} \tag{A2}$$

The dot product of two vectors, $A \cdot B$, is a scalar functional whose value is given by the sum of the products of the corresponding elements. The operation is commutative

$$A \cdot B = B \cdot A = a_1 b_1 + a_2 b_2 + a_3 b_3 \tag{A3}$$

Thus, $A \cdot A$ is the square of the Cartesian length of the vector;

$$A \cdot A = a_1^2 + a_2^2 + a_3^2 = a^2 \tag{A4a}$$

and we have for the magnitude of A ,

$$a = |A| = (A \cdot A)^{\frac{1}{2}} \tag{A4b}$$

The unit vector , $\hat{A}$, is given by

$$\hat{A} = \frac{1}{a} A \tag{A5}$$

If we consider the dot product of the sum of two vectors into itself, we have

$$(A + B) \cdot (A + B) = a^2 + b^2 + 2 A \cdot B \tag{A6}$$

From the cosine law in trigonometry, we have, if $C = A + B$

$$c^2 = a^2 + b^2 + 2 ab \cos \theta \tag{A7a}$$

Thus, if θ is the angle between A and B, we have

$$A \cdot B = ab \cos \theta \tag{A7b}$$

The cross product of two vectors, $A \times B$, is a vector , C , whose components are defined by ,

$$A \times B = C = \begin{Bmatrix} a_2 b_3 - a_3 b_2 \\ a_3 b_1 - a_1 b_3 \\ a_1 b_2 - a_2 b_1 \end{Bmatrix} \tag{A8}$$

It is plain that $A \times B = -B \times A$.

The cross product of a vector into itself is the null vector

$$A \times A = \begin{Bmatrix} 0 \\ 0 \\ 0 \end{Bmatrix} \tag{A9}$$

The operation of cross product and dot product commute, that is, given three vectors A , B and C

$$(A \times B) \cdot C = A \cdot (B \times C) = B \cdot (C \times A) \tag{A10}$$

It follows from (A10) that if $C = A$, or $C = B$, we have

$$\begin{aligned} (A \times B) \cdot B &= A \cdot (B \times B) = 0 \\ (A \times B) \cdot A &= B \cdot (A \times A) = 0 \end{aligned} \tag{A11}$$

It follows from (A11) that the cross product vector, $A \times B$, is a vector perpendicular to both A and B. Thus $A \times B$ is a vector normal to the plane defined by A and B .

The triple cross product of three vectors, $(A \times B) \times C$ is a vector which is contained in the plane defined by A and B and is orthogonal to C. Thus, we have

$$(A \times B) \times C = B (A \cdot C) - A (B \cdot C) \tag{A12}$$

The square of the length of the cross product vector, $A \times B$, is given by

$$(A \times B) \cdot (A \times B) = (A \cdot A) (B \cdot B) - (A \cdot B)^2 \tag{A13}$$

Thus, we have

$$|A \times B| = a\,b\,|\sin\theta| \tag{A13a}$$

where θ is the angle between vectors A and B.

B. Rotation of a Vector About a Unit Vector Through an Angle

The differential equation for the instantaneous rotation of vector, R, about a fixed unit vector, $\hat{A}$, is given by

$$\frac{d}{dt} R = w \hat{A} \times R \tag{A14}$$

where w is a scalar equal to the instantaneous rotation rate.

To acquire the solution of Eq. (A14) we may interpret the operation $\hat{A} \times$ as a matrix. We have, from Eq. (A8), for any vector, B,

$$\hat{A} \times B = \begin{pmatrix} 0 & -a_3 & a_2 \\ a_3 & 0 & -a_1 \\ -a_2 & a_1 & 0 \end{pmatrix} \begin{Bmatrix} b_1 \\ b_2 \\ b_3 \end{Bmatrix} \tag{A15}$$

where a_1, a_2, and a_3 are the components of $\hat{A}$.

Thus, the operation, $\hat{A} \times$, is a skew symmetric 3 x 3 matrix given by

$$\hat{A} \times = \begin{pmatrix} 0 & -a_3 & a_2 \\ a_3 & 0 & -a_1 \\ -a_2 & a_1 & 0 \end{pmatrix} \tag{A15a}$$

The matrix satisfies the characteristic equation

$$(\hat{A} \times)^3 = -a^2 (\hat{A} \times) \tag{A16}$$

To prove this, we note that

$$\hat{A} \times \left(\hat{A} \times \left[\hat{A} \times B \right] \right) = \hat{A}\ \hat{A} \cdot (\hat{A} \times B) - \hat{A} \cdot \hat{A} (\hat{A} \times B) \tag{A17}$$

Since

$$\hat{A} \cdot (\hat{A} \times B) = 0 \tag{A17a}$$

and B is any vector, we have, for $(\hat{A} \times)$ the identity

$$(\hat{A} \times) (\hat{A} \times) (\hat{A} \times) = - \hat{A} \cdot \hat{A} (\hat{A} \times) \tag{A17b}$$

which proves Eq. (A16).

Since $\hat{A}$ is of unit length, $a^2 = 1$, the eigenvalues of $(\hat{A} \times)$ are $0 , i , -i$; where $i = \sqrt{-1}$.

The formal solution of Eq. (1.14) is

$$R(t) = e^{w t (\hat{A} \times)} R (t_o) \tag{A18}$$

Since the roots of the characteristic equation of $(A \times)$ are $\lambda = 0 , i$, and $-i$, we have, from the Lagrange interpolation formula,

$$e^{wt\,(Ax)} = \sum_{k=1}^{3} \frac{\prod_{\substack{j=1 \\ j \neq k}}^{3} [\, (Ax) - \lambda j I \,]}{\prod_{\substack{j=1 \\ j \neq k}}^{3} (\lambda_k - \lambda_j)} e^{\lambda_k wt} \tag{A19a}$$

where $$I = \begin{Bmatrix} 1 & 0 & 0 \\ 0 & 1 & 0 \\ 0 & 0 & 1 \end{Bmatrix} . \tag{A19b}$$

Evaluating Eq. (A19) for $\lambda = 0$, i and $-i$, we have

$$e^{wt(\hat{A}\,x)} = (I + (1 - \cos wt)\,(\hat{A}\,x)\,(\hat{A}\,x) + \sin wt\,\hat{A}\,x) \tag{A20}$$

The inverse (or reverse) transformation is $e^{-wt(\hat{A}\,x)}$ since

$$e^{-wt(\hat{A}\,x)}\,e^{wt(\hat{A}\,x)} = e^{o} = I \tag{A21}$$

Furthermore, the inverse is the transpose since $(\hat{A}\,x)$ is skew symmetric. It follows that the transformation is orthogonal and represents a rigid rotation of every vector $R(t_o)$ into a corresponding vector $R(t)$ about the unit vector, $\hat{A}$, through the angle, $w\,t$.

If we choose the three unit vectors along the coordinate axes of the rotated system for $R(t_o)$, the corresponding columns in the matrix, $e^{wt(\hat{A}\,x)}$, given by Eq. (A20) will be the images of the three axes in the fixed coordinate system.

Since the transformation depends only on wt and $\hat{A}$ we define

$$T(\alpha_i\,,\,\hat{A}) = e^{\alpha_i(\hat{A}\,x)} \tag{A22}$$

If we have a sequence of rotations of α_1 about $\hat{A}_1$, α_2 about $\hat{A}_2$ in the rotated system resulting from the first rotation, and α_3 about $\hat{A}_3$ in the system rotated about $\hat{A}_2$, etc., we have

$$G = T(\alpha_1\,,\,\hat{A}_1)\,T(\alpha_2\,,\,\hat{A}_2)\,T(\alpha_3\,,\,\hat{A}_3) \tag{A23}$$

a transformation from the rotated system into the fixed original system.

As an illustration of the method we choose an inertial fixed reference frame, given by

x_1 along the Earth North Pole;

x_2 at the intersection of the Greenwich Meridian and the equator at the initial time, t_o;

x_3 at the intersection of the -90^o meridian and the equator at t_o.

As the Earth rotates about its North Pole with constant rate, w_E, we seek the transformation between the initial inertial reference frame and a rotating frame fixed in the rotating planet. We define the transformation to be G_{IE}, from Earth fixed to inertial. Let $\Delta t = t - t_o$

$$G_{IE} = T(w_E \Delta t, \hat{x}_1) \tag{A24}$$

Evaluating Eq. (A20) with

$$\hat{x}_1 = \begin{Bmatrix} 1 \\ 0 \\ 0 \end{Bmatrix} \tag{A25}$$

we have

$$G_{IE} = \begin{bmatrix} 1 & 0 & 0 \\ 0 & \cos w_E \Delta t & -\sin w_E \Delta t \\ 0 & \sin w_E \Delta t & \cos w_E \Delta t \end{bmatrix} \tag{A25a}$$

It is convenient to define a level earth coordinate system with its $\hat{x}_3$ axis to the point on the Earth's surface with right ascension, α_1, and declination δ. We obtain the transformation from level Earth to inertial coordinates through

$$G_{IL} = T(\alpha_1 \hat{x}_1) T(\delta_1 \hat{x}_2) \tag{A26}$$

In matrix form, Eq. (A26) is given by

$$G_{IL} = \begin{bmatrix} \cos\delta & 0 & \sin\delta \\ \sin\delta \sin\alpha_1 & \cos a & -\cos\delta \sin\alpha_1 \\ -\sin\delta \cos\alpha_1 & \sin a & \cos\delta \cos\alpha_1 \end{bmatrix} \tag{A26a}$$

In Earth level coordinates, the $\hat{x}_3$ axis is the radius vector from the Earth center in the inertial system; the $\hat{x}_2$ vector points due west and the $\hat{x}_1$ vector is due north.

C. Rotation Rates

The matrix , $T(\alpha, \hat{A})$, is an orthogonal transformation. Thus it leaves the length of every vector invariant.

$$\{ R \} = T \{ R_o \} \tag{A27}$$

then

$$R \cdot R = [R_o]^T T^{-1} T \{ R_o \} = R_o \cdot R_o \tag{A27a}$$

Furthermore, given any two vectors A and B , the angle between them θ , is invariant under the transformation of (T) . Let

$$\{ A^1 \} = T \{ A \}$$

and (A28)

$$\{ B^1 \} = T \{ B \}$$

then

$$A^1 \cdot B^1 = a^1 b^1 \cos \alpha \tag{A28a}$$

where α is the angle between A^1 and B^1.

From Eq. (A28) we have

$$A^1 \cdot B^1 = [A] T^{-1} T \{ B \} = A \cdot B = a\, b \cos \theta \tag{A28b}$$

Since $a^1 = a$ and $b^1 = a$ we conclude that $\alpha = \theta$.

Since the cross product of two vectors is a vector, we have that

$$(T) [A \times B \} = (T) \{ A \} \times (T) \{ B \} \tag{A29}$$

Furthermore, we have

$$(T)\{A \times B\} = (T)(A\times)T^{-1}\,T\{B\} = (T)\{A\}\times(T)\{B\} \quad \text{(A29a)}$$

Since $T\{B\}$ is an arbitrary vector, we conclude that for all (T) and $\{A\}$

$$(T)(A\times)T^{-1} \equiv \left((T)\{A\}\times\right) \quad \text{(A30)}$$

The result enables us to relate the rotation rate in one coordinate system to the rotation rates in the transformed system.

Let

$$G = T(w_1 t, \hat{A}_1)\,T(w_2 t, \hat{A}_2)\,T(w_3 t, \hat{A}_3) \quad \text{(A31)}$$

We have that

$$\frac{dG}{dt} = w(\hat{B}\times)G \quad \text{(A32)}$$

where $\hat{B}$ is the unit instantaneous rotation axis of the transformation, G and w is its scalar rotation rate.

Differentiating Eq. (A31) we have

$$\frac{d}{dt}G = w_1(\hat{A}_1\times)G + T(w_1 t,\hat{A}_1)\,w_2(\hat{A}_2\times)\,T(w_2 t,\hat{A}_2)\,T(w_3 t,\hat{A}_3) + T(w_1 t,\hat{A}_1)\,T(w_2 t,\hat{A}_3)\,w_3(\hat{A}_3\times)\,T(w_3 t,\hat{A}_3) \quad \text{(A33)}$$

Equating Eq's. (A32) and (A33) we have

$$\hat{w}(\hat{B}x) \equiv w_1(\hat{A}_1 x) + T(w_1 t, \hat{A}_1)\, w_2(\hat{A}_2 x)\, T^{-1}(w_1 t, \hat{A}_1) + T(w_1 t, \hat{A}_1)\, T(w_2 t, \hat{A}_2)\, w_3(\hat{A}_3 x)\, T^{-1}(w_2 t, \hat{A}_2)\, T^{-1}(w_1 t, \hat{A}_1) \tag{A33a}$$

Using the vector cross product identity of Eq. (A30) we have

$$\hat{w}(\hat{B}x) = w_1(\hat{A}_1 x) + w_2\left(\{T(w_1 t, \hat{A}_1)\,\hat{A}_2\}\, x\right) + w_3\left(\{T(w_1 t, \hat{A}_1)\, T(w_2 t, \hat{A}_2)\,\hat{A}_3\}\, x\right) \tag{A34}$$

Since the identity is true for all vectors we may remove the cross product operator and obtain the desired instantaneous rotation rate vector $\hat{w}_B$ in terms of the components in the rotating systems.

$$\hat{w}_B = w_1\hat{A}_1 + w_2\, T(w_1 t, \hat{A}_1)\,\hat{A}_2 + w_3\, T(w_1 t, \hat{A}_1)\, T(w_2 t, \hat{A}_2)\,\hat{A}_3 \tag{A35}$$

To obtain the inverse relationship we note that

$$\frac{d}{dt} G^{-1} = -\hat{w}(\hat{B}x)\, G^{-1} \tag{A36}$$

Following the same logic as in Eq's. (A31) through (A35) we obtain

$$\hat{w}_B = w_3\hat{A}_3 + w_2\, T(w_2 t, \hat{A}_3)\,\hat{A}_2 + w_1\, T(w_2 t, \hat{A}_3)\, T(w_1 t, \hat{A}_2)\,\hat{A}_1 \tag{A37}$$

Equation (1.37) may be used to obtain the body rotation rate in the local level coordinate system, Ω_{BL}, from the knowledge of the measured body rotation rate with respect to the inertial system, Ω_{BI}. We have

$$\frac{d}{dt} T_{BI} = -\Omega_{BI} \times T_{BI} \tag{A38}$$

where

$$T_{BI} = T(\hat{i}, -\varphi)\, T(\hat{j}, -\theta)\, T(\hat{k}, -\psi)\, T(\hat{i}, \pi)\, T(\hat{j}, -\delta)\, T(\hat{i}, -a) \tag{A39}$$

It follows that

$$\begin{aligned}\Omega_{BI} = {} & \dot{\varphi}\,\hat{i} + \dot{\theta} \begin{Bmatrix} 0 \\ \cos\varphi \\ -\sin\varphi \end{Bmatrix} + \dot{\psi} \begin{Bmatrix} -\sin\theta \\ \sin\varphi\cos\theta \\ \cos\varphi\cos \end{Bmatrix} \\ & + T_{BG}\, T(\hat{i}, \pi) \left(\left\{ \hat{j}, \dot{\delta} \right\} + \dot{a} \begin{Bmatrix} \cos\delta \\ 0 \\ \sin\delta \end{Bmatrix} \right)\end{aligned} \tag{A40}$$

Since

$$\delta = \sin^{-1} \frac{x}{r}$$

and (A40a)

$$a = \tan^{-1} \left(\frac{-y}{z} \right)$$

We have

$$\dot{\delta} = \frac{x\,\dot{R} - \dot{R}\,r^2\,\dot{x}}{r^2\,(y^2+z^2)^{\frac{1}{2}}}$$

$$\dot{a} = \frac{-\dot{y} - \tan a\,\dot{z}}{(y^2+z^2)^{\frac{1}{2}}} \tag{A40b}$$

We may now solve for the Euler angle rates, $\dot{\varphi}$, $\dot{\theta}$, and $\dot{\psi}$, from the differential equation

$$\dot{\varphi}\,\hat{i} + \dot{\theta} \begin{Bmatrix} 0 \\ \cos\varphi \\ -\sin\varphi \end{Bmatrix} + \dot{\psi} \begin{Bmatrix} -\sin\theta \\ \sin\varphi\cos\theta \\ \cos\varphi\cos\theta \end{Bmatrix} = \Omega_{BI} - T_{BG} \begin{Bmatrix} \cos\delta\,\dot{a} \\ -\dot{\delta} \\ -\sin\delta\,\dot{a} \end{Bmatrix} \tag{A41}$$

APPENDIX B

Waypoint Path Construction

This appendix derives the equations for constructing a desired path consisting of straight lines (great circles on the surface of a spherical Earth) connected by arcs of circles, fixed on the surface of a rotating spherical Earth, and rotating with the Earth.

The input data required for generating the path is minimal, consisting of the latitude and longitude of a sequence of way points, the radius of the connecting circular arcs, and the desired altitude and airspeed at each way point.

The path is constructed by sequentially connecting each pair of way points by a great circle arc on the surface of the Earth. At each interior way point, a circle is constructed by the intersection of a circular cone from the center of the Earth to the surface of the Earth. The radius of the circular conical base is taken to be the input turn radius at that interior way point. The center of the cone is chosen so that the circle is tangent to both the incoming great circle and the outgoing great circle.

The coordinates of the unit vectors from the Earth center to the two tangent points on the surface of the spherical Earth are designated as additional way points, and the unit vector to the middle of each turn replaces each interior way point. The vertical construction of the path is now accomplished by generating a piecewise linear altitude variation from the middle of each turn to the middle of the next turn as a linear function of the ground track distance between the middle turn points. The initial and final segments are the two great circles connecting the initial way point to the first incoming tangent way point, and the great circle connecting the outgoing final tangent way point to the final way point.

A. Initial Data

Let N be the number of way points (N must be at least three). At each way point we must supply the following:

$$\begin{aligned} &\lambda\,(I) = \text{longitude in degrees} \\ &\delta\,(I) = \text{latitude in degrees} \\ &h\,(I) = \text{altitude in meters} \\ &v_D(I) = \text{airspeed in meters/sec} \end{aligned} \tag{B1}$$

$$I = 1, N$$

and at each interior way point we must supply the following:

$$R_T(I) = \text{radius of the turn (meters)} \tag{B2}$$

$$I = 1, N - 2$$

B. Vector Representation of Each Way Point

The vector representation of each way point is in the Earth fixed frame. Converting the angle data to radians, the way point unit vectors are given by,

$$\hat{WR}\,(I) = \begin{Bmatrix} \sin\delta\,(I) \\ -\cos\delta\,(I)\,\sin\lambda\,(I) \\ \cos\delta\,(I)\,\cos\lambda\,(I) \end{Bmatrix} \tag{B3}$$

$$I = 1, N$$

C. The Unit Normal Vectors

Between each consecutive pair of way points we pass a plane which intersects the Earth surface in a great circle. The unit normal to that plane is given by

$$\hat{WN}(I) = \frac{\hat{WR}(I) \times \hat{WR}(I+1)}{\left|\hat{WR}(I) \times \hat{WR}(I+1)\right|} \qquad (B4)$$

$$I = 1, N-1$$

The vector magnitude of the cross product is required for the computation of the change in yaw heading angle at each interior corner way point. Let

$$DN(I) = \left|\hat{WR}(I) \times \hat{WR}(I+1)\right| \qquad (B4a)$$

$$I = 1, N-1$$

D. The Change in Yaw Heading

The change in yaw heading at each interior way point is the angle through which the unit normal vector $\hat{WN}(I)$ must be rotated about the unit way point, $\hat{WR}(I+1)$, in order to coincide with the outgoing unit normal vector, $\hat{WN}(I+1)$. (See Fig. 23). Since the interior waypoint vector, $\hat{WR}(I+1)$ is perpendicular to both the incoming and the outgoing normals, we have

$$\hat{WN}(I+1) = \cos[\Delta\psi(I)]\,\hat{WN}(I) - \sin[\Delta\psi(I)]\,\hat{WR}(I+1) \times \hat{WN}(I) \qquad (B5)$$

From Eq. (B5) we have

$$\hat{WN}(I) \cdot \hat{WN}(I+1) = \cos[\Delta\psi(I)] \qquad (B6a)$$

$$I = 1, N-2$$

and

$$\hat{WR}(I+1) \times \hat{WN}(I) \cdot \hat{WN}(I+1) = -\sin[\Delta\psi(I)] \qquad (B6b)$$

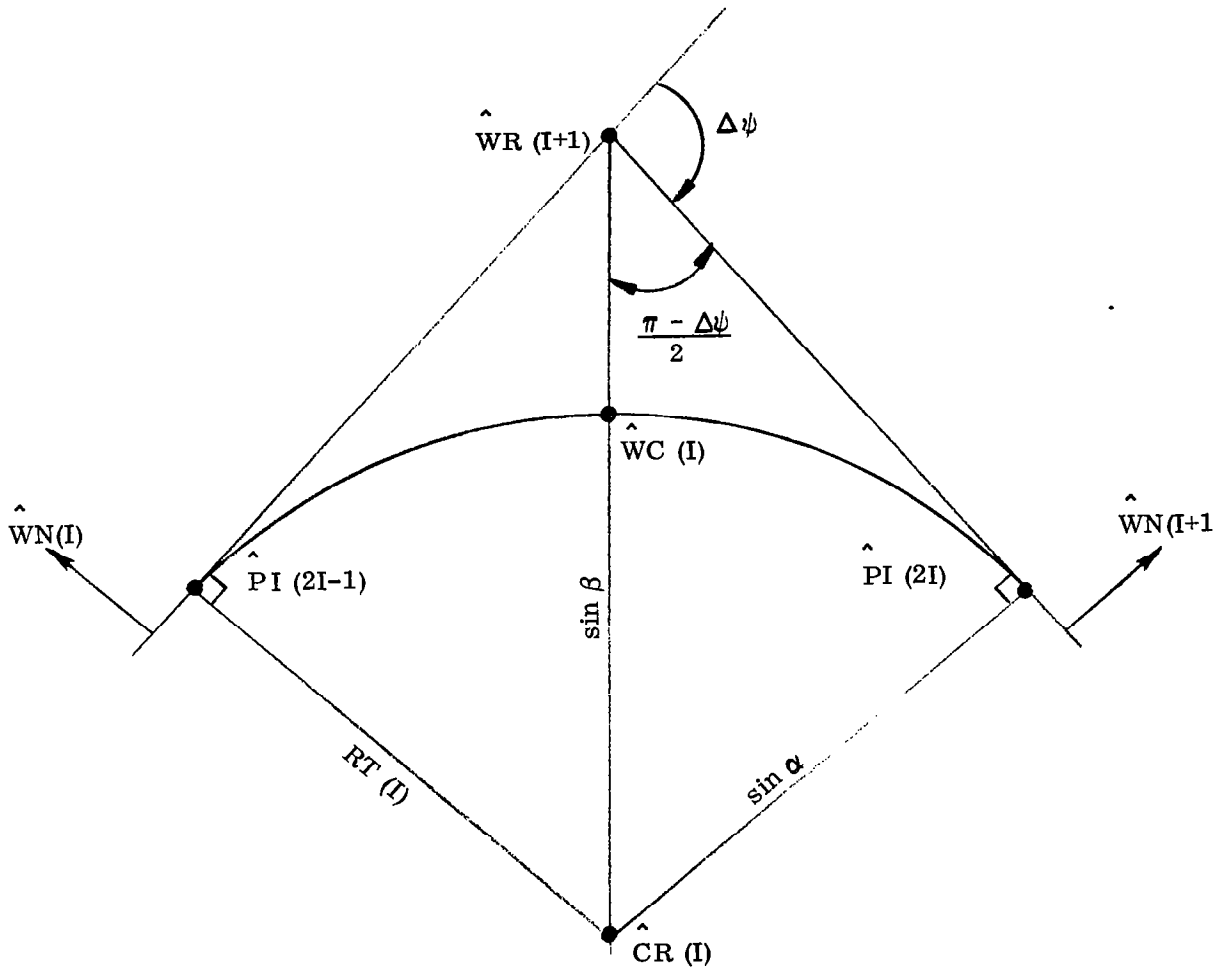

Figure 23.–Turn Circle Geometry for Positive Heading Change

Since, from Eq. (B4),

$$\hat{WN}(I) = \frac{\hat{WR}(I) \times \hat{WR}(I+1)}{DN(I)} \tag{B6c}$$

we have

$$\hat{WR}(I+1) \times \hat{WN}(I) = \frac{\hat{WR}(I) - \hat{WR}(I+1)\left(\hat{WR}(I) \cdot \hat{WR}(I+1)\right)}{DN(I)} \tag{B6d}$$

and Eq. (B6b) becomes

$$\frac{\hat{WR}(I) \cdot \hat{WN}(I+1)}{DN(I)} = -\sin\left[\Delta\psi(I)\right] \tag{B6e}$$

$$I = 1, N-2$$

It follows that the change in heading is given by

$$\Delta\psi = \tan^{-1}\left(\frac{-\hat{WR}(I) \cdot \hat{WN}(I+1)}{DN(I)\left(\hat{WN}(I) \cdot \hat{WN}(I+1)\right)}\right) \tag{B7}$$

$$I = 1, N-2$$

The four quadrant definition of arc tangent should be used to evaluate Eq. (B 7).

E. Center of the Circular Turn

We note that for each interior way point $\hat{WR}(I+1)$, the unit radius vector at the center of the turn $\hat{CR}(I)$, the unit vector at the middle of the turn $\hat{WC}(I)$, and $\hat{WR}(I+1)$ all lie in a plane. (See Fig. 24). Furthermore, since $\hat{WN}(I)$ and $\hat{WN}(I+1)$ are perpendicular to $\hat{WR}(I+1)$, it follows that the sum $\hat{WN}(I) + \hat{WN}(I+1)$ is perpendicular to $\hat{WR}(I+1)$ and also lies in the same plane.

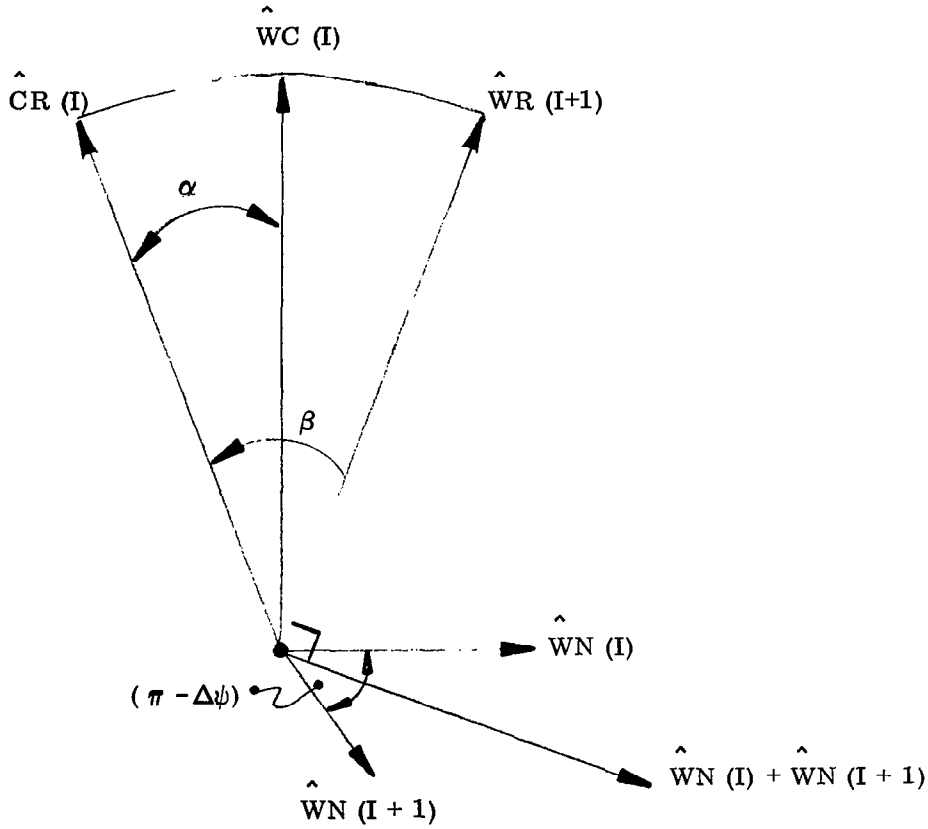

Note: For a negative ($\Delta\psi$) the vectors $\hat{WN}$ (I) and $\hat{WN}$ (I + 1) will be in the opposite direction.

Figure 24.—Center of Turn and Middle of Turn Vectors

We have

$$\hat{SUMV}(I) = \frac{\hat{WN}(I) + \hat{WN}(I+1)}{\left|\hat{WN}(I) + \hat{WN}(I+1)\right|} \qquad (B8)$$

$$I = 1, N-2$$

where

$$\left|\hat{WN}(I) + \hat{WN}(I+1)\right| = 2\left|\cos\frac{\Delta\psi}{2}\right| \qquad (B8a)$$

It follows that $\hat{WN}(I+1)$ and $\hat{SUMV}(I)$ form a perpendicular basis for all vectors in the common plane. Let β be the angle between the center of the turn, $\hat{CR}(I)$ and $\hat{WR}(I+1)$; then the unit vector at the center of the circle is

$$\hat{CR}(I) = \cos\beta\,\hat{WR}(I+1) - \text{sign}(\Delta\psi)\sin\beta\,\hat{SUMV}(I) \qquad (B9)$$

$$I = 1, N-2$$

Let α be the angle between $\hat{CR}(I)$ and $\hat{WC}(I)$ on the circle with radius, $R_T(I)$. Then, we have

$$\sin\alpha = \frac{R_T(I)}{r_E} \qquad (B10)$$

and the unit vector to the middle of the turn, $\hat{WC}(I)$, is given by

$$\hat{WC}(I) = \cos(\beta-\alpha)\,\hat{WR}(I+1) \pm \text{sign}(\Delta\psi)\sin(\beta-\alpha)\,\hat{SUMV}(I) \qquad (B11)$$

$$I = 1, N-2$$

To obtain an expression for the angle , β , we have from spherical triangles, using Fig. 23 ,

$$\sin\beta = \frac{\sin\alpha}{\cos\frac{\Delta\psi}{2}} \qquad (B12a)$$

$$\cos\beta = \sqrt{1 - \sin^2\beta} \tag{B12b}$$

From Eq. (B12a) we conclude that since the maximum value of $\sin\beta = 1.$, that the limiting value of $\frac{\Delta\psi}{2}$ is given by

$$\frac{\Delta\psi}{2} = \cos^{-1}\left(\sin\left(\frac{R_T}{r_e}\right)\right) \tag{B13}$$

This value occurs when the two great circle paths are parallel meridians meeting at a point halfway around the Earth sphere from the circle center. For this limiting value of $\frac{\Delta\psi}{2}$, the two radii from the center to the incoming and outgoing tangent points lie a great circle, containing $\hat{CR}$ (I) .

The normal at the middle of the turn is required in the guidance parameter equations in order to compute the distance to go to complete the half turn. We have

$$\hat{WNE}\ (I) = \hat{SUMV}\ (I) \tag{B13a}$$

$$I = 1\ ,\ N - 2$$

For the end of the turn we note that the normal at the outgoing tangent way point is $\hat{WN}\ (I + 1)$.

F. The Incoming and Outgoing Tangent Unit Vectors

To obtain the equation for the unit vector tangent way points, we note that the circle center $\hat{CR}$ (I) and the normal to the great circle, $\hat{WN}$ (I) lie in a plane containing the incoming tangent waypoint $\hat{PI}$ (I). (See Fig. 25). Since $\hat{PI}$ (I) is perpendicular to $\hat{WN}$ (I) , we have

$$\hat{PI}\ (2I - 1) = \frac{1}{\cos\alpha}\left(\hat{CR}\ (I) + \text{sign}\ (\Delta\psi)\ \sin\alpha\ \hat{WN}\ (I)\right) \tag{B14}$$

$$I = 1\ ,\ N - 2$$

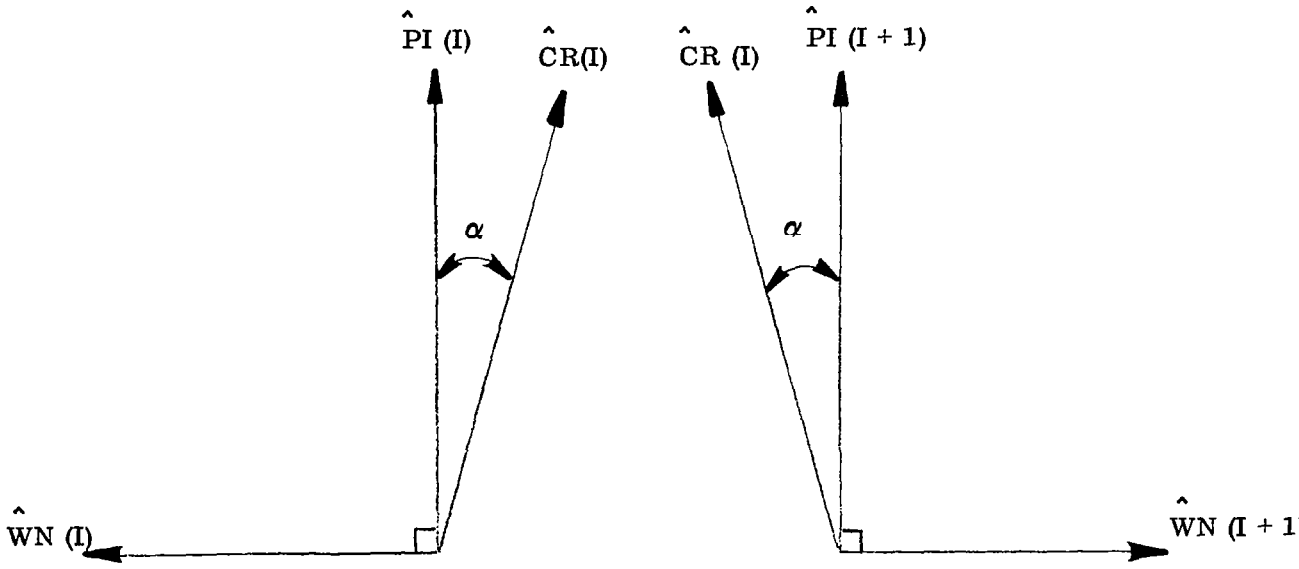

Note: For negative ($\Delta\psi$) the directions of $\hat{WN}$ (I + 1) and $\hat{WN}$ (I) will be reverses in the figure.

Figure 25.–Incoming and Outgoing Tangent Vectors

Similarly, for the outgoing unit tangent way point we have

$$\hat{PI}(2I) = \frac{1}{\cos\alpha}\left(\hat{CR}(I) + \text{sign}(\Delta\psi)\sin\alpha\,\hat{WN}(I+1)\right) \qquad (B15)$$

$$I = 1,\ N-2$$

G. Altitude and Airspeed Gradients

To compute the gradient in altitude and airspeed, we assign to the initial and final unit way points, as well as to each interior unit middle of the turn way points, $\hat{WC}(I)$, a desired altitude and airspeed. By determining the ground track distance between these successive way points, we may compute the gradient in altitude and airspeed over each element. (See Figs. (26a), (26b) and (26c).

The distance between the initial way point and the first middle way point is given by

$$DST(1) = r_E \sin^{-1}\left(\left|\hat{WR}(1) \times \hat{PI}(1)\right|\right) + R_T(1)\left|\frac{\Delta\psi}{2}(1)\right| \qquad (B16)$$

The distance between each of two successive middle of the turn unit way points is given by

$$DST(I) = R_T(I-1)\left|\frac{\Delta\psi}{2}(I-1)\right| + r_e \sin^{-1}\left(\left|\hat{PI}(2I-2) \times \hat{P}(2I-1)\right|\right) + R_T(I)\left|\frac{\Delta\psi}{2}(I)\right| \qquad (B17a)$$

$$I = 2,\ N-2$$

$$(N > 3)$$

Finally, the distance between the last middle of the turn way point and the final touch down way point $\hat{WR}(N)$, is given by

$$DST(N-1) = R_T(N-2)\left|\frac{\Delta\psi}{2}(N-2)\right| + r_e \sin^{-1}\left(\left|\hat{PI}(2N-4) \times \hat{WR}(N)\right|\right) \qquad (B17b)$$

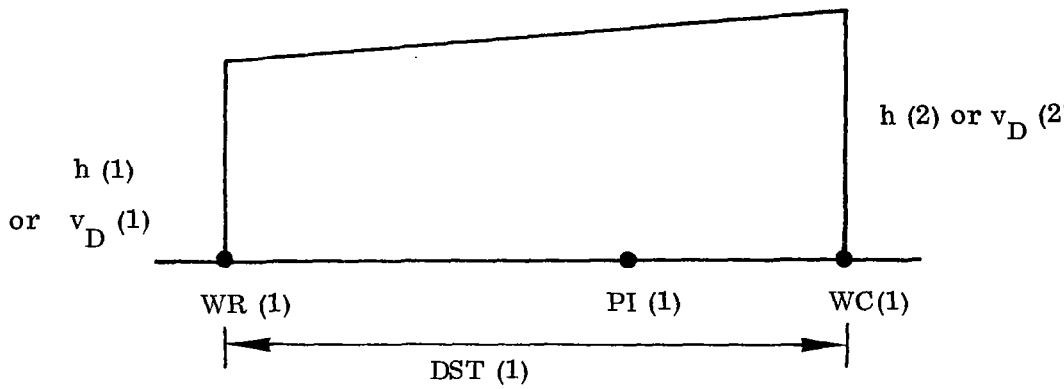

(a) Initial Gradients

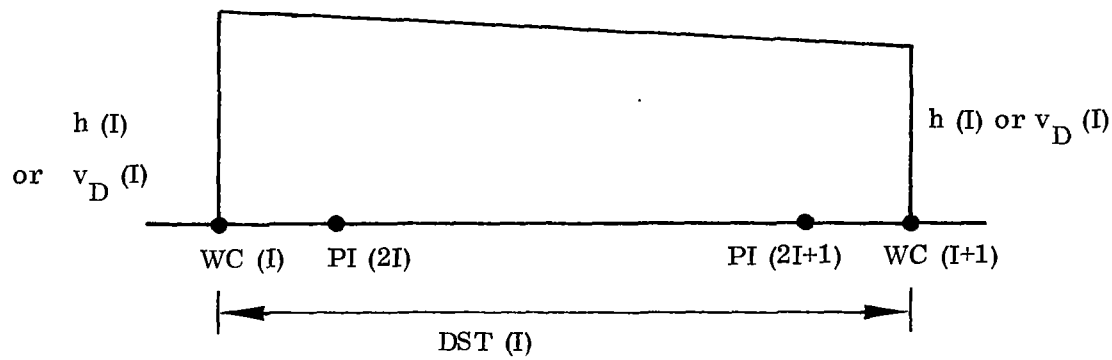

(b) Interior Gradients

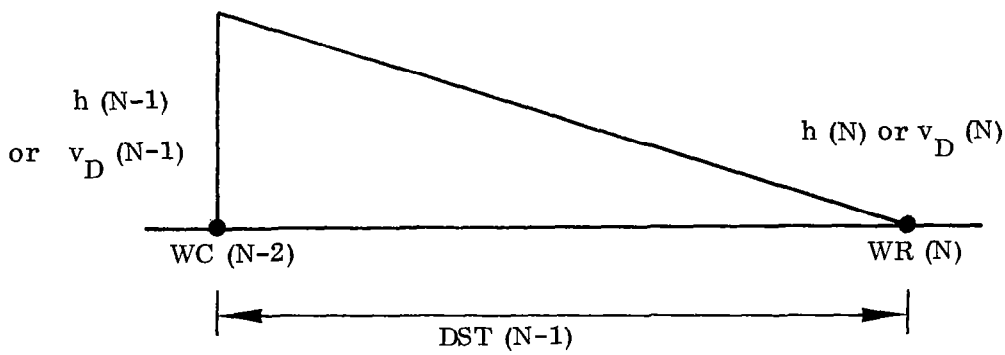

(c) Final Gradients

Figure 26.-Vertical Path Construction

The gradient in altitude for each element is given by

$$\text{GRAD (I)} = \frac{h\,(I+1) - h\,(I)}{\text{DST (I)}} \qquad \text{(B18)}$$

$$I = 1,\ N-1$$

The gradient in airspeed is given by

$$\text{DVG (I)} = \frac{v_D\,(I+1) - v_D\,(I)}{\text{DST (I)}} \qquad \text{(B19)}$$

H. Way Point Guidance Array

If the initial input contains N way points, the final path contains 3N - 4 way points. These way points subtend 3N - 5 segments; N - 1 of these are arcs of great circles and 2 (N - 2) comprise N - 2 pairs of half turns. Each segment is described by a vector array of 19 elements used in RNAV guidance on that particular segment.

The guidance parameters, detailed in Section I (b) (page 12) of this report, require data which are constant over each of the 3N - 5 segments. These data are conveniently arranged in 3N - 5 guidance parameter vector arrays to be computed initially at the beginning of each flight and called by the guidance logic in sequence as required. The elements of each array are listed below for both great circles and half turn circles.

Let II go from 1 to 3N - 5

$$\begin{aligned} &J = \text{Integer part } (II/3) + 1 \\ &K = 2J - 1 \\ &\text{If MODULO } (II,3) = 2, \text{ then } L = J \\ &\text{If MODULO } (II,3) = 0, \text{ then } L = J - 1 \end{aligned} \qquad \text{(B20)}$$

For Great Circles

$$WP(1) = \hat{WN}(J, 1)$$
$$WP(2) = \hat{WN}(J, 2)$$
$$WP(3) = \hat{WN}(J, 3)$$
$$WP(4) = \hat{PI}(K, 1)$$
$$WP(5) = \hat{PI}(K, 2)$$
$$WP(6) = \hat{PI}(K, 3)$$

(B20)
Cont'd.

If $II = 3N - 5$,

$$\left(\begin{array}{l} WP(4) = \hat{WR}(N, 1) \\ WP(5) = \hat{WR}(N, 2) \\ WP(6) = \hat{WR}(N, 3) \end{array}\right)$$

$$WP(7) = \text{sign}\left(\Delta\psi(J)\right)$$
$$WP(8) = \hat{CR}(J, 1)$$
$$WP(9) = \hat{CR}(J, 2)$$
$$WP(10) = \hat{CR}(J, 3)$$
$$WP(11) = 0$$
$$WP(12) = R_T(J)$$
$$WP(13) = 0$$
$$WP(14) = \sin\left(\tan^{-1}(GRAD(J))\right)$$

If $II = 1$

$$\left(\begin{array}{l} HEND = H(1) \\ VEND = V_D(1) \end{array}\right)$$

If $II > 1$, but $< 3N - 5$

$$\left(\begin{array}{l} HEND = HEND + GRAD(J)\left(r_E \sin^{-1}\left(\left|\hat{PI}(2J-2) \times \hat{PI}(2J-1)\right|\right)\right) \\ VEND = VEND + DVD(J)\left(r_E \sin^{-1}\left(\left|\hat{PI}(2J-2) \times \hat{PI}(2J-1)\right|\right)\right) \end{array}\right)$$

If $II = 3N - 5$

$$\left(\begin{array}{l} HEND = H(N) \\ VEND = V_D(N) \end{array}\right)$$

$$WP(15) = HEND$$
$$WP(16) = GRAD(J)$$
$$WP(17) = VEND$$
$$WP(18) = DVD(J)$$
$$WP(19) = J$$
$$WP(20) = \left| \Delta\psi\,(J)/2 \right|$$

(B20) Cont'd.

For Half Turn Circles

If MODULO (I I,3) = 2, then L = J

$$WP(1) = \hat{WNE}(L, 1)$$
$$WP(2) = \hat{WNE}(L, 2)$$
$$WP(3) = \hat{WNE}(L, 3)$$

If MODULO (I I,3) = 0, then L = J-1

$$WP(1) = \hat{WN}(J, 1)$$
$$WP(2) = \hat{WN}(J, 2)$$
$$WP(3) = \hat{WN}(J, 3)$$

(B21)

$$WP(4) = 0$$
$$WP(5) = 0$$
$$WP(6) = 0$$
$$WP(7) = \text{sign}\left(\Delta\psi\,(L)\right)$$
$$WP(8) = \hat{CR}(L, 1)$$
$$WP(9) = \hat{CR}(L, 2)$$
$$WP(10) = \hat{CR}(L, 3)$$
$$WP(11) = \left| \Delta\psi\,(L) / 2 \right|$$
$$WP(12) = R_T(L)$$
$$WP(13) = 0$$
$$WP(14) = \sin\left(\tan^{-1}\left(GRAD\,(J)\right)\right)$$
$$HEND = HEND + GRAD\,(J)\left(R_T(L)\left|\Delta\psi\,(L) / 2\right|\right)$$
$$VEND = VEND + DVD\,(J)\left(R_T(L)\left|\Delta\psi\,(L) / 2\right|\right)$$

WP (15) = HEND

WP (16) = GRAD (J)

WP (17) = VEND

WP (18) = DVD (J)

WP (19) = J

WP (20) = 0

(B21)
Cont'd.

APPENDIX C

Discrete Formulation of a Third Order Complementary Filter

This appendix derives a closed form solution of the third order complementary filter for use in implementing a discrete formulation of the filter for flight computers. The solution permits the use of input gains to yield either 3 real or 1 real and 2 complex conjugate roots. It provides for fixed coefficients to update the aircraft state position, velocity and acceleration directly from input noisy accelerometer data, and navigation aids such as MLS, VORTAC, and barometric data, etc., without requiring Runge Kutta integration.

In what follows, the measurements are converted into a runway Cartesian vector ($\bar{x}$, $\bar{y}$, $\bar{z}$). The details of the transformation are contained in Section II of this report and is not repeated here. Each component of the coordinate system is estimated by means of three first order linear differential equations driven by the converted measurement, say $\bar{x}$, and the measurement of acceleration in that coordinate, $\ddot{x}$.

A. The Third Order Complementary Filter

The differential equations for the third order complementary filter for one of the three coordinates, (say x (t)) may be written as

$$\dot{x}_1 = K_1 (\bar{x} (t) - x_1) + x_2 \qquad \text{(C1a)}$$

$$\dot{x}_2 = K_2 (\bar{x} (t) - x_1) + x_3 + \ddot{x} (t) \qquad \text{(C1b)}$$

$$\dot{x}_3 = K_3 (\bar{x} (t) - x_1) \qquad \text{(C1c)}$$

where

K_1 , K_2 and K_3 are the filter gains.

$\bar{x}$ (t) is the navigation aid pseudo measurement of the coordinate, in the x direction.

$\ddot{x}$ (t) is the measured noisy acceleration, assumed constant over the internal $0 \leq t \leq \tau$.

From Eq. (C1c) we may solve for $x_1 - \bar{x}$ (t)

$$x_1 - \bar{x}(t) = - \frac{1}{K_3} \dot{x}_3 \tag{C2}$$

Differentiating Eq. (C 2) we get

$$\dot{x}_1 - \dot{\bar{x}}(t) = - \frac{1}{K_3} \ddot{x}_3 \tag{C2a}$$

Substituting for $\dot{x}_1$ from Eq. (C 1a) we obtain

$$K_1 (\bar{x}(t) - x_1) + x_2 - \dot{\bar{x}}(t) = - \frac{1}{K_3} \ddot{x}_3 \tag{C2b}$$

We may replace $(\bar{x}(t) - x_1)$ in Eq. (C2b) by its equivalent in Eq. (C 2) and obtain

$$x_2 - \dot{\bar{x}}(t) = - \frac{1}{K_3} (\ddot{x}_3 + K_1 \dot{x}_3) \tag{C3}$$

Differentiating Eq. (C 3) we obtain

$$x_2 - \ddot{\bar{x}}(t) = - \frac{1}{K_3} (\dddot{x}_3 + K_1 \ddot{x}_3) \tag{C3a}$$

Replacing $\dot{x}_2$ by Eq. (C 1b) , we obtain

$$K_2 (\bar{x}(t) - x_1) + x_3 + \dot{\bar{x}}(t) - \ddot{\bar{x}} = - \frac{1}{K_3} (\dddot{x}_3 + K_1 \ddot{x}_3) \tag{C3b}$$

Again we replace $\bar{x}$ (t) - x_1 in Eq. (C 3b) by its equivalent in Eq. (C 2) and obtain

$$\ddot{x}(t) - \ddot{\bar{x}}(t) = - \frac{1}{K_3} (\ddddot{x}_3 + K_1 \dddot{x}_3 + K_2 \ddot{x}_3 + K_3 \dot{x}_3) \tag{C4}$$

We now make the assumption that the navigation aid measurement $\bar{x}(t)$ is modeled as a quadratic polynomial of time.

$$\bar{x}(t) = \bar{x}_o + \dot{\bar{x}}_o\, t + \ddot{\bar{x}}_o \frac{t^2}{2} \tag{C5}$$

We determine the initial coefficient as follows:

At $t = 0$ (the beginning of the discrete time interval).

$$\dot{\bar{x}}(0) = \dot{\bar{x}}_o = x_2(0) \tag{C5a}$$

$$\ddot{\bar{x}}(0) = \ddot{\bar{x}}_o = \ddot{x}(\tau) + x_3(0) \tag{C5b}$$

At $t = \tau$ we set the navigation aid measurement equal to $\bar{x}(\tau)$.

$$\bar{x}(\tau) = \bar{x}_o + x_2(0)\,\tau + \left(\ddot{x}(\tau) + x_3(0)\right)\frac{\tau^2}{2} \tag{C5c}$$

We may now solve for the initial value of $\bar{x}(0)$, namely $\bar{x}_o$

$$\bar{x}_o = \bar{x}(\tau) - x_2(0)\,\tau - \left(\ddot{x}(\tau) + x_3(0)\right)\frac{\tau^2}{2} \tag{C6}$$

Subtracting $x_1(0)$ from both sides we have

$$\bar{x}_o - x_1(0) = \bar{x}(\tau) - \left(x_1(0) + x_2(0)\,\tau + \left(x_3(0) + \ddot{x}\right)\frac{\tau^2}{2}\right) \tag{C6a}$$

Thus we have succeeded to model the observation $\bar{x}(\tau)$ in such a manner that if the difference between the observation $\bar{x}(\tau)$ and its prediction, as a quadratic function of $x_1(0)$, $x_2(0)$, $x_3(0)$ and $\ddot{x}(\tau)$ vanishes, then the initial value of $\bar{x}_o - x_1(0)$ also vanishes.

Returning to Eq. (C4), we note that the right hand side is a constant and using Eq. (C5b), Eq. (C4) becomes

$$\dddot{x}_3 + K_1 \ddot{x}_3 + K_2 x_2 \dot{x}_3 + K_3 x_3 = K_3 x_3 (0) \tag{C4a}$$

The solution of Eq. (C4a) is either

$$x_3 - x_3 (0) = a e^{-\alpha_1 t} + b e^{-\alpha_2 t} \cos \beta t + c e^{-\alpha_2 t} \frac{\sin \beta t}{\beta} \tag{C7}$$

(if the gains K_1, K_2, and K_3 produce 1 real root and a pair of complex conjugate roots), or else

$$x_3 - x_3 (0) = a e^{-\alpha_1 t} + b e^{-\alpha_2 t} + c e^{-\alpha_3 t} \tag{C8}$$

if K_1, K_2 and K_3 produce 3 real roots of the characteristic equation

$$z^3 + K_1 z^2 + K_2 z + K_3 = 0 \tag{C9}$$

For the case of only one real root, Eq. (C7), we have

$$(z + \alpha_1)\left((z + \alpha_2)^2 + \beta^2\right) = 0 \tag{C7a}$$

and

$$K_1 = \alpha_1 + 2\alpha_2 \tag{C7b}$$

$$K_2 = 2\alpha_2 \alpha_1 + \alpha_2^2 + \beta^2 \tag{C7c}$$

$$K_3 = \alpha_1 (\alpha_2^2 + \beta^2) \tag{C7d}$$

For the case of 3 real roots, Eq. (C 8) , we have

$$(z+\alpha_1)(z+\alpha_2)(z+\alpha_3) = 0 \tag{C8a}$$

$$\alpha_1 + \alpha_2 + \alpha_3 = K_1 \tag{C8b}$$

$$\alpha_1\alpha_2 + \alpha_1\alpha_3 + \alpha_2\alpha_3 = K_2 \tag{C8c}$$

$$\alpha_1\alpha_2\alpha_3 = K_3 \tag{C8d}$$

We now proceed to solve the discrete third order complementary filter for the two cases.

Let the roots of the characteristic equation be α_1 , $\alpha_2 + i\,\beta$, $\alpha_2 - i\,\beta$; then, the solution of Eq. (C 4a) is Eq. (C 7). We may now differentiate Eq. (C 7) to obtain a solution of Eq. (C 2). We have

$$K_3(x_1 - \bar{x}(t) = \dddot{x}_3 = \left\{ \begin{array}{l} a\,\alpha_1 e^{-\alpha_i t} \\ +b\,e^{-\alpha_2 t}(\alpha_2 \cos\beta t + \beta \sin\beta t) \\ +c\,e^{-\alpha_2 t}(\alpha_2 \frac{\sin\beta t}{\beta} - \cos\beta t) \end{array} \right\} \tag{C10}$$

Similarly, we may obtain an expression for $\ddot{x}_3 + K_1\dot{x}_3$. Recalling that $K_1 = \alpha_1 + 2\alpha_2$ we may solve Eq. (C 3) and obtain

$$K_3\left(x_2 - \dot{\bar{x}}(t)\right) = -\ddot{x}_3 - K_1\dot{x}_3 = \left\{ \begin{array}{l} a\,e^{-\alpha_1 t} 2\alpha_1\alpha_2 \\ +b\,e^{-\alpha_2 t}\left((\alpha_2^2 + \beta^2 + \alpha_1\alpha_2)\cos\beta t + \alpha_1\beta^2 \frac{\sin\beta t}{\beta}\right) \\ +c\,e^{-\alpha_2 t}\left((\alpha_2^2 + \beta^2 + \alpha_1\alpha_2)\frac{\sin\beta t}{\beta} - \alpha_1\cos\beta t\right) \end{array} \right\} \tag{C11}$$

We may combine Eq's. (C 10) , (C11) and (C 7) in matrix form to obtain

$$\begin{Bmatrix} K_3 \, (x_1 - \bar{x} \, (t) \,) \\ K_3 \, (x_2 - \dot{\bar{x}} \, (t) \,) \\ x_3 - x_3 \, (0) \end{Bmatrix} = (A) \begin{Bmatrix} a \, e^{-\alpha_1 t} \\ b \, e^{-\alpha_2 t} \\ c \, e^{-\alpha_2 t} \end{Bmatrix} \qquad \text{(C12)}$$

where the elements of the 3 x 3 matrix (A) are given by

$$a_{11} = \alpha_1$$

$$a_{12} = \alpha_2 \cos \beta t + \beta \sin \beta t$$

$$a_{13} = \alpha_2 \frac{\sin \beta t}{\beta} - \cos \beta t$$

$$a_{21} = 2 \alpha_1 \alpha_2$$

$$a_{22} = (\alpha_2^2 + \beta^2 + \alpha_1 \alpha_2) - \cos \beta t + \alpha_1 \beta \sin \beta t \qquad \text{(C12a)}$$

$$a_{23} = (\alpha_2^2 + \beta^2 + \alpha_1 \alpha_2) \frac{\sin \beta t}{\beta} - \alpha_1 \cos \beta t$$

$$a_{31} = 1$$

$$a_{32} = \cos \beta t$$

$$a_{33} = \frac{\sin \beta t}{\beta}$$

Setting $t = 0$, Eq. (C12) becomes

$$\begin{Bmatrix} K_3(x_1(0) - \bar{x}_o) \\ 0 \\ 0 \end{Bmatrix} \begin{bmatrix} \alpha_1 & \alpha_2 & -1 \\ 2\alpha_1\alpha_2 & \alpha_2^2 + \beta^2 + \alpha_1\alpha_2 & -\alpha_1 \\ 1 & 1 & 0 \end{bmatrix} \begin{Bmatrix} a \\ b \\ c \end{Bmatrix} \quad \text{(C13)}$$

The solution for a, b, and c is given by

$$\begin{aligned} a &= \frac{\alpha_1}{\Delta} K_3 (x_1(0) - \bar{x}_o) \\ b &= \frac{-\alpha_1}{\Delta} K_3 (x_1(0) - \bar{x}_o) \\ c &= \frac{\alpha_2\alpha_1 - \alpha_2^2 - \beta^2}{\Delta} K_3 (x_1(0) - \bar{x}_o) \end{aligned} \quad \text{(C14)}$$

where Δ is the determinant of the matrix (A)

$$\Delta = \alpha_2^2 + \beta^2 + \alpha_1^2 - 2\alpha_2\alpha_1 \quad \text{(C14a)}$$

From Eq. (C6a) we may substitute for $x_1(0) - \bar{x}_o$ in Eq. (C14) and obtain

$$\begin{aligned} a &= \frac{\alpha_1}{\Delta} K_3 (\hat{x}_1(\tau) - \bar{x}(\tau)) \\ b &= \frac{-\alpha_1}{\Delta} K_3 (\hat{x}_1(\tau) - \bar{x}(\tau)) \\ c &= \frac{\alpha_2\alpha_1 - \alpha_2^2 - \beta^2}{\Delta} K_3 (\hat{x}_1(\tau) - \bar{x}(\tau)) \end{aligned} \quad \text{(C14b)}$$

$$\hat{x}_1 = x_1(0) + x_2(0)\tau + (x_3(0) + \dddot{x}(\tau)) \frac{\tau^2}{2} \quad \text{(C14c)}$$

After substituting the solution for a , b , and c into Eq. (C12) we have

$$\begin{Bmatrix} x_1(\tau) \\ x_2(\tau) \\ x_3(\tau) \end{Bmatrix} = \begin{Bmatrix} \bar{x}(\tau) \\ x_2(0) + (x_3(0) + \ddot{\bar{x}})\tau \\ x_3(0) \end{Bmatrix} + \begin{Bmatrix} G_1(\hat{x}_1(\tau) - \bar{x}(\tau)) \\ G_2(\hat{x}_1(\tau) - \bar{x}(\tau)) \\ G_3(\hat{x}_1(\tau) - \bar{x}(\tau)) \end{Bmatrix} \quad \text{(C15)}$$

where

$$G_1 = \begin{pmatrix} \alpha_1^2 e^{-\alpha_1\tau} + (\beta^2 + \alpha_2^2 - 2\alpha_1\alpha_2) e^{-\alpha_2\tau}\cos\beta\tau \\ +\left(\alpha_1(\alpha_2^2 - \beta^2) - (\alpha_2^2 + \beta^2)\alpha_2\right) e^{-\alpha_2\tau}\frac{\sin\beta\tau}{\beta} \end{pmatrix} \frac{1}{\Delta}$$

$$G_2 = \begin{pmatrix} 2\alpha_1^2\alpha_2\left(e^{-\alpha_1\tau} - e^{-\alpha_2\tau}\cos\beta\tau\right) \\ +\left(\alpha_1^2(\alpha_2^2 - \beta^2) - (\alpha_2^2 + \beta^2)^2\right) e^{-\alpha_2\tau}\frac{\sin\beta\tau}{\beta} \end{pmatrix} \frac{1}{\Delta} \quad \text{(C15a)}$$

$$G_3 = \begin{pmatrix} \alpha_1\left(e^{-\alpha_1\tau} - e^{-\alpha_2\tau}\cos\beta\tau\right) \\ -(\beta^2 + \alpha_2^2 - \alpha_1\alpha_2) e^{-\alpha_2\tau}\frac{\sin\beta\tau}{\beta} \end{pmatrix} \frac{K_3}{\Delta}$$

A somewhat more convenient form for the solution is obtained by replacing G_1 by $G_1 - 1$. Then Eq. (C15) becomes

$$\begin{Bmatrix} x_1(\tau) \\ x_2(\tau) \\ x_3(\tau) \end{Bmatrix} = \begin{Bmatrix} \hat{x}_1(\tau) \\ x_2(0) + (x_3(0) + \ddot{\bar{x}})\tau \\ x_3(0) \end{Bmatrix} + \begin{Bmatrix} (G_1 - 1)(\hat{x}_1(\tau) - \bar{x}(\tau)) \\ G_2(\hat{x}_1(\tau) - \bar{x}(\tau)) \\ G_3(\hat{x}_1(\tau) - \bar{x}(\tau)) \end{Bmatrix} \quad \text{(C16)}$$

In this form it is clear that if the residual $x_1(\tau) - \bar{x}(\tau)$ is zero, then the solution of $x_1(\tau)$, $x_2(\tau)$ and $x_3(\tau)$ is the so called "dead reckoning" solution obtained for a linear system under constant acceleration.

Let the roots of the characteristic equation be α_1, α_2 and α_3.

In place of Eq. (C10) we now have

$$K_3\left(x_1 - \bar{x}(\tau)\right) = a\alpha_1 e^{-\alpha_1\tau} + b\alpha_2 e^{-\alpha_2\tau} + c\alpha_3 e^{-\alpha_3\tau} \qquad \text{(C17)}$$

In place of Eq. (C11) we now have

$$K_3\left(x_2 - \dot{\bar{x}}(\tau)\right) = a\alpha_1(\alpha_2+\alpha_3)e^{-\alpha_1\tau} + b\alpha_2(\alpha_1+\alpha_3)e^{-\alpha_2\tau} + c\alpha_3(\alpha_1+\alpha_2)e^{-\alpha_3\tau} \qquad \text{(C18)}$$

For the equation for $x_3 - x_3(0)$ we have from Eq. (C8)

$$x_3 - x_3(0) = a e^{-\alpha_1\tau} + b e^{-\alpha_2\tau} + c e^{-\alpha_3\tau} \qquad \text{(C19)}$$

The matrix equation replacing Eq. (C12) is given by

$$\begin{Bmatrix} K_3\left(x_1 - \bar{x}(\tau)\right) \\ K_3\left(x_2 - \dot{\bar{x}}(\tau)\right) \\ x_3 - x_3(0) \end{Bmatrix} = \begin{Bmatrix} \alpha_1 & \alpha_2 & \alpha_3 \\ \alpha_1(\alpha_2+\alpha_3) & \alpha_2(\alpha_1+\alpha_3) & \alpha_3(\alpha_1+\alpha_2) \\ 1 & 1 & 1 \end{Bmatrix} \begin{Bmatrix} a e^{-\alpha_1\tau} \\ b e^{-\alpha_2\tau} \\ c e^{-\alpha_3\tau} \end{Bmatrix} \qquad \text{(C20)}$$

Setting $t = 0$ in Eq. (C20) and solving for a, b and c we obtain

$$\begin{aligned} a &= \frac{\alpha_1}{(\alpha_1-\alpha_2)(\alpha_1-\alpha_3)} K_3\left(x_1(0) - \bar{x}_o\right) \\ b &= \frac{\alpha_2}{(\alpha_2-\alpha_1)(\alpha_2-\alpha_3)} K_3\left(x_1(0) - \bar{x}_o\right) \\ c &= \frac{\alpha_3}{(\alpha_3-\alpha_1)(\alpha_3-\alpha_2)} K_3\left(x_1(0) - x_o\right) \end{aligned} \qquad \text{(C21)}$$

The final solution equivalent to Eq. (C16) is given by the G_i coefficients

$$G_1 - 1 = \left\{ \frac{\alpha_1^2}{(\alpha_1-\alpha_2)(\alpha_1-\alpha_3)} e^{-\alpha_1 \tau} + \frac{\alpha_2^2}{(\alpha_2-\alpha_1)(\alpha_2-\alpha_3)} e^{-\alpha_2 \tau} + \frac{\alpha_3^2}{(\alpha_3-\alpha_1)(\alpha_3-\alpha_2)} e^{-\alpha_3 \tau} \right\} - 1$$

$$G_2 = \left\{ \frac{\alpha_1^2(\alpha_2+\alpha_3)}{(\alpha_1-\alpha_2)(\alpha_1-\alpha_3)} e^{-\alpha_1 \tau} + \frac{\alpha_2^2(\alpha_1+\alpha_3)}{(\alpha_2-\alpha_1)(\alpha_2-\alpha_3)} e^{-\alpha_2 \tau} + \frac{\alpha_3^2(\alpha_1+\alpha_2)}{(\alpha_3-\alpha_1)(\alpha_3-\alpha_2)} e^{-\alpha_3 \tau} \right\} \quad \text{(C22)}$$

$$G_3 = \left\{ \frac{K_3 \alpha_1}{(\alpha_1-\alpha_2)(\alpha_1-\alpha_3)} e^{-\alpha_1 \tau} + \frac{K_3 \alpha_2}{(\alpha_2-\alpha_1)(\alpha_2-\alpha_3)} e^{-\alpha_2 \tau} + \frac{K_3 \alpha_3}{(\alpha_3-\alpha_1)(\alpha_3-\alpha_2)} e^{-\alpha_3 \tau} \right\}$$

B. Determination of the Characteristic Roots From the Filter Gains

It is sometimes more convenient to input the three gains, K_i, rather than the roots of the characteristic equation. In that case it is necessary to determine the values of the three roots and to find whether two are complex.

Let the gains be K_1, K_2 and K_3. The characteristic equation is

$$z^3 + K_1 z^2 + K_2 z + K_3 = 0 \quad \text{(C23)}$$

with

$$K_i \geq 0 \quad \text{(C23a)}$$

First form the discriminant to test for reality of the roots.

Let

$$C = K_1^2 \quad \text{(C24)}$$

$$P = K_2 - C/3$$

$$Q = K_3 - (K_2/3 - \tfrac{2}{27} C) K_1$$

The discriminant is given by

$$D = 4P^3 + 27Q^2 \tag{C25}$$

If $D < 0$ 3 real negative roots

If $D \geq 0$ 1 real negative and 2 complex conjugate

For $D < 0$

$$A = 2\left(-P/3\right)^{\frac{1}{2}} \tag{C26a}$$

$$\theta = \cos^{-1}\left(\frac{-Q}{2\left(\frac{-P^3}{27}\right)^{\frac{1}{2}}}\right) \tag{C26b}$$

$$\alpha_1 = \frac{K_1}{3} - A\cos\theta$$

$$\alpha_2 = \frac{K_1}{3} + \frac{A}{2}\left(\cos\theta + \sqrt{3}\sin\theta\right) \tag{C27}$$

$$\alpha_3 = \frac{K_1}{3} + \frac{A}{2}\left(\cos\theta - \sqrt{3}\sin\theta\right)$$

For $D \geq 0$

$$B = \left(\frac{D}{108}\right)^{\frac{1}{2}} \tag{C28a}$$

$$E = -\tfrac{1}{2}Q + B \tag{C28b}$$

$$F = -\tfrac{1}{2}Q - B \tag{C28c}$$

$$G = \text{sgn}(E)\left|E\right|^{\frac{1}{3}} \tag{C28d}$$

$$H = \text{sgn}(F)\left|F\right|^{\frac{1}{3}} \tag{C28e}$$

$$\alpha_1 = \frac{K_1}{3} - (G + H)$$

$$\alpha_2 = \frac{K_1}{3} + \frac{1}{2}(G + H) \qquad \text{(C29)}$$

$$\beta = \frac{\sqrt{3}}{2} \left| G - H \right|$$

APPENDIX D

Wind Estimator Models

The physical model used to estimate the winds is based on the assumption that the aircraft attitude is maintained in a trimmed condition, aligned with the relative wind. In this equilibrium condition, we have for the horizontal components of the wind

$$w_x = \dot{R}_G(1) - v_{airspeed} \cos\psi \tag{D1}$$

$$w_y = \dot{R}_G(2) - v_{airspeed} \sin\psi \tag{D2}$$

If we retain the initial value of w_x and w_y as the best estimate of the constant winds in a local level coordinate frame, we may model the deviation from this original estimate as an exponentially correlated random variable.

Thus for the Kalman filter we have

$$\tilde{b}w_x(t) = \tilde{b}w_x(t - \Delta t)\, e^{-\frac{\Delta t}{t_w}} + \sigma_w \sqrt{\frac{2\,\Delta t}{t_w}} \tag{D3}$$

$$\tilde{b}w_y(t) = \tilde{b}w_y(t - \Delta t)\, e^{-\frac{\Delta t}{t_w}} + \sigma_w \sqrt{\frac{2\,\Delta t}{t_w}} \tag{D4}$$

where

$$\sigma_w = 1.\ \text{m/sec}\ ,\ t_w = 100.\ \text{sec}\ ,\ \Delta t = .05\ \text{sec}$$

The best estimate of the horizontal winds for the Kalman filter is

$$\hat{w}_x(t) = w_x(t_o) + \tilde{b}w_x(t) \tag{D5}$$

$$\hat{w}_y(t) = w_y(t_o) + \tilde{b}w_y(t) \tag{D6}$$

The observation of the winds are supplied by Eq's. (D1) and (D2) and the residual for the Kalman filter equations are given by

$$\Delta w_x = w_x(y)_{\text{Eq. (4.1)}} - \hat{w}_x(t) \tag{D7}$$

$$\Delta w_y = w_y(t)_{\text{Eq. (4.2)}} - \hat{w}_y(t) \tag{D8}$$

The Kalman gains are computed in a manner already described in Ref. 1 (page 31) and are not repeated here. The updated value of the wind biases are given by

$$\hat{bw}_x(t) = \hat{bw}_x(t) + \Delta bw_x \tag{D9}$$

$$\hat{bw}_y(t) = \hat{bw}_y(t) + \Delta bw_y \tag{D10}$$

For the case of the complementary filter we chose a first order exponential model without reference to any estimate of the variance. We have

$$bw_x(t) = bw_x(t - \Delta t) + e^{-\Delta t/t_w}\left(w_x(t_o) + bw_x(t - \Delta t) - w_{x_{\text{Eq. (D1)}}}(t)\right) \tag{D11}$$

$$bw_y(t) = bw_y(t - \Delta t) + e^{-\Delta t/t_w}\left(w_y(t_o) + bw_y(t - \Delta t) - w_{y_{\text{Eq. (D2)}}}(t)\right) \tag{D12}$$

where $bw_x(t_o) = bw_y(t_o) = 0$,

$t_w = 100$ sec, $\Delta t = .05$ sec.

1. Report No.	2. Government Accession No.	3. Recipient's Catalog No.
NASA CR-3511		

4. Title and Subtitle	5. Report Date
TERMINAL AREA AUTOMATIC NAVIGATION, GUIDANCE, AND CONTROL RESEARCH USING THE MICROWAVE LANDING SYSTEM (MLS) PART 2 - RNAV/MLS TRANSITION PROBLEMS FOR AIRCRAFT	January 1982
	6. Performing Organization Code

7. Author(s)	8. Performing Organization Report No.
Samuel Pines	AMA 80-12
	10. Work Unit No.

9. Performing Organization Name and Address	11. Contract or Grant No.
Analytical Mechanics Associates, Inc. 17 Research Road Hampton, Virginia 23666	NAS1-15116
	13. Type of Report and Period Covered

12. Sponsoring Agency Name and Address	13. Type of Report and Period Covered
National Aeronautics and Space Administration Washington, D. C. 20546	Contractor Report
	14. Sponsoring Agency Code

15 Supplementary Notes

Langley Technical Monitor: Richard M. Hueschen
Final Report - Part 2

16. Abstract

This report contains the results of an investigation carried out for the NASA Langley Research Center TCV B-737 program to study the problems in navigation and guidance encountered by aircraft in the initial transition period in changing from DME, VORTAC, and barometric instruments to the more precise MLS data type navaids in the terminal area. The report investigates the effects of the resulting discontinuities on the estimates of position and velocity for both optimal (Kalman type navigation schemes) and fixed gain (complementary type) navigation filters, and the effects of the errors in cross track, track angle, and altitude on the guidance equations and control commands during the critical landing phase. A method is presented to remove the discontinuities from the navigation loop and to reconstruct an RNAV path designed to land the aircraft with minimal turns and altitude changes.

17. Key Words (Suggested by Author(s))	18. Distribution Statement
Automatic Landing Navigation and Guidance Path Redesign MLS Navaids Transition	Unclassified - Unlimited Subject Category 04

19. Security Classif. (of this report)	20. Security Classif. (of this page)	21. No. of Pages	22. Price
Unclassified	Unclassified	137	A07

For sale by the National Technical Information Service, Springfield, Virginia 22161